R-935

May 1991

NCEL

Technical Report

By G.E. Warren and L.J. Malvar

Sponsored By Naval Facilities
Engineering Command

LATERAL LOAD DISTRIBUTION IN ONE-WAY FLAT SLABS

ABSTRACT Results of laboratory model tests, inservice pier tests, classical plate theory, and finite element analyses provide the basis for changes in Military Handbook 1025/1 addressing flat slab pier deck design to distribute truck crane outrigger loads. The concentrated load distribution efficiency of Navy pier slabs can be doubled over current AASHTO allowables. For pier deck designs where large, truck-mounted cranes dominate load requirements, this will result in higher load capacity, longer spans, and less construction material. Further, the verified effectiveness of lateral load distribution would almost double outrigger load-carrying efficiency of current Navy pier decks.

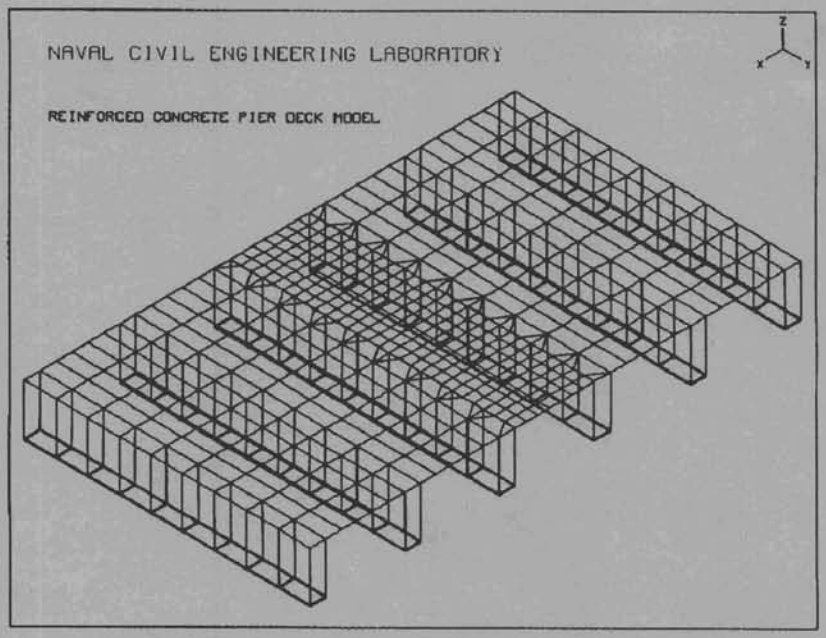

NAVAL CIVIL ENGINEERING LABORATORY PORT HUENEME CALIFORNIA 93043-5003

METRIC CONVERSION FACTORS

Approximate Conversions to Metric Measures

Symbol	When You Know	Multiply by	To Find	Symbol
		LENGTH		
in	inches	*2.5	centimeters	cm
ft	feet	30	centimeters	cm
yd	yards	0.9	meters	m
mi	miles	1.6	kilometers	km
		AREA		
in^2	square inches	6.5	square centimeters	cm^2
ft^2	square feet	0.09	square meters	m^2
yd^2	square yards	0.8	square meters	m^2
mi^2	square miles	2.6	square kilometers	km^2
	acres	0.4	hectares	ha
		MASS (weight)		
oz	ounces	28	grams	g
lb	pounds	0.45	kilograms	kg
	short tons (2,000 lb)	0.9	tonnes	t
		VOLUME		
tsp	teaspoons	5	milliliters	ml
Tbsp	tablespoons	15	milliliters	ml
fl oz	fluid ounces	30	milliliters	ml
c	cups	0.24	liters	l
pt	pints	0.47	liters	l
qt	quarts	0.95	liters	l
gal	gallons	3.8	liters	l
ft^3	cubic feet	0.03	cubic meters	m^3
yd^3	cubic yards	0.76	cubic meters	m^3
		TEMPERATURE (exact)		
°F	Fahrenheit temperature	5/9 (after subtracting 32)	Celsius temperature	°C

*1 in = 2.54 (exactly). For other exact conversions and more detailed tables, see NBS Misc. Publ. 286, Units of Weights and Measures, Price $2.25, SD Catalog No. C13.10:286.

Approximate Conversions from Metric Measures

Symbol	When You Know	Multiply by	To Find	Symbol
		LENGTH		
mm	millimeters	0.04	inches	in
cm	centimeters	0.4	inches	in
m	meters	3.3	feet	ft
m	meters	1.1	yards	yd
km	kilometers	0.6	miles	mi
		AREA		
cm^2	square centimeters	0.16	square inches	in^2
m^2	square meters	1.2	square yards	yd^2
km^2	square kilometers	0.4	square miles	mi^2
ha	hectares (10,000 m^2)	2.5	acres	
		MASS (weight)		
g	grams	0.035	ounces	oz
kg	kilograms	2.2	pounds	lb
t	tonnes (1,000 kg)	1.1	short tons	
		VOLUME		
ml	milliliters	0.03	fluid ounces	fl oz
l	liters	2.1	pints	pt
l	liters	1.06	quarts	qt
l	liters	0.26	gallons	gal
m^3	cubic meters	35	cubic feet	ft^3
m^3	cubic meters	1.3	cubic yards	yd^3
		TEMPERATURE (exact)		
°C	Celsius temperature	9/5 (then add 32)	Fahrenheit temperature	°F

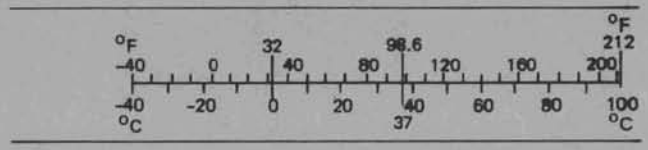

REPORT DOCUMENTATION PAGE

Form Approved
OMB No. 0704-018

1. AGENCY USE ONLY *(Leave blank)*	2. REPORT DATE	3. REPORT TYPE AND DATES COVERED
	May 1991	Final - May 1987 through Sep 1990

4. TITLE AND SUBTITLE

LATERAL LOAD DISTRIBUTION IN ONE-WAY FLAT SLABS

5. FUNDING NUMBERS

PR - 51-157
WU - DN666334

6. AUTHOR(S)

G.E. Warren, NCEL and
L.J. Malvar, Research Engineer, UC Davis

7. PERFORMING ORGANIZATION NAME(S) AND ADDRESSE(S)

Naval Civil Engineering Laboratory
Port Hueneme, CA 93043-5003

8. PERFORMING ORGANIZATION REPORT NUMBER

TR - 935

9. SPONSORING/MONITORING AGENCY NAME(S) AND ADDRESSE(S)

Naval Facilities Engineering Command
Alexandria, Virginia 22332

10. SPONSORING/MONITORING AGENCY REPORT NUMBER

11. SUPPLEMENTARY NOTES

12a. DISTRIBUTION/AVAILABILITY STATEMENT

Approved for public release; distribution unlimited.

12b. DISTRIBUTION CODE

13. ABSTRACT *(Maximum 200 words)*

Results of laboratory model tests, inservice pier tests, classical plate theory, and finite element analyses provide the basis for changes in Military Handbook 1025/1 addressing flat slab pier deck design to distribute truck crane outrigger loads. The concentrated load distribution efficiency of Navy pier slabs can be doubled over current AASHTO allowables. For pier deck designs where large, truck-mounted cranes dominate load requirements, this will result in higher load capacity, longer spans, and less construction material. Further, the verified effectiveness of lateral load distribution would almost double outrigger load-carrying efficiency of current Navy pier decks.

14. SUBJECT TERMS

Reinforced concrete, slabs, pier decks, patch loads, load distribution, finite element modeling

15. NUMBER OF PAGES

71

16. PRICE CODE

17. SECURITY CLASSIFICATION OF REPORT	18. SECURITY CLASSIFICATION OF THIS PAGE	19. SECURITY CLASSIFICATION OF ABSTRACT	20. LIMITATION OF ABSTRACT
Unclassified	Unclassified	Unclassified	UL

CONTENTS

INTRODUCTION

Navy experience with large, truck-mounted crane outrigger loads on pier decks has demonstrated that current American Association of State Highway and Transportation Officials (AASHTO) wheel load distribution formulas applied to the case of patch loads on reinforced concrete slabs are very conservative. An initial numerical parameter study of flat plates subjected to concentrated loads showed that lateral load distribution is more significant than allowed by AASHTO. An existing pier was tested concurrently to verify the parameter study.

Two prototype reinforced concrete pier decks were designed: the first one following AASHTO's formula, the second assuming a more efficient lateral load distribution as determined in the parameter study. The second design represented large savings in materials and labor. A one-third scale model of the latter design was constructed and tested at the Naval Civil Engineering Laboratory (NCEL).

The objectives of the study were to:

1. Verify the soundness and safety of a more economical pier design.

2. Measure the lateral distribution of patch loads in the scale model.

3. Establish experimentally the load capacity and mode of failure of the scale model.

4. Obtain the lateral distribution by using a finite element model.

5. Determine the lateral distribution analytically by using influence surfaces based on classical plate theory.

6. Derive simple, empirical design criteria for outrigger load distribution that would provide a more accurate alternative to current designs.

"Distribution of Crane Loads and Concrete Pier Deck Design," is a Naval Facilities Engineering Command (NAVFAC) sponsored project in the Operations and Maintenance, Navy (O&MN) funded Engineering Investigation (EI) Program.

BACKGROUND

Navy experience using portable truck cranes on reinforced pier decks strongly suggests that AASHTO wheel load distribution formulas (Ref 1) are very conservative. Tests on full-scale isotropic bridge decks have shown ultimate capacities far in excess of the allowable (Ref 2). The current Ontario (Canada) Bridge Design Code (Ref 3) allows a reduction in flexural reinforcing steel in concrete decks on laterally restrained supports. An analytical and experimental study on load distribution for haunched deck panels (Ref 4) concluded that AASHTO load distribution design allowables could be increased up to 45 percent for 20-foot spans.

The AASHTO approach (Ref 5) is to calculate an "effective" width, E, over which the concentrated wheel load is assumed to be uniformly distributed:

$$E = 4.0 + 0.06S \quad \text{(feet)}$$

where S is the span length. A larger value of E equates to more efficient (effective) distribution of load. Flexural reinforcement is then determined from an equivalent strip of width, E, carrying the total load. The maximum value of E is limited to 7 feet. AASHTO does not address shear distribution, change in moment distribution away from the point of load, or change in moment distribution due to load position (near support or edge).

Navy pier decks are subjected to large patch loads from mobile truck crane outrigger pads. Maximum loads are on the order of 140 kips (90-ton crane) and are applied through square outrigger pads. Current design loads for Navy pier decks also include concentrated wheel loads of forklifts, trucks, and mobile cranes. It is current practice to treat mobile crane outrigger loads the same as wheel loads and apply AASHTO distribution formulas. Since outrigger loads are much larger than vehicular wheel loads, they often are the critical live loads for Navy pier decks.

PARAMETER STUDY

The initial finite element parameter study examined one-way slabs with span lengths ranging from 14 feet to 24 feet and pier widths from 50 feet to 150 feet. Loads were applied over a 2-foot square area. The finite element discretization used 1-foot square plate elements. Two types of elements were examined: a 3-node discrete Kirchhoff formulation plate element and a 9-node Mindlin/Reissner formulation shell element. The computer code ADINA was used (Ref 6).

Early observations revealed that concentrated load distribution did not change for widths beyond 40 feet for the range of spans considered. The effect of shear deformation was determined negligible and the simplified 3-node plate element was more effective. Support conditions were varied from pinned to fully fixed.

In addition to load application at midspan, the effect on distribution of moving the load toward a support as well as toward a free edge was quantified. The effect of load-pad-size-to-span-length ratio was also investigated.

FIELD TESTS ON PIER 5002

Load tests were conducted on an inservice pier (Pier 5002) at the Navy Submarine Base, San Diego. Single patch loads were applied at midspan and quarterspan. Pier 5002 was selected because its deck was newly constructed and uncluttered with design features such as trenches, duct banks, manholes or curbs, which detract from pure slab behavior. The test area is shown in Figure 1. The center of the test span (Figure 2) was 80 feet from the end of the pier and 20 feet from the pier centerline. The deck consisted of a layer of cast-in-place concrete over precast, prestressed planks. The total deck thickness was 18 inches.

Fifteen, paper-backed wire, SR-4 strain gages with 6-inch gage length were mounted at the locations shown in Figure 3. The gages were cemented to the deck surface one day prior to testing. The gages were aligned longitudinally with the pier except for gage 5 (at midspan) which was set transversely.

Load was applied by stacking two crane calibration weights. A 38-kip and a 42-kip weight were used. They were positioned over a 2-foot square, 3/4-inch-thick plywood pad using a mobile truck crane. Four load tests were conducted at locations shown in Figure 3: (1) load applied at midspan over gages 4 and 5, (2) load at quarterspan over gage 12, (3) load at midspan over gage 6, and (4) a repeat test with the load over gages 4 and 5.

PROTOTYPE DESIGN CHANGES

For a typical Navy pier span of 18 feet, AASHTO's effective width is 5.08 feet. A reinforced concrete deck design resulting from AASHTO load distribution for an 18-foot span is detailed in Figure 4. However, the finite element parameter study and experimental work on Pier 5002 revealed that actual lateral distribution would correspond to effective width values in excess of 10 feet. In view of this more efficient load distribution, a prototype pier deck of equal span was also designed based on an effective width value of 10 feet. This prototype design is shown in Figure 5.

SCALE MODEL

Field testing on Pier 5002 sustained high noise-to-signal ratios and ambient vibrations from waves and operations. In contrast, laboratory tests of a pier deck model would allow for proper control of the environment and enhanced monitoring of loading and response. A one-third scale model of the prototype design shown in Figure 5 was constructed at NCEL for laboratory testing. The model size was manageable in a laboratory and still large enough to preclude special similitude conditions associated with the nonhomogeneous nature of reinforced concrete. The deck consisted of a flat slab supported on rectangular pile cap beams.

The model structural drawings appear in Figure 6. Figure 7 shows the test model during the construction phase and Figure 8 shows the completed structure. It included five spans with pile bent spacing of 6 feet. The prototype has a 16-inch-thick deck with 15-foot clear spans (18 feet center-to-center) between pile cap supports. Principal reinforcing of the prototype included No. 6 and No. 9, grade 60, deformed bars with end spans having heavier reinforcement than intermediate spans. Material properties of the model were identical to the prototype, but dimensions and bar sizes were scaled. In the model D5 deformed wire (equivalent to a No. 2 deformed, grade 60 bar) and No. 3 deformed, grade 60 bars were used with 4,000-psi concrete (design compression strength). The model clear span was 5 feet and the slab thickness was 5-3/8 inches. Reinforcing clear cover was one-third of the prototype's (1 inch on the bottom and 5/8 inch on top). Model dimensional and reinforcement placement tolerances were reduced threefold.

Since material densities are the same for both prototype and model, dead weight of the model was one-third of the required weight for direct similitude. Dead weight contributes moments of about 7 percent of those produced by live service loads at the center of the model. This discrepancy does not affect the determination of lateral load distribution, and is acceptable in determining ultimate failure.

The model supports were designed to match the torsional rigidity of the prototype pile and cap beams support system such that there was no impact on the load distribution into the deck. Finite element analyses showed that the pile rotational rigidity is small compared to the flexural rigidity of the deck and the torsional rigidity of the pile cap. The cap beams were then provided only with uniform vertical support and rested on the floor of the test building.

The model concrete mix is indicated in Table 1. The maximum aggregate size was scaled down to 3/8 inch. A higher relative content of fine aggregate and the use of a high-range, water-reducing admixture (superplasticizer) allowed the concrete to be pumped. The model was cast from three concrete trucks. The concrete from the first load was pumped into the supports up to near the deck level, the second truckload completed the supports plus spans 2, 3, 4, and 5, while the final load went into span 1 and completion of span 2. Concrete cylinder tests in accordance with ASTM C-469 provided concrete strengths. The concrete mix design was constant but the cylinder strength was 5,000 psi for span 1, and 7,500 psi for spans 2, 3, 4, and 5. The measured modulus of elasticity for the central spans was 4,000 ksi and the measured Poisson ratio was 0.15.

Coupon tests of the reinforcing in the loaded areas were conducted in accordance with ASTM E8-87. The No. 2 bars had a yield strength of 81,000 psi and an ultimate strength of 85,000 psi, while the No. 3 bars had a yield strength of 69,000 psi and ultimate strength of 109,000 psi.

SCOPE OF MODEL TESTS

The load tests were limited to static loads applied over a one-third scale simulation of a crane outrigger pad footprint. Points were loaded individually. Load points were moved from midspan to near

supports and from structure centerline to free edge providing a range of positions and flexure/shear combinations. Continuous monitoring of sensors provided a full load range response.

Cyclic loads were applied in the service stress range of the concrete and reinforcement (concrete stresses remained less than 45 percent of the 28-day cylinder strength and steel stresses remained less than one-half of its yield strength). Loads were applied smoothly and without impact or dynamic effect.

After completion of the service load tests, static, monotonic loads to failure were applied. Failure was defined as exceeding ultimate capacity with sufficient displacement where the failure mode and crack/deformation pattern was visibly evident.

Test Setup

The pier deck model was constructed on the rail-reinforced concrete floor of NCEL Building 570. Figure 9 is a schematic of the test setup and loading fixtures. Loads were applied using a 100-ton, hollow-ram, hydraulic jack bearing on an 8-inch by 8-inch steel plate. The jack pulled a high-strength steel rod anchored to the rail system built into the floor of Building 570. The bearing pad consisted of a 1-1/2-inch steel plate with a rectangular 8-inch by 8-inch "rim" modeling 90-ton crane outrigger supports. A flat plate and circular shaped rim were also tested as bearing pads with comparable, but better, load distribution results.

Load locations are indicated in Figure 10. Load testing concentrated in three general areas for each span: (1) in the center of the span (D15, D1, D4), (2) at the free edge (D5, D17), and (3) near the support edge (D18, D3).

Instrumentation

The instrumentation layout focused on providing the load-deformation (strain and deflection) response over a grid around the loaded areas and at discrete points in neighboring spans. Typical strain gage locations are shown in Figure 11. A photograph of concrete strain gage layout for span 3 is provided in Figure 12. Deflection gages were positioned laterally to the load points, as shown in Figure 13. The following sensors were employed:

1. Concrete Strain Gages - 4-inch gage length, 350-ohm, paper-backed, SR-4 resistance wire gages.

2. Steel Strain Gages - HITEC hermetically-sealed weldable strain gage, 350-ohm resistance, 7/8-inch gage length.

3. Deflection Gages - Temposonics Linear Displacement Transducer (LDT) (with analog output) senses position of an external reference (magnet target) to measure differential displacement between the target and LDT.

4. Load Cell - Fabricated by strain gaging the high-strength reaction rod and calibrating it to a known tensile load.

Concrete strain gages were epoxied to the compression face of the deck slab. Weldable strain gages were attached to the tension reinforcement opposite the compression gages. Tandem strain gages at each point provided a measure of resistant flexural distribution away from the load points. The load cell on the high-strength rod measured load applied by the hydraulic ram.

Test Procedure

Two types of load tests were conducted on the structural model: service loading and load to failure. Load testing was conducted at all load points within the three general load areas identified previously (seven individual load points shown in Figure 10).

Service load tests consisted of the following load cycles at each location:

1. 0 to 10 kips (prior to flexural cracking) for 15 cycles
2. 0 to 30 kips for 15 cycles
3. 0 to 60 kips for 15 cycles
4. 0 to 90 kips for 20 cycles

The loads were cycled at each load level until the crack growth ceased and the measured strain values stabilized. A model load of 30 kips on an 8-inch by 8-inch pad is equivalent to a prototype load of 270 kips applied by a 2-foot by 2-foot outrigger pad. Thus, the "model service load" cycles listed above far exceed design outrigger loads for a 90-ton crane.

Loads to failure at each load point followed the cyclic load tests at all locations. During tests to failure, the hydraulic ram operator applied load monotonically until ultimate resistance was exceeded, a failure pattern was well defined, and the strength of the slab had been spent.

ANALYTICAL MODELING

Influence Surfaces

Influence surfaces for the bending moment at the center and edge of rectangular plates with varying edge conditions have been developed by A. Pucher (Ref 7). These influence surfaces have been obtained for elastic, homogeneous, isotropic material properties. For uncracked concrete, this model is accurate but some deviation is expected in the post cracking range where orthotropic section properties corresponding to different orthogonal steel percentages are present.

Solutions for infinite strips with two edges restrained or one edge restrained and one simply supported are given for the case of plates with large ratios of width-to-length. These two cases approximate an interior and an exterior span, respectively. Applying Maxwell's reciprocity law, the moment at a point away from the center due to a center

patch load is equal to the moment in the center due to a patch load at that point. The moment along the centerline due to a center patch load can thus be determined directly.

Refined Orthotropic Finite Element Analysis

The initial finite element model used in the parameter study was refined with orthotropic shell elements. Using the ADINA finite element code and an orthotropic material model allows for consideration of orthotrophy caused by cracking and orthogonal steel percentage difference. Two material properties were then implemented: an isotropic uncracked concrete material in the load range before flexural cracking, and an orthotropic cracked reinforced concrete material at service loads after cracking. The materials are considered linearly elastic and deflections are small compared to plate thickness. Because concrete is nonlinear at higher loads, these assumptions are limited to the service load range.

A finite element mesh of the scale model employing ADINA's shell and three-dimensional (3-D) elements is shown in Figure 14. A finer mesh was always used for the span in which the load was applied.

RESULTS OF THE PARAMETER STUDY

The parameter study yielded the following quantitative results for typical ranges of depth, span, and widths for Navy piers:

- Negligible distribution variation occurs due to change of the width-to-span ratio.
- Negligible variation occurs due to effect of slab depth.
- More effective distribution results for midspan loads than loads near a support.
- Less effective distribution results as load is moved toward a free edge.
- Enhanced distribution results for increasing span length.

The parametric study also indicated that the lateral distribution of the 2-foot patch load is more extensive than allowed by AASHTO's formula. For midspan applied loads an effective width in excess of 10 feet was consistently obtained.

Figure 15 shows the effect on load distribution (effective width) of moving the patch load from the center toward the support. The lateral distribution is shown to be less effective near the support. AASHTO's effective width for an 18-foot span is indicated. As the load is applied near the free edge, the distribution is less effective, as shown on Figure 16. It should be noted that an edge beam is typically required which would contribute to load carrying and distribution. The increase in effective width with increasing span length for a 2-foot pad is shown in Figure 17.

FIELD TEST RESULTS

For each location strain was plotted versus time for 15 minutes prior to loading, then for 15 minutes after applying an 80-kip load. Averaged strain differentials were obtained for comparison with numerical values.

Figures 18 through 21 are examples of strain versus time for the unloaded and loaded states. Figures 18 and 21 are typical plots, Figure 19 shows a maximum differential, and Figure 20 is indicative of locations away from the load where random oscillations dominate the strain gage output. The random oscillations were due to operational activity on the pier, sea action, mooring reactions, wind loading, and temperature changes.

Figures 22 through 24 are comparisons of measured and finite element model strain differentials, by location. The strain differential values were normalized. Discrepancies are due to random oscillations and different support conditions between the actual and finite element model.

SCALE MODEL TEST RESULTS

Service Load Response

Load-deflection response exhibited a positive nonlinear slope which decreased as the load increased. Load-deflection curves for a load applied in the center of a span are shown in Figures 25 through 27. Load-deflection curves for loads at the free edge are shown in Figures 28 and 29, and for loads near the support edges in Figures 30 and 31. Lateral deflection distribution about a center load point is depicted in Figure 32. Strain readings recorded on both sides of the load point provided a direct measurement of moment distribution. The lateral variation of the principal bending moment is shown in Figure 33 for a center load. Moment magnitude exhibited a sharp decay away from the load location. A more detailed normalized lateral load distribution from two test load levels, finite element model results and Pucher's approach (Ref 7), is provided in Figure 34 for a center patch load on span 2. If Hooke's Law applies and stresses and moments are linearly related, then the normalized lateral distributions of strain, moment, and influence factors should coincide. Similar distribution curves were derived for a load at center of spans 3 and 5 (Figures 35 and 36), and for loads at the edge of spans 3 and 5 (Figures 37 and 38). Measured distribution for loads at support edges are reported in Figures 39 and 40.

Failure Modes

The failure mode in all load locations was punching shear, complemented by diagonal cracking near the supports for the load points near the free edge of the slab. Midspan ultimate loads were in excess of 120 kips. For an effective slab depth, d, equal to 4-3/16 inches, this

translates to an ultimate shear stress of 6.8 to 7.6 times $\sqrt{f'_c}$ for an 8-inch by 8-inch patch load print, away from the slab edges. Ultimate loads (and ultimate shear stresses) were:

127 kips (7.2 $\sqrt{f'_c}$) for span 2 at midspan (D15)
121 kips (6.8 $\sqrt{f'_c}$) for span 3 at midspan (D1)
130 kips (7.3 $\sqrt{f'_c}$) for span 5 at midspan (D4)

110 kips (7.6 $\sqrt{f'_c}$) for span 1 at edge of support (D18)
121 kips (6.8 $\sqrt{f'_c}$) for span 4 at edge of support (D3)

69 kips (3.9 $\sqrt{f'_c}$) for span 3 at edge of span (D5)
70 kips (4.0 $\sqrt{f'_c}$) for span 5 at edge of span (D17)

A close view of the punching shear failure for the center of span 5 (D4) is shown in Figures 41 and 42. The punching shear crack on the top surface matched the footprint of the square steel-plywood pad and conically propagated into the slab at an angle of approximately 45 degrees. Figure 43 is a typical view of the crack pattern on the deck bottom. Failure at the edge of span 5 (D17) with diagonal tension cracks near the supports is depicted in Figure 44.

Concrete strain failure did not exceed 2,400 microstrain and steel strain did not exceed 1,800. Failure deflections were less than 0.38 inches at the point of load.

Strain gage readings were less than 5 percent error. LDT error was less than 2 percent. Errors in the load measurements were less than 5 percent.

Effective Width Calculation

A load distribution factor may be calculated from the distribution of internal moments determined from the tests, finite element analyses, and influence surfaces of Reference 7. The sum of the internal moments or the total area under the internal moment distribution curve is equivalent to the externally applied moment due to the concentrated load. Assuming the plate material is isotropic and homogeneous and follows Hooke's law, the internal moments are proportional to the internal strains. Thus, the effective width, E, is equal to the ratio of the total area under the internal force curve to the maximum internal force, the internal force being moment, strain, or influence factor. The distribution factor is the reciprocal of the effective width.

Applying laws of similitude, the effective widths corresponding to the prototype will be threefold of those found for the model. Similarly, for any other span size, if all dimensions (including patch size) increase simultaneously, E will increase proportionally. Hence a plot of E versus clear span would yield a straight line through the origin. This is shown in Figures 45 to 48. On the other hand, if the patch load size is kept constant, and all other dimensions are varied proportionally, the resulting curve would originate with an effective width equal

to the patch size and extend linearly toward the value of E for a point load case of an infinitely large span. This indicates the importance of considering point loads in the analysis.

The effective width relationship for midspan patch loads (e.g., on spans 2, 3 and 5) is shown in Figures 45 and 46 as a function of clear span width. Effective widths were obtained for test values, for Pucher's approach, and for the finite element analyses. Since point loads would yield lower, more conservative effective widths, they were also considered whenever possible. In the numerical analyses the use of uncracked section properties also yielded more conservative effective widths.

Effective widths were also calculated at the midspan edge: interior span (Figure 47) and exterior span (Figure 48). Results from all three approaches are displayed.

Crack Patterns

Cracks on the deck top surface for a midspan load formed almost concentric circles around the load point (Figure 49). On the deck bottom surface, all cracks radiated from the load point except for those formed on the last cycle, which corresponded to the intersection of the conical punching shear surface with the deck bottom surface (Figure 50). These crack patterns closely match the ones reported in Reference 3.

DISCUSSION OF SCALE MODEL RESULTS

Load-Deflection Curves

For a given load range and point of application, the load-deflection curves are very similar regardless of span. For example, midspan load-deflection plots at D1, D4 and D15 (spans 3, 5, and 2, respectively) could not be differentiated if they were superimposed (Figures 25, 26, 27). This increases the confidence in the experimental data, and indicates that endspan effects on deflection magnitude and distribution are small. Load deflections at the free edge of interior and exterior spans (Figures 28 and 29) are also similar while those for near support loading (Figures 30 and 31) coincide up to 100 kips.

Service Load Response

For midspan loads first flexural cracking was expected around 7 kips and yielding of the bottom flexural reinforcing at midspan was expected around 55 kips. First flexural cracking occurred between 10 and 15 kips. The load response of the deck upon reloading was linear up to at least 60 kips for centered loads (equivalent to 540 kips in prototype) which would represent conservative limits on service loading (Figures 25 to 27).

For the cases of midspan load on center span (Figures 34, 35, 36) and load on free edge (Figures 37 and 38), the normalized lateral distributions of strain, moment, and influence factors coincided. In all cases the finite element model with uncracked and cracked properties

provided a lower and upper bound, respectively, to the experimental distribution. Pucher's influence surface method also yielded very close agreement.

Due to decreased stiffness, load resistance decreased while deflection increased for loads applied near the slab free edge. Loads close to the edge displayed less lateral distribution resulting in larger moments under the load point. The load response at the edge of the slab was linear up to 45 kips (405 kips in prototype). There was no perceptible difference in load distribution into the exterior span (span 5) and into the middle span (span 3).

Failure Modes

Due to superior load distribution, neither flexural yield mechanisms in the span nor yielding along the supports occurred as was expected (at about 109 kips). Instead, all failures occurred from punching shear. This is consistent with experimental observations from Reference 3 and is a result of the arching mechanism of the short span-to-depth of the slab.

For tests away from the slab edges the experimental ultimate shear stress of 6.8 to 7.6 times $\sqrt{f'_c}$ is in excess of the design value of 4 $\sqrt{f'_c}$ allowed by the American Concrete Institute (ACI) (Ref 8).

For tests at slab free edges it should be noted that the test model did not have an edge beam which would have significantly increased shear and moment capacities.

A disturbing result of the tests is the ultimate failure mode. A punching shear failure occurs without warning, without large deflections, and without redistribution or redundancy. Even though the failure loads are far above the expected range, shear failure is very undesirable. An increase in deck depth without a commensurate increase in flexural capacity will lessen the likelihood of a shear failure resulting in a more redundant and desirable flexural failure mode.

Analytical Model Factors Affecting Effective Width

The following parameter effects are noted in the analytical results:

1. Effect of Load Type - Point loads represent the most conservative case in analytical modeling in terms of lateral distribution.

2. Effect of Flexural Cracking and Orthotropy - The corresponding relatively high stiffness corresponding to uncracked concrete properties resulted in much lower lateral distribution. This provided a conservative lower bound for the effective width since service loads should always induce cracking. Effective width values with uncracked properties were consistently 20 percent lower than for cracked properties.

3. Effect of Boundary Conditions (pile supports) - Pile cap bottoms are restrained by the bending stiffness of the piles which is relatively small compared to the deck. If the pile caps were allowed to displace laterally all effective width values would increase by 20 percent.

4. Effect of Transverse Reinforcement - In order to obtain proper lateral distribution, a minimum amount of transverse steel must be provided. AASHTO provides requirements for transverse steel under 1.3.2(E) Distribution Reinforcement. For main reinforcement parallel to traffic, the amount is the percentage of the main reinforcement required for positive moment given by:

Percentage = $100/\sqrt{S}$ (maximum 50 percent, with S in feet).

In order to evaluate the direct effect on effective width, a center patch load was applied on span 3 for three different amounts of transverse reinforcement of the finite element model: (a) 50 percent, representing the maximum allowed, and the amount used in the test, (b) 25 percent, representing the required amount for a 15-foot clear span, and (c) 7 percent, representing the minimum allowed by temperature and shrinkage considerations. The effective width only decreased from 51 inches in case (a) to 50 inches in case (c). The required amount of transverse steel therefore appears conservative at first, but further investigation is required to observe the effects on ultimate capacity.

Effective Width and Slab Design

Effective widths were calculated for the values obtained from tests, Pucher's approach, and finite element analyses. All sources indicate the current practice of using AASHTO procedures is very conservative for patch loads on Navy piers. More efficient load distribution and the high probability of shear failure mode suggests a more liberal design relationship for effective width should be employed for decks subjected to patch loads, such as:

$E = 0.5\ S \qquad E < 10$ feet.

which is about two times more liberal that AASHTO but still conservative compared to analytical and experimental relationships.

For loads away from the edges, the more liberal value matches the most conservative case of point load, uncracked properties, and restrained pile caps. The limit of 10 feet reflects a safe effective width for the Navy pier prototype modeled in this study according to both tests and the initial numerical parameter study. The above relationship provides up to 100 percent better distribution than allowed by AASHTO while being 50 percent lower than the patch load test results.

For a load at the edge of a support, experimental effective width values are more conservative than the above relationship. Further, these load points (D18 and D3) are near the inflection points and do not have much moment to distribute.

For an edge load case, only the finite element analysis with uncracked properties is not conservative with respect to the above relationship. However, edge beams are required by AASHTO 1.3.2(D), which should be able to carry a moment of 0.08 P·S for continuous spans (0.1 P·S for simple span) where P is the applied concentrated force. An edge beam will then carry almost half the total moment due to P which is 0.17 P·S for continuous spans.

Deck parameters can be optimized to take advantage of the increase in effective width. The following two options should be considered:

1. The span length may be increased while maintaining cross-sectional properties similar to current designs. As a consequence, the number of piles can be reduced with considerable savings.

2. The moment capacity of the section may be reduced by reducing the steel area while maintaining depths and span lengths similar to current designs. The savings in steel weight and placement will also be substantial. Deflections due to moment will increase.

CONCLUSIONS

Parameter Study and Field Tests

For typical Navy piers, with spans ranging from 14 feet to 24 feet:

1. An effective width in excess of 10 feet was determined.

2. Effective width increases with increasing span.

3. Moving the patch load toward a support or a free edge decreases the effective width.

Pier Deck Model

Model tests and analyses of a prototype pier deck design revealed:

1. Cyclic testing at several load levels produced no signs of deterioration at working load levels.

2. Finite element predictions of deflection and moment distribution closely reproduced experimental data.

3. Finite element analyses, experiments, and influence surface analyses yielded almost identical lateral load distribution patterns and very similar effective widths values.

4. An effective width relationship, $E = 0.05\ S$ ($E < 10$ feet), is up to two times more liberal than AASHTO but still conservative with respect to all analytical models and experimental values.

5. For locations away from the slab edges, punching shear stress capacities were all above $6.8\sqrt{f'_c}$.

REFERENCES

1. American Association of State Highway and Transportation Officials. Standard specifications for highway bridges, Washington, DC, 1977.

2. I.K. Fang, C.K.T. Tsui, N.H. Burns, and R.E. Klingner. "Load capacity of isotropically reinforced, cast-in-place and precast panel bridge decks," Portland Cement Association Journal, Jul-Aug 1990.

3. Ontario Highway Bridge Design Code, Ontario Ministry of Transportation and Communications, 2nd Edition, 1983.

4. ABAM Engineers, Inc. Concentrated loads on haunched deck panels, Tacoma, WA, 1967.

5. Naval Facilities Engineering Command. Military Handbook 1025/1: Piers and Wharfs. Alexandria, VA, Oct 1987.

6. ADINA R&D Inc. ADINA: A finite element program for automatic dynamic incremental nonlinear analysis. Watertown, MA, Dec 1987.

7. Adolf Pucher. Influence surfaces of elastic plates. New York-Wien, Springer-Verlag, 1977.

8. American Concrete Institute. ACI 318-89: Building code requirements for reinforced concrete. Detroit, MI, 1989.

Table 1. Concrete Mix

Constituent	Amount
Type I Cement	658 lb/yd^3
Fly Ash	100 lb/yd^3
Water	350 lb/yd^3
3/8-Inch Gravel	1,080 lb/yd^3
Sand	1,740 lb/yd^3
Water Reducing Admixture (Sikament 86) Per Manufacturer	

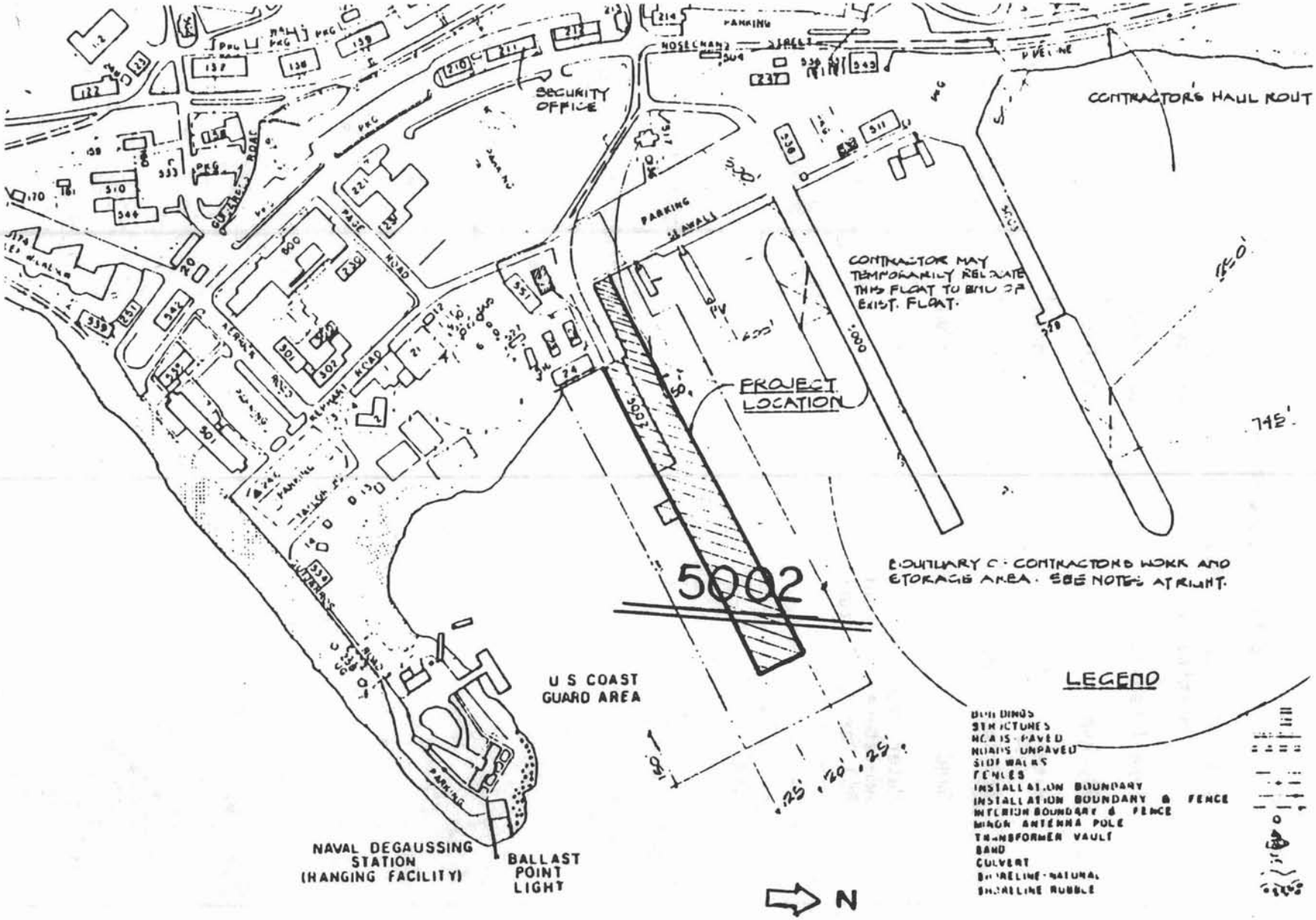

Figure 1. Pier 5002 located at Navy Submarine Base, San Diego, CA.

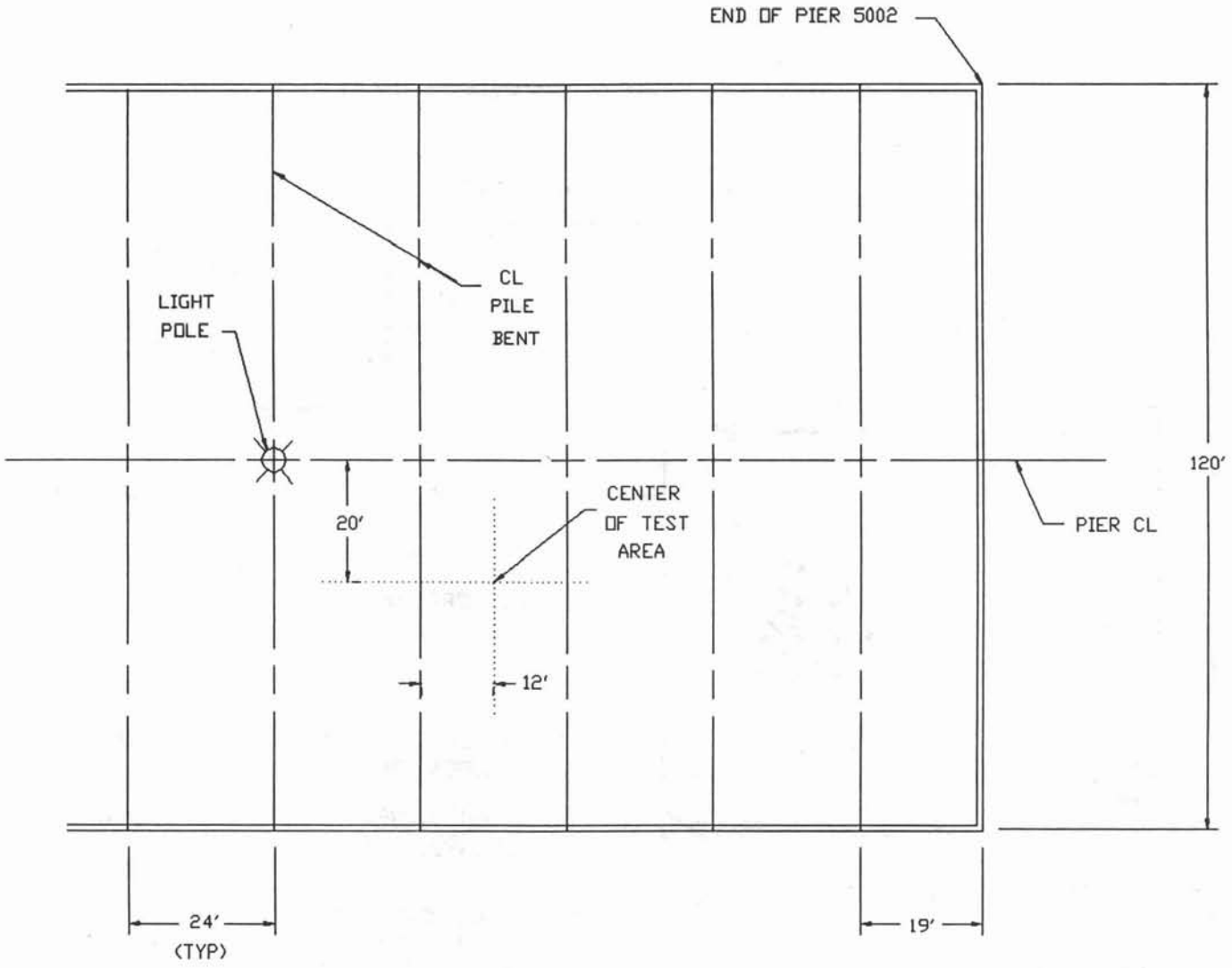

Figure 2. Test area at the end of Pier 5002.

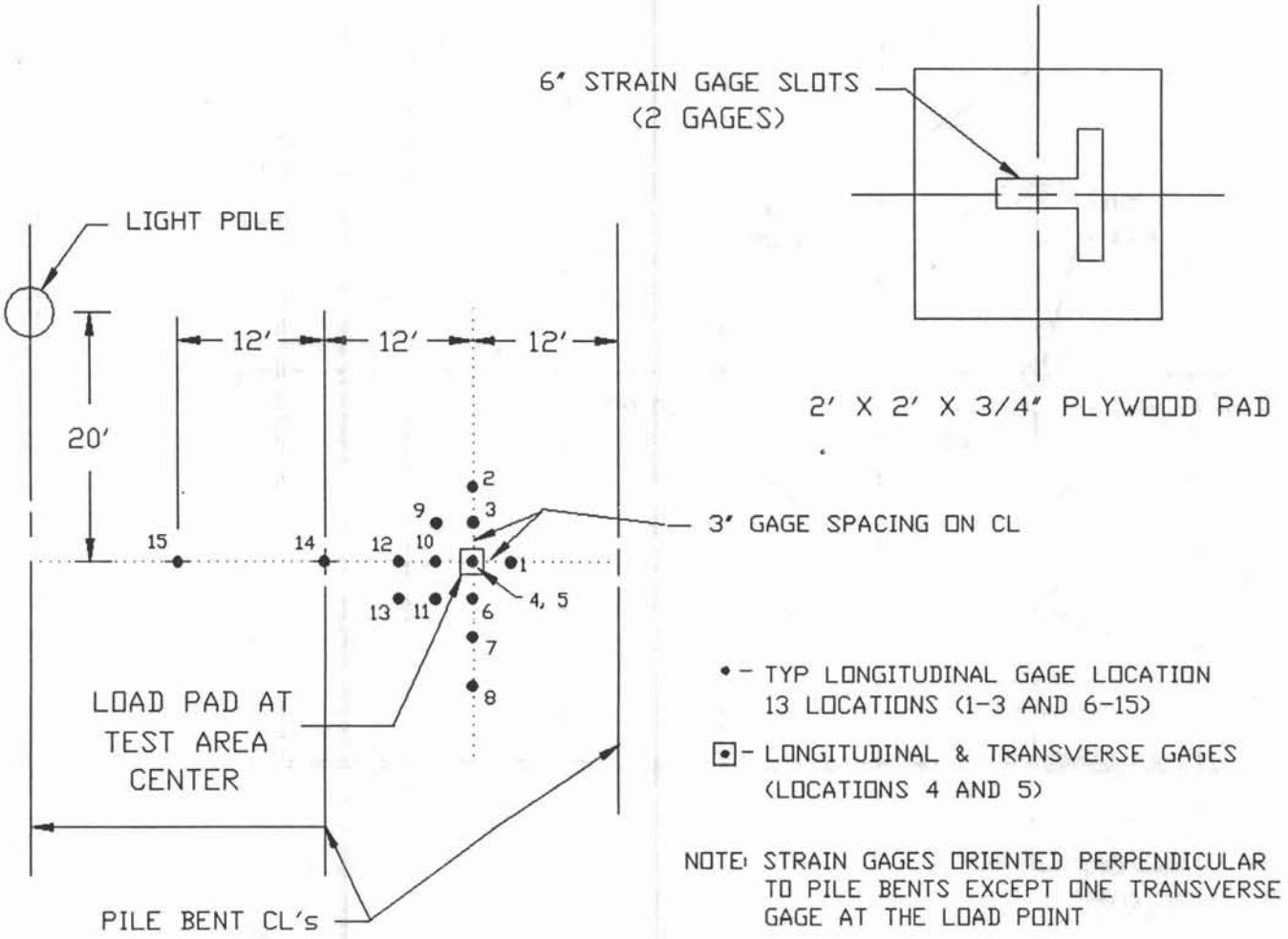

Figure 3. Stain gage locations at test site on Pier 5002.

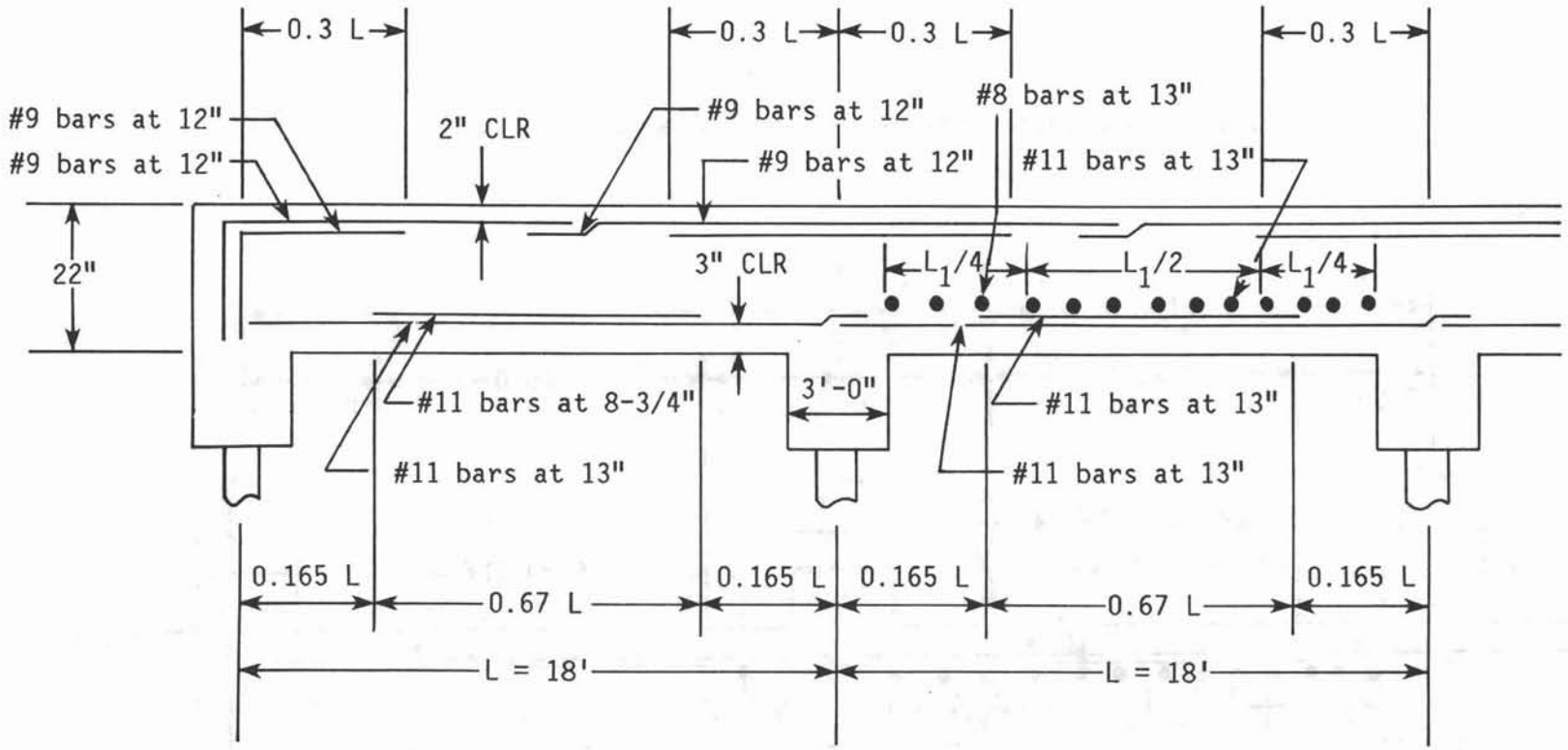

Figure 4. Prototype pier deck - AASHTO design.

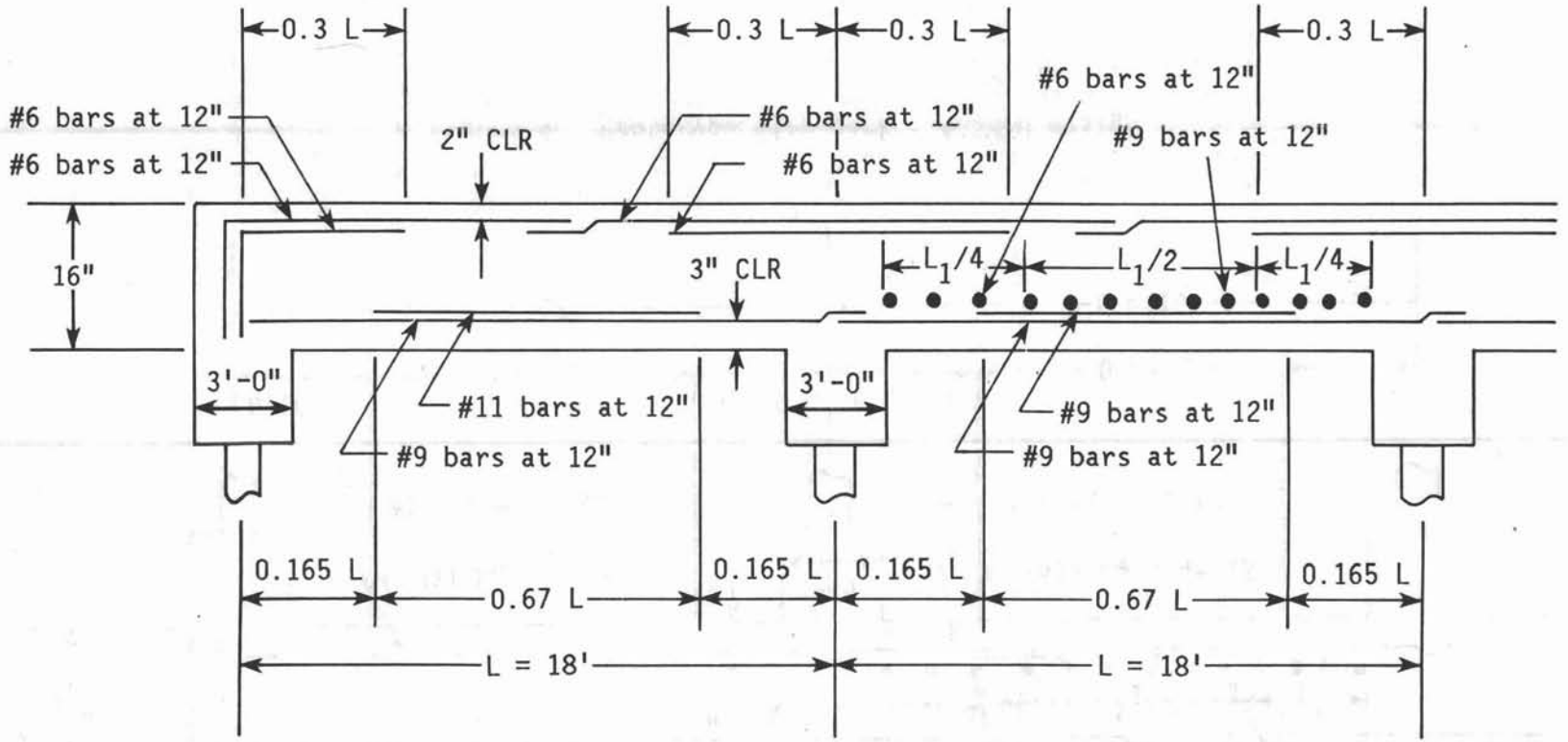

Figure 5. Prototype pier deck - 10-foot effective width design.

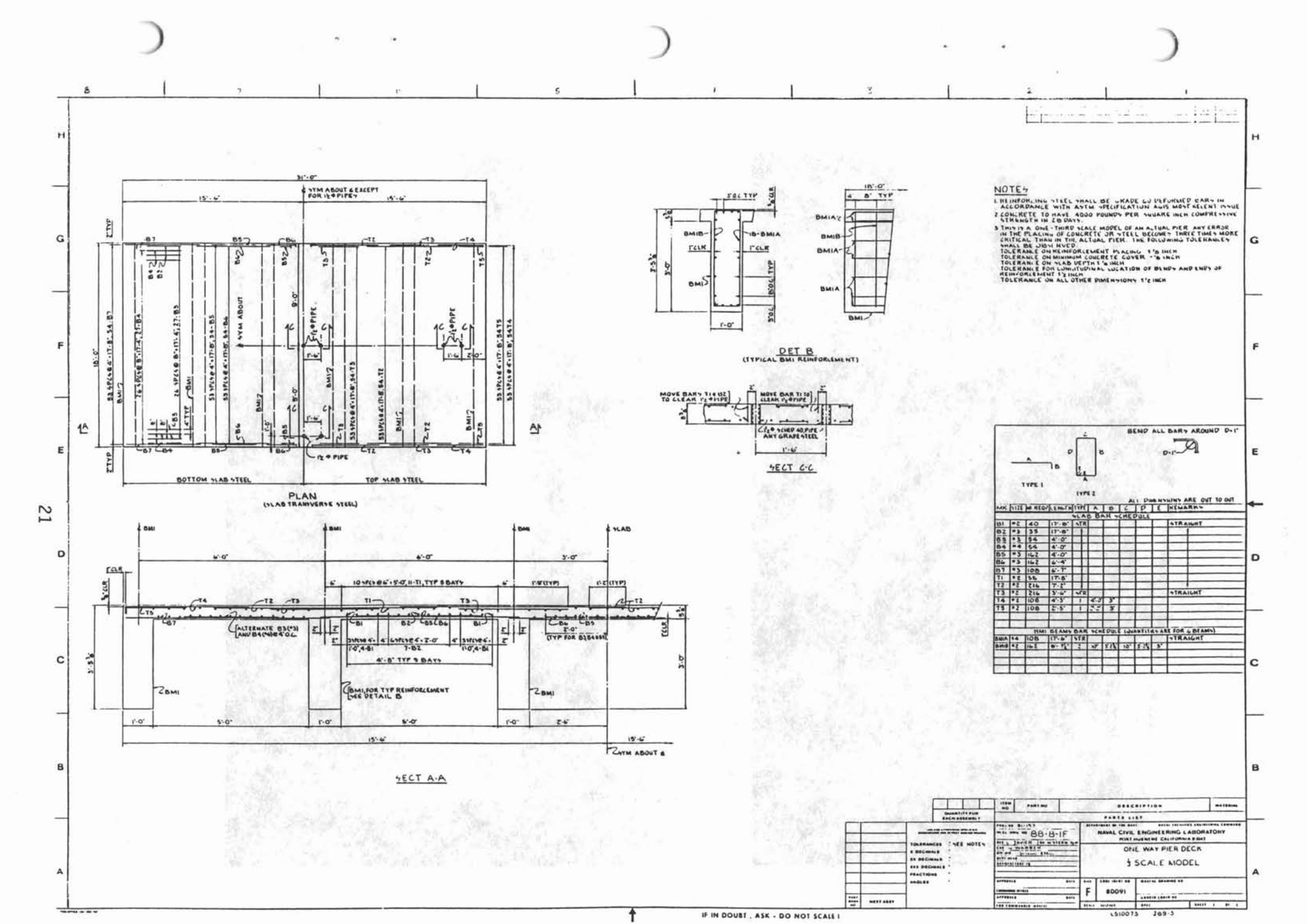

Figure 6. Construction drawings of pier deck scale model.

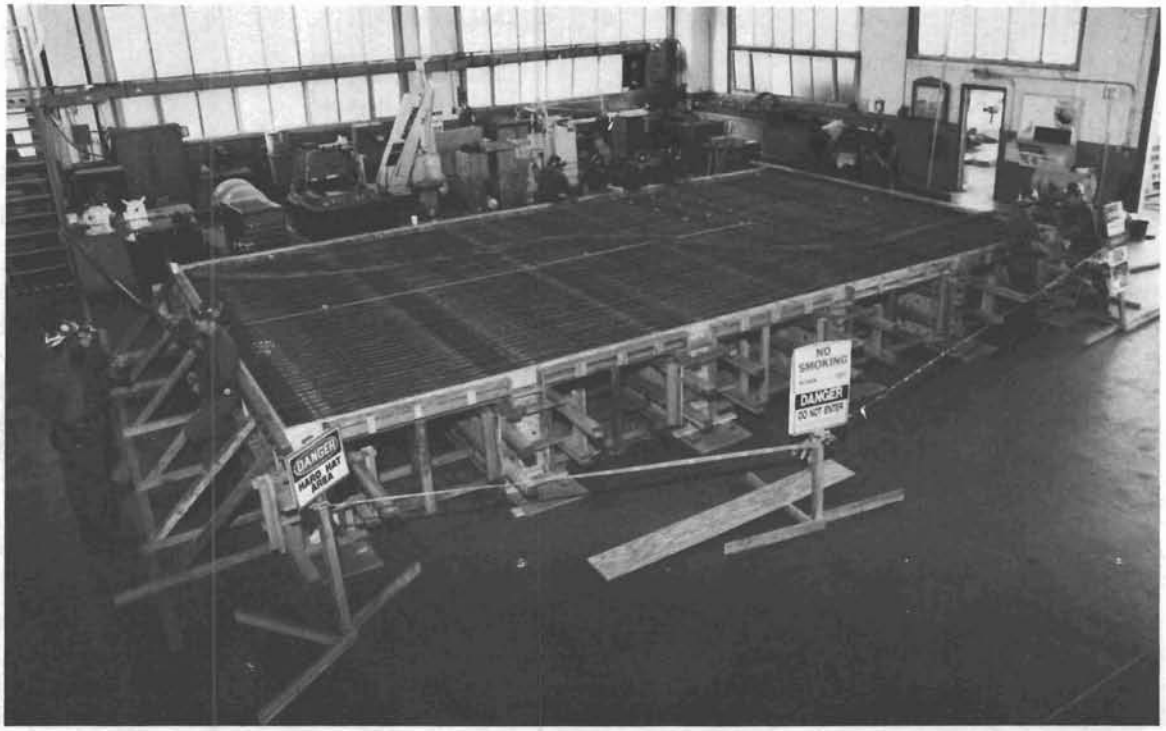

Figure 7. Pier deck model - reinforcing cage and formwork.

Figure 8. Completed pier deck scale model.

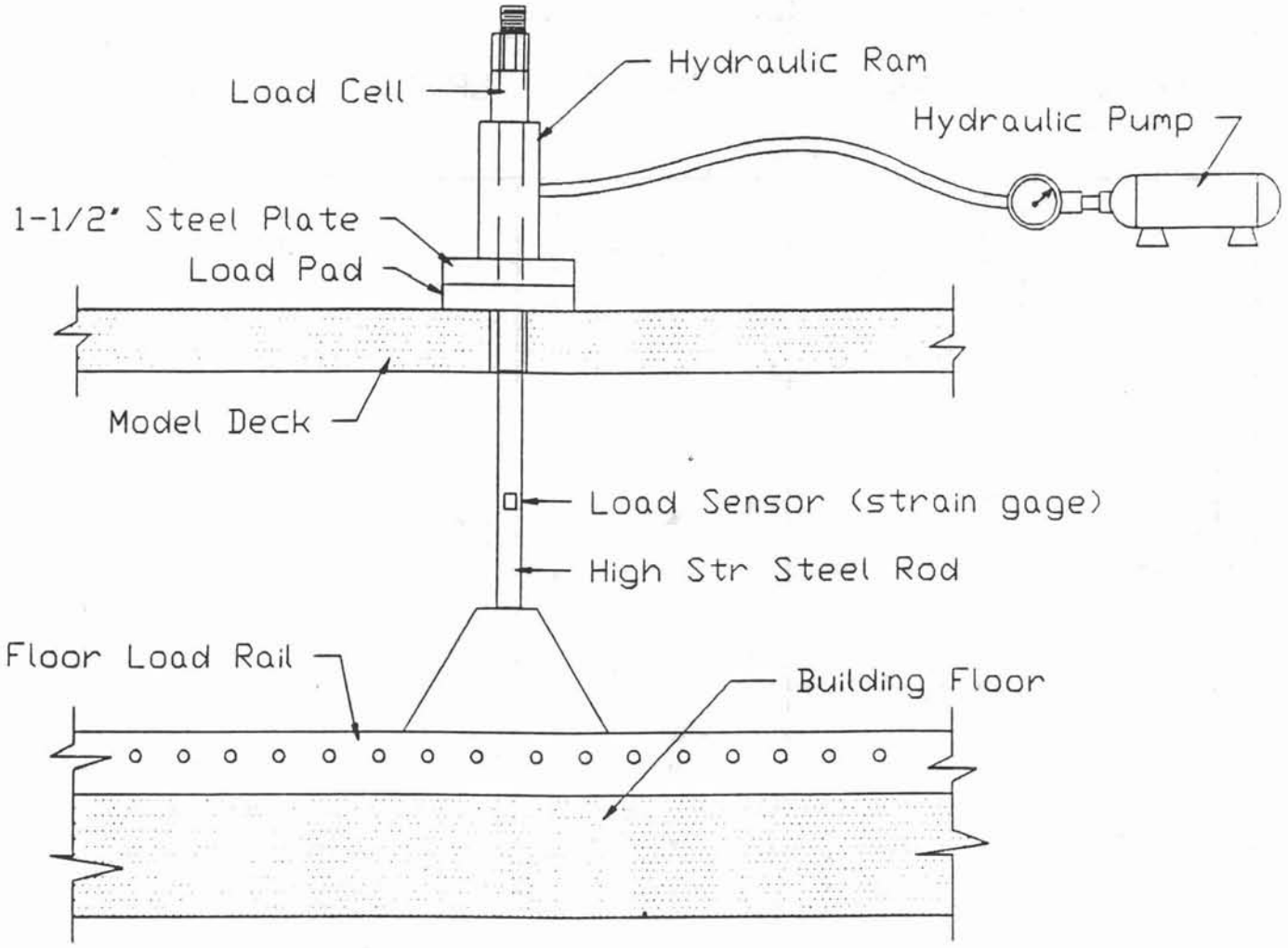

Figure 9. Schematic of loading apparatus.

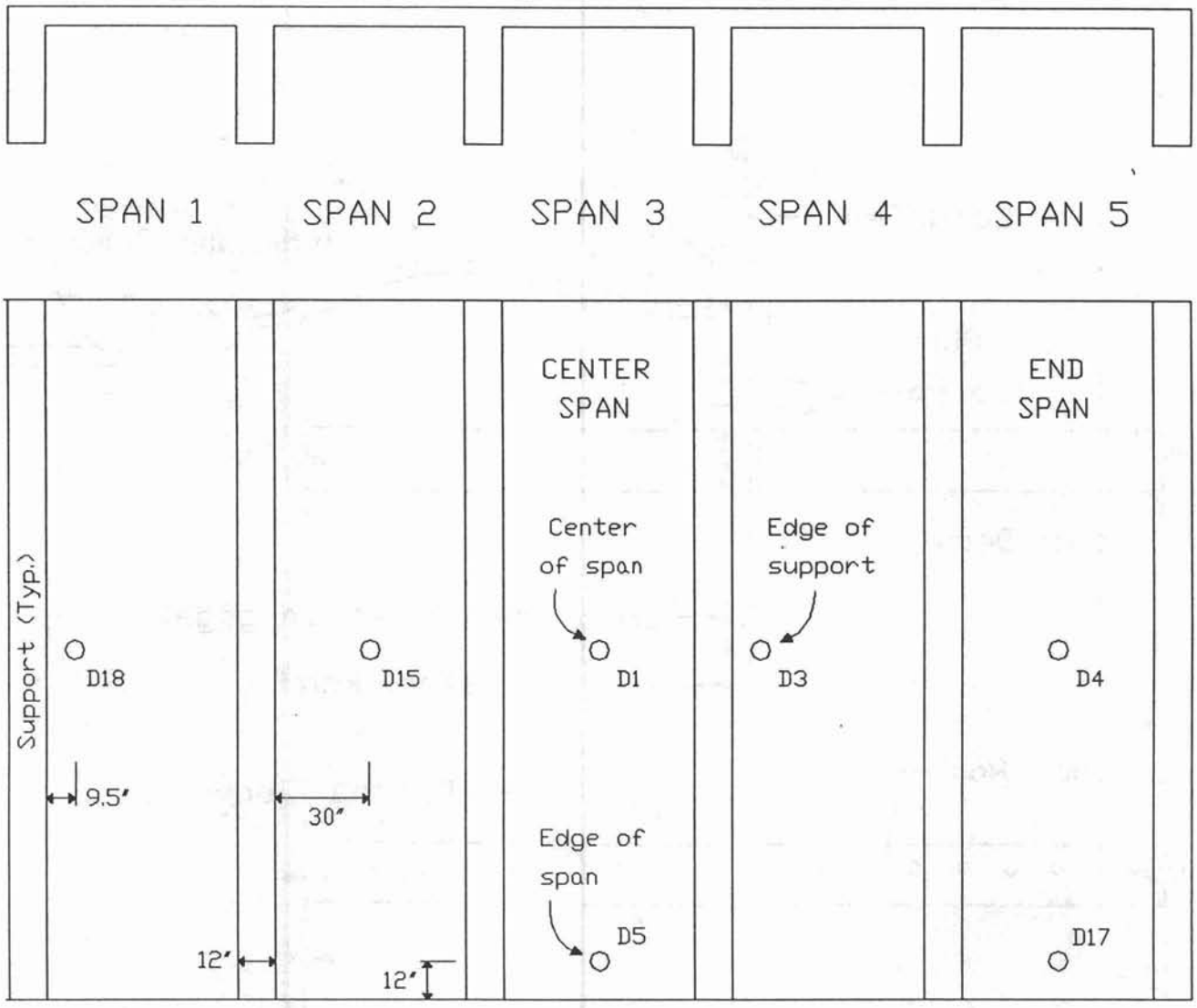

Figure 10. Pier deck model - load point locations.

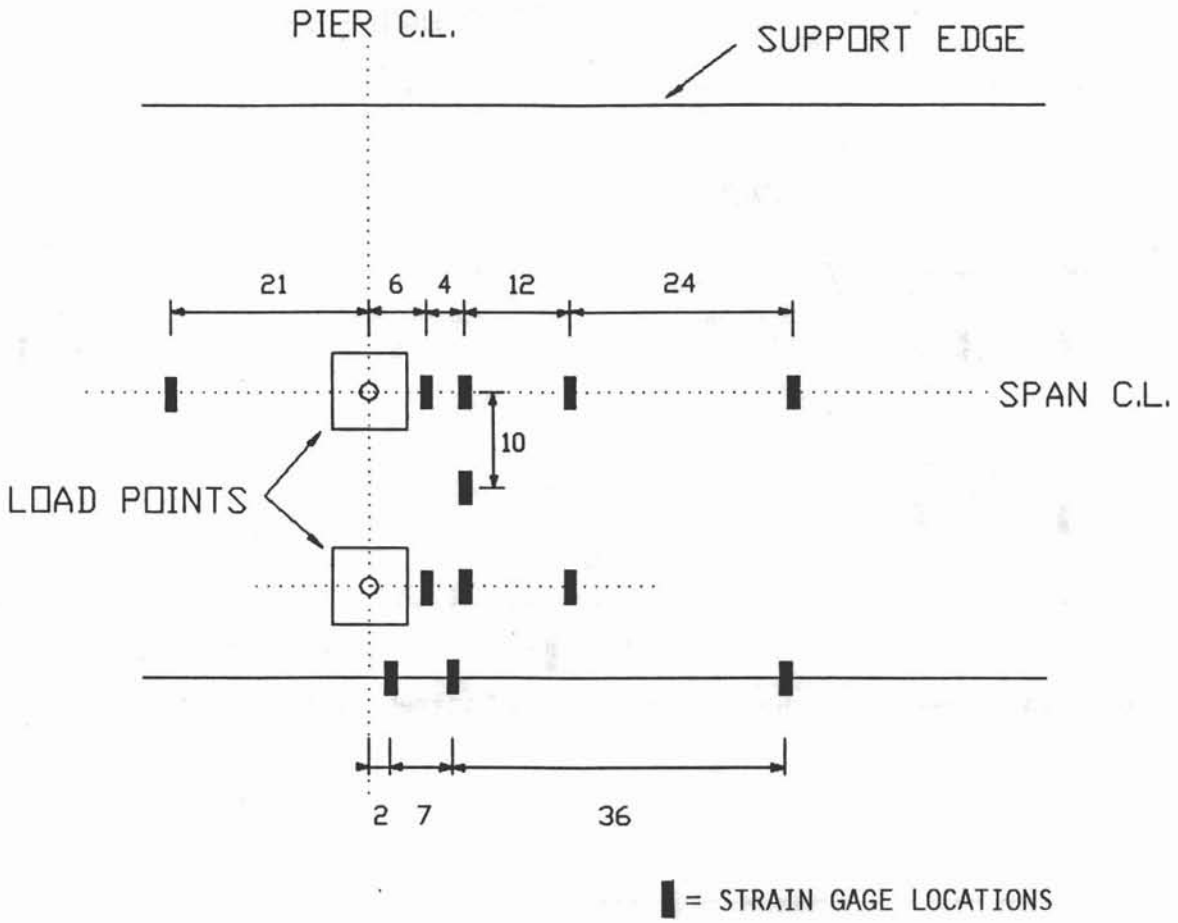

Figure 11. Pier deck model - typical strain gage locations.

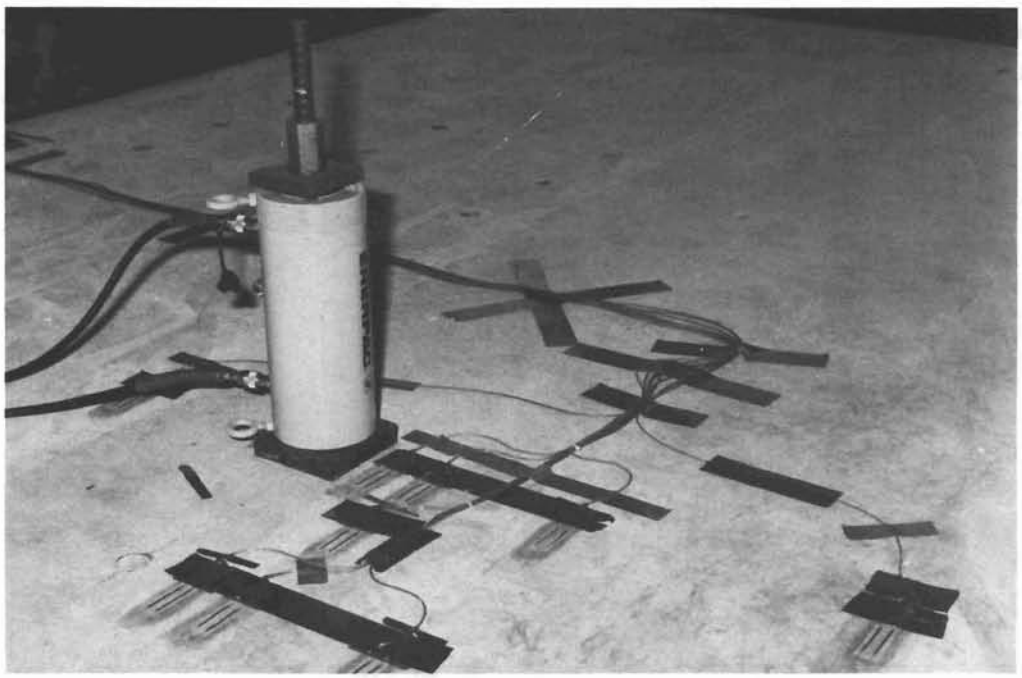

Figure 12. Strain gage locations for load point D1, span 3.

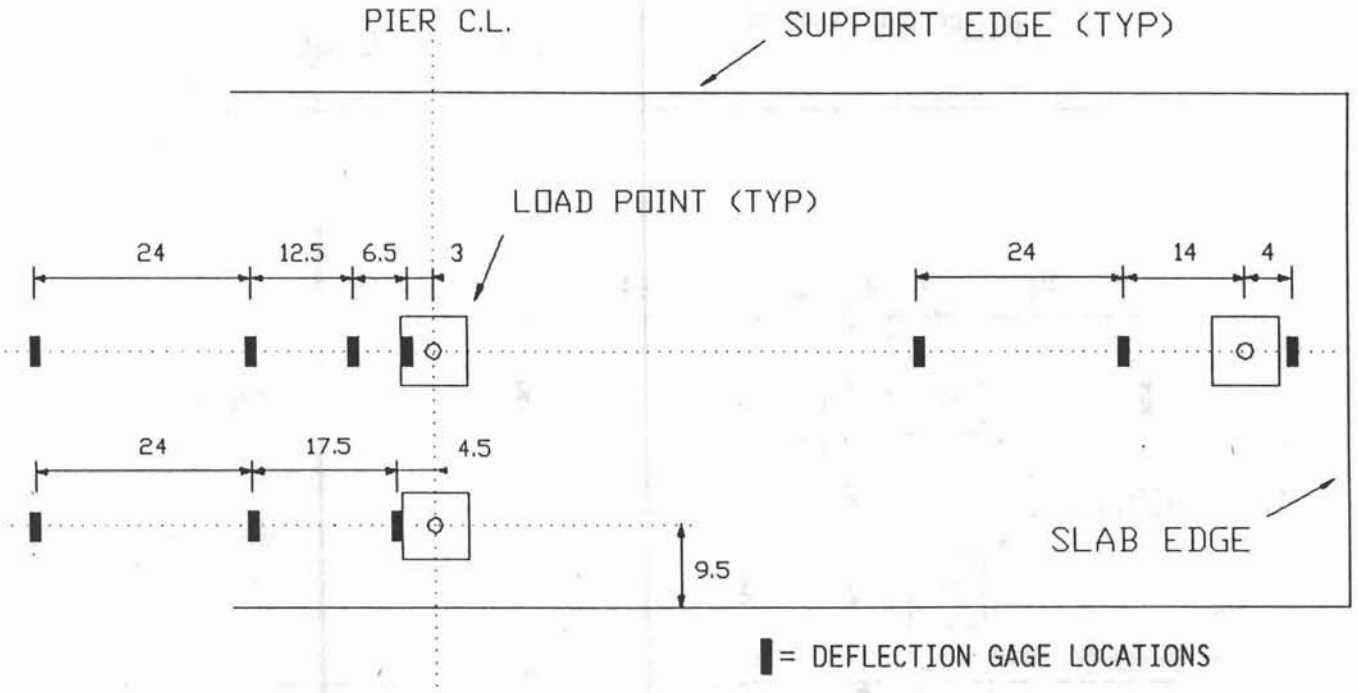

Figure 13. Pier deck model - typical displacement gage locations.

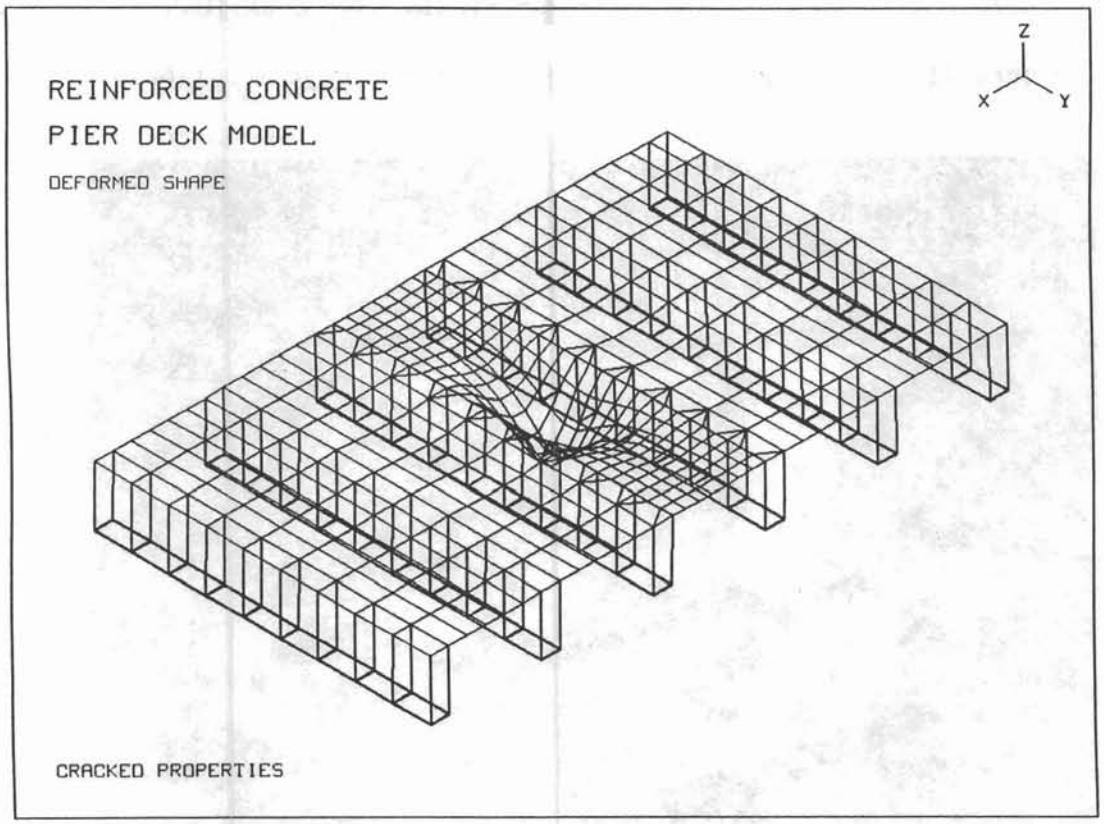

Figure 14. Pier deck model - deformed finite element mesh.

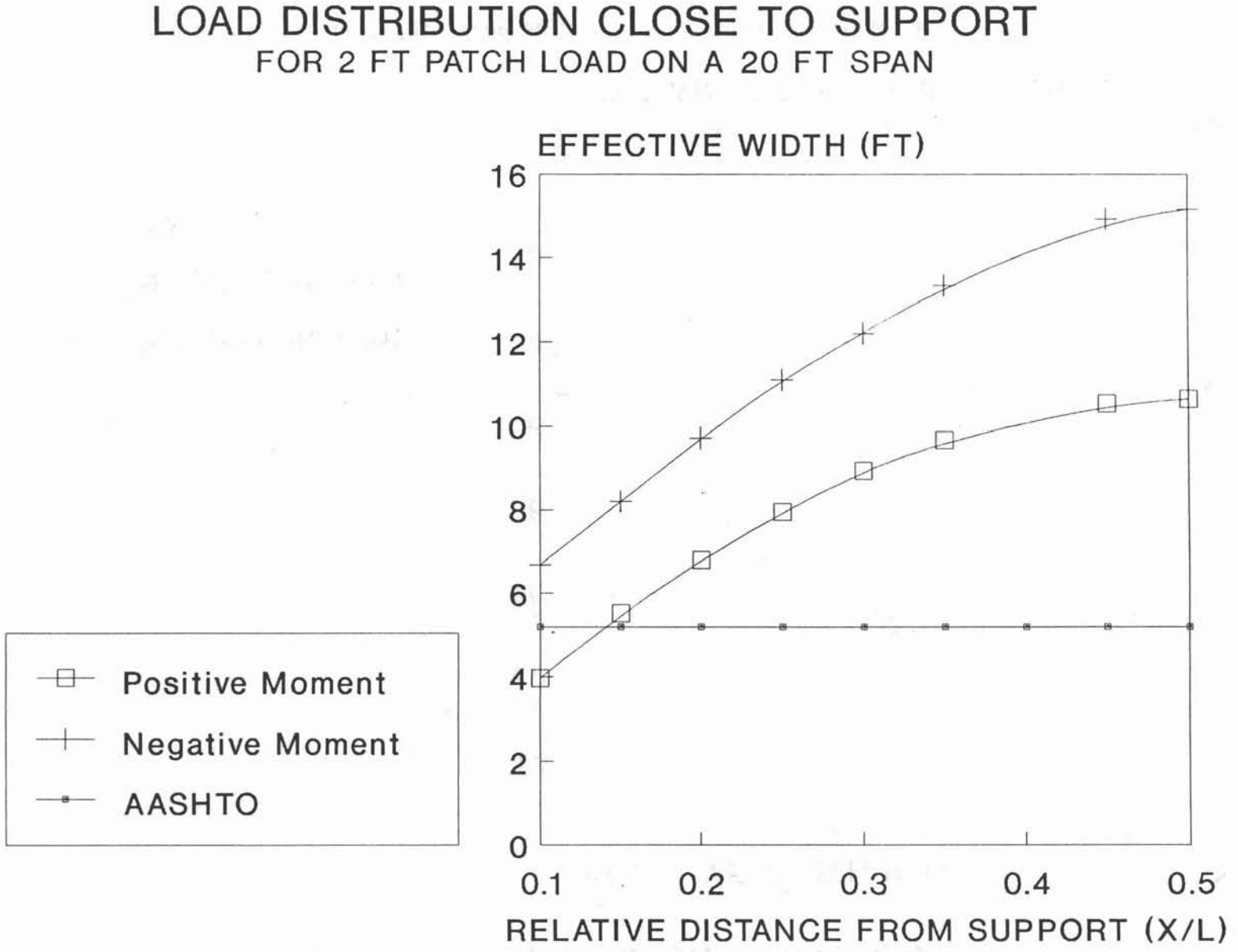

Figure 15. Effect of load position on load distribution.

LOAD DISTRIBUTION CLOSE TO FREE EDGE
FOR 2 FT PATCH LOAD ON A 20 FT SPAN

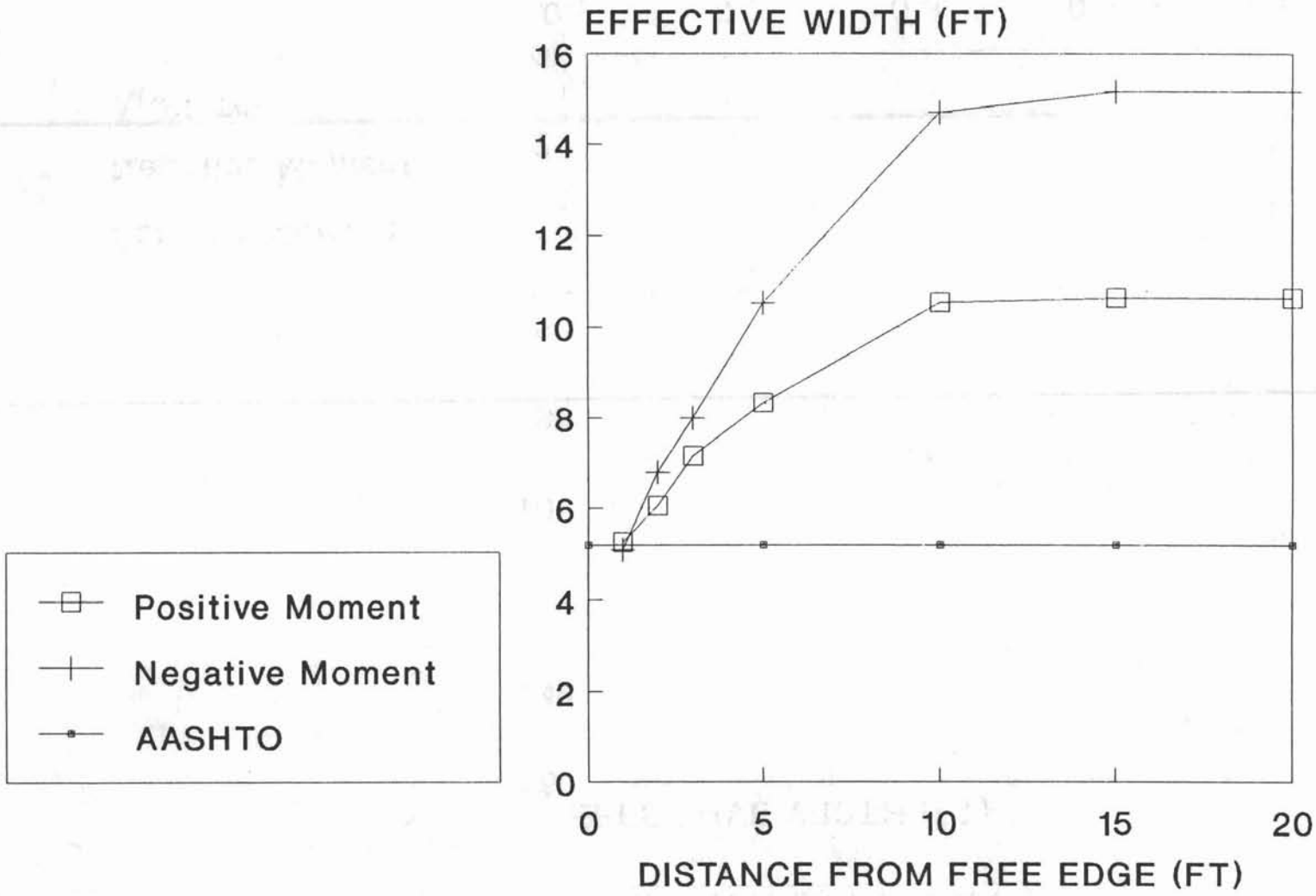

Figure 16. Free edge effect on load distribution.

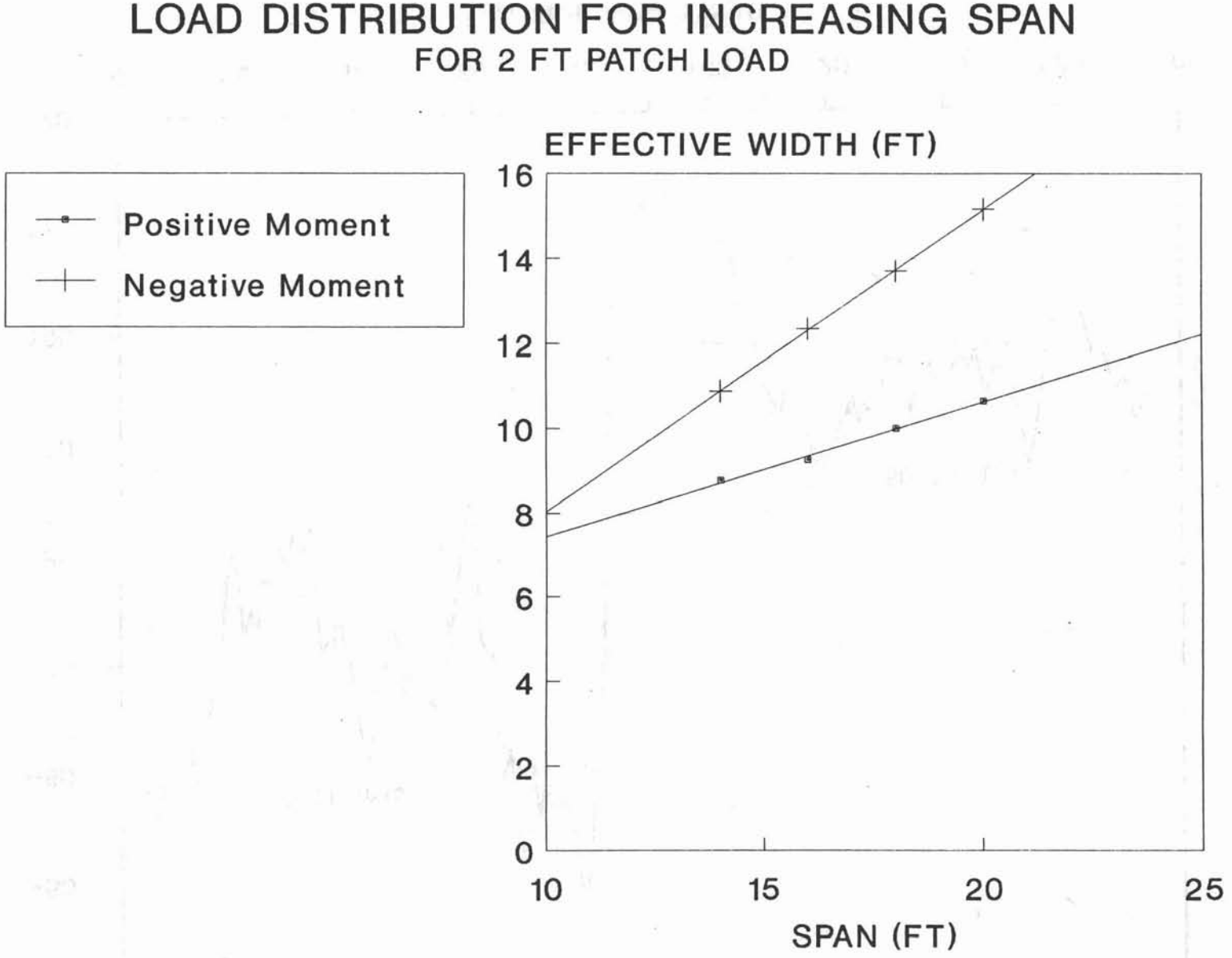

Figure 17. Span length effect on load distribution.

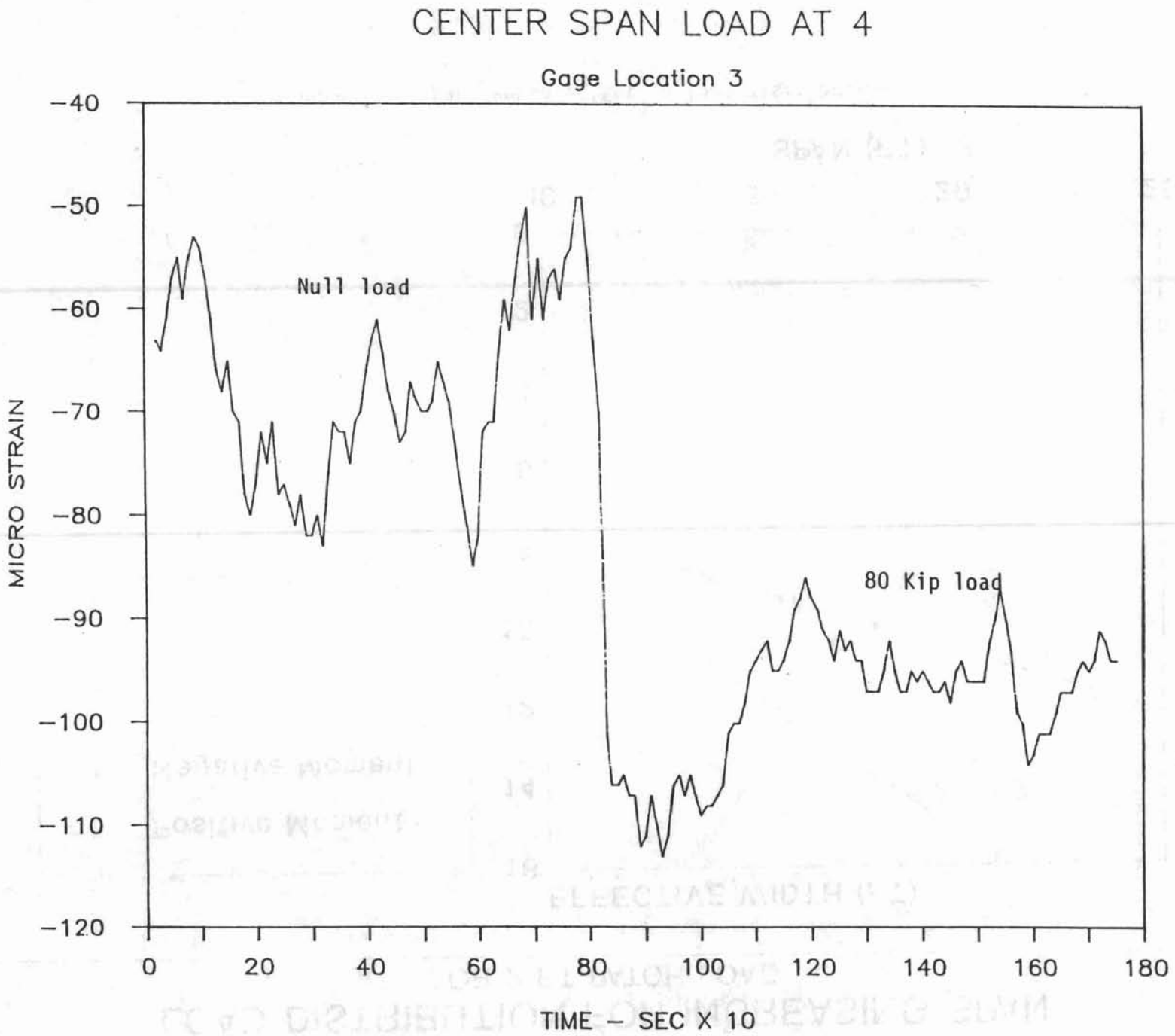

Figure 18. Strain differential near midspan load point.

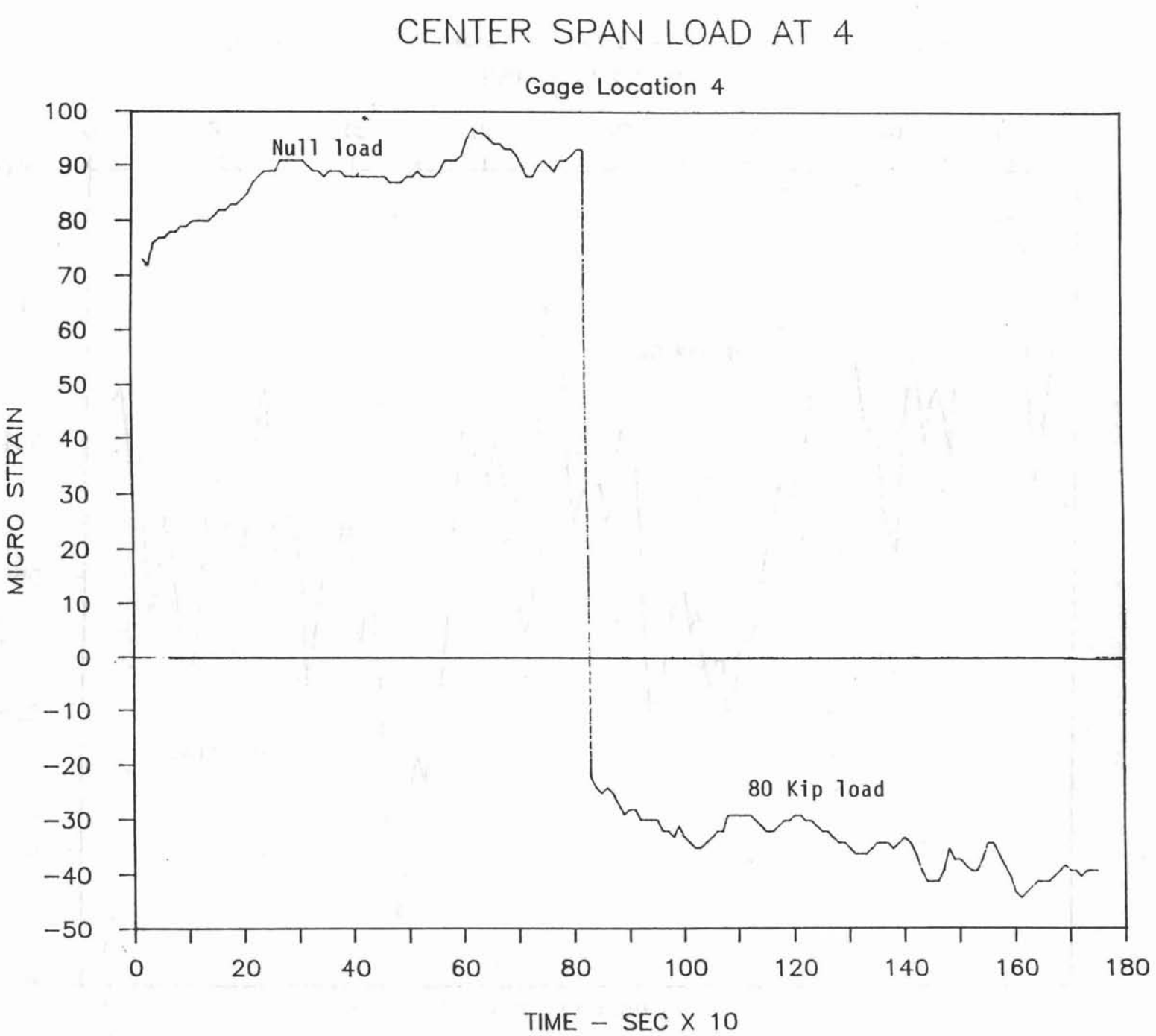

Figure 19. Strain differential at midspan load point.

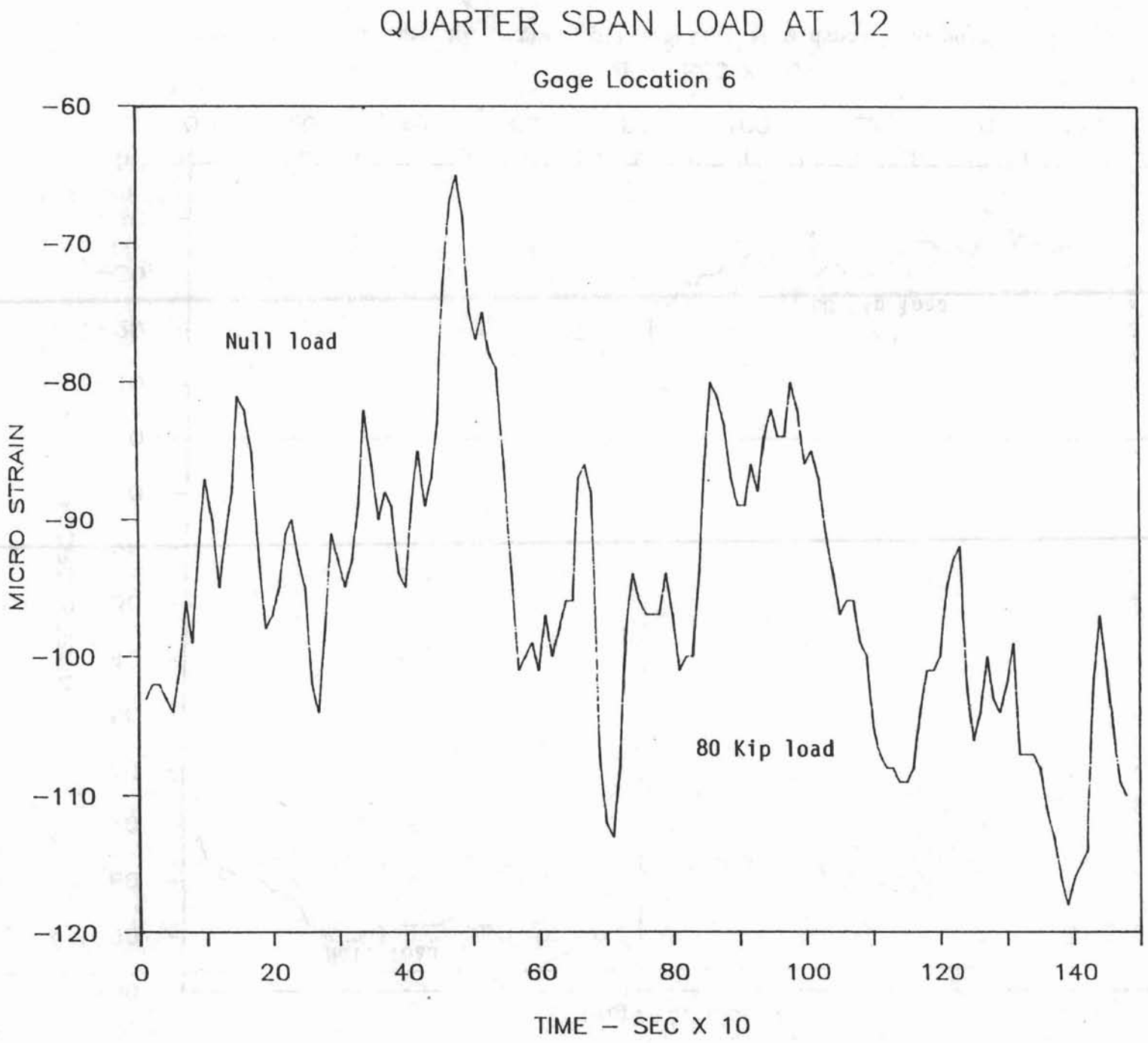

Figure 20. Strain variation away from quarterspan load point.

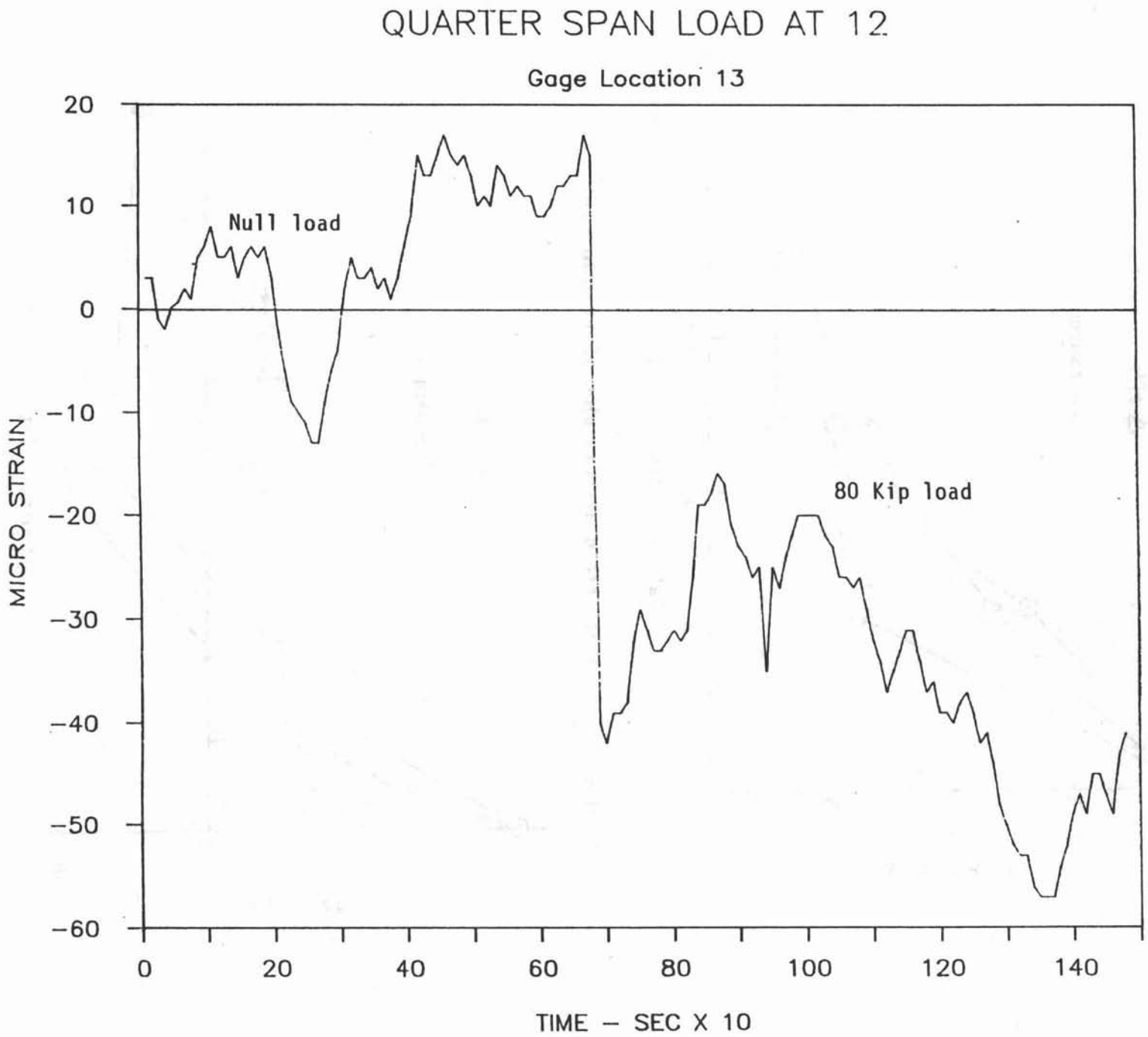

Figure 21. Strain differential near quarterspan load point.

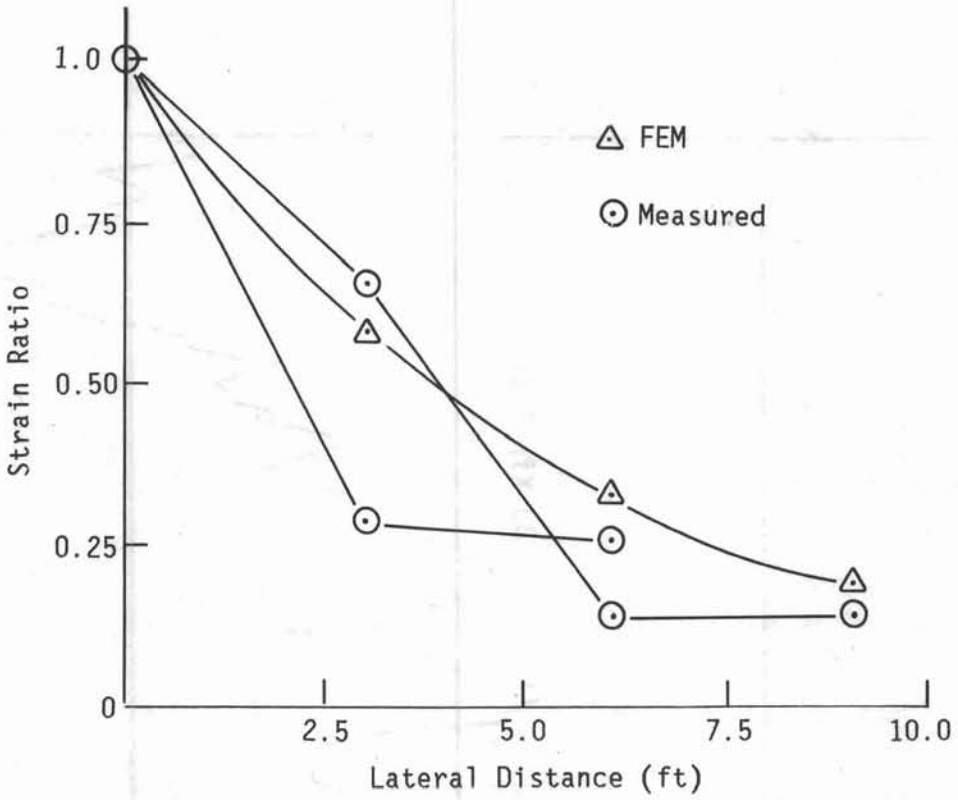

Figure 22. Lateral strain distribution of midspan load.

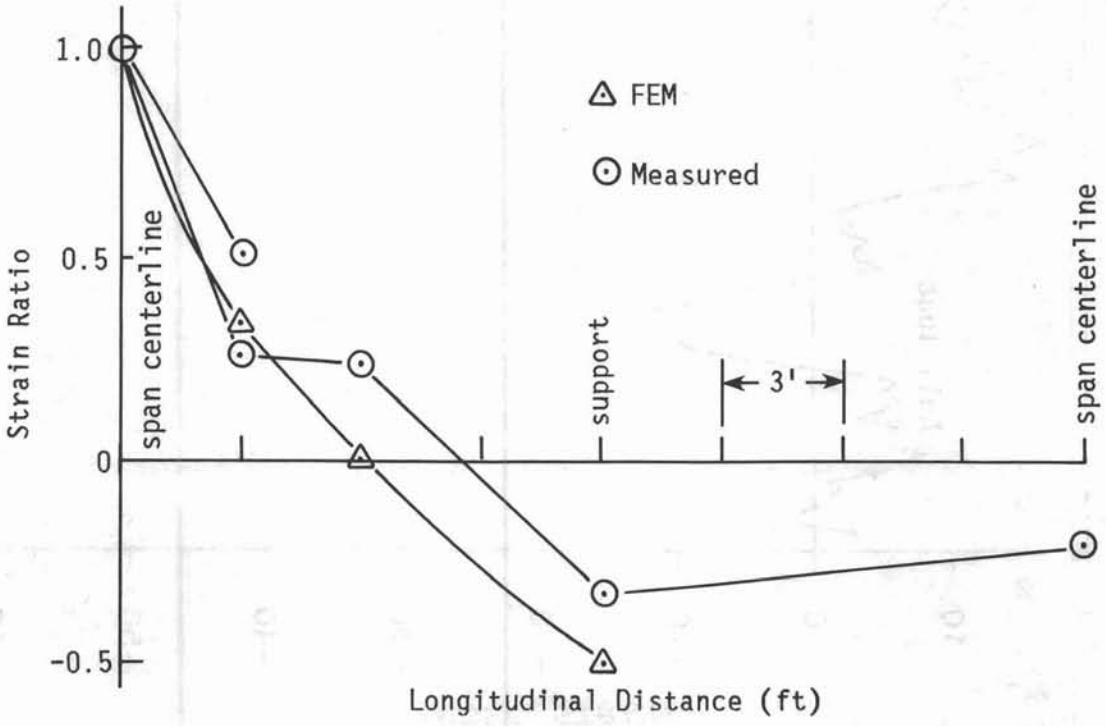

Figure 23. Longitudinal strain distribution of midspan load.

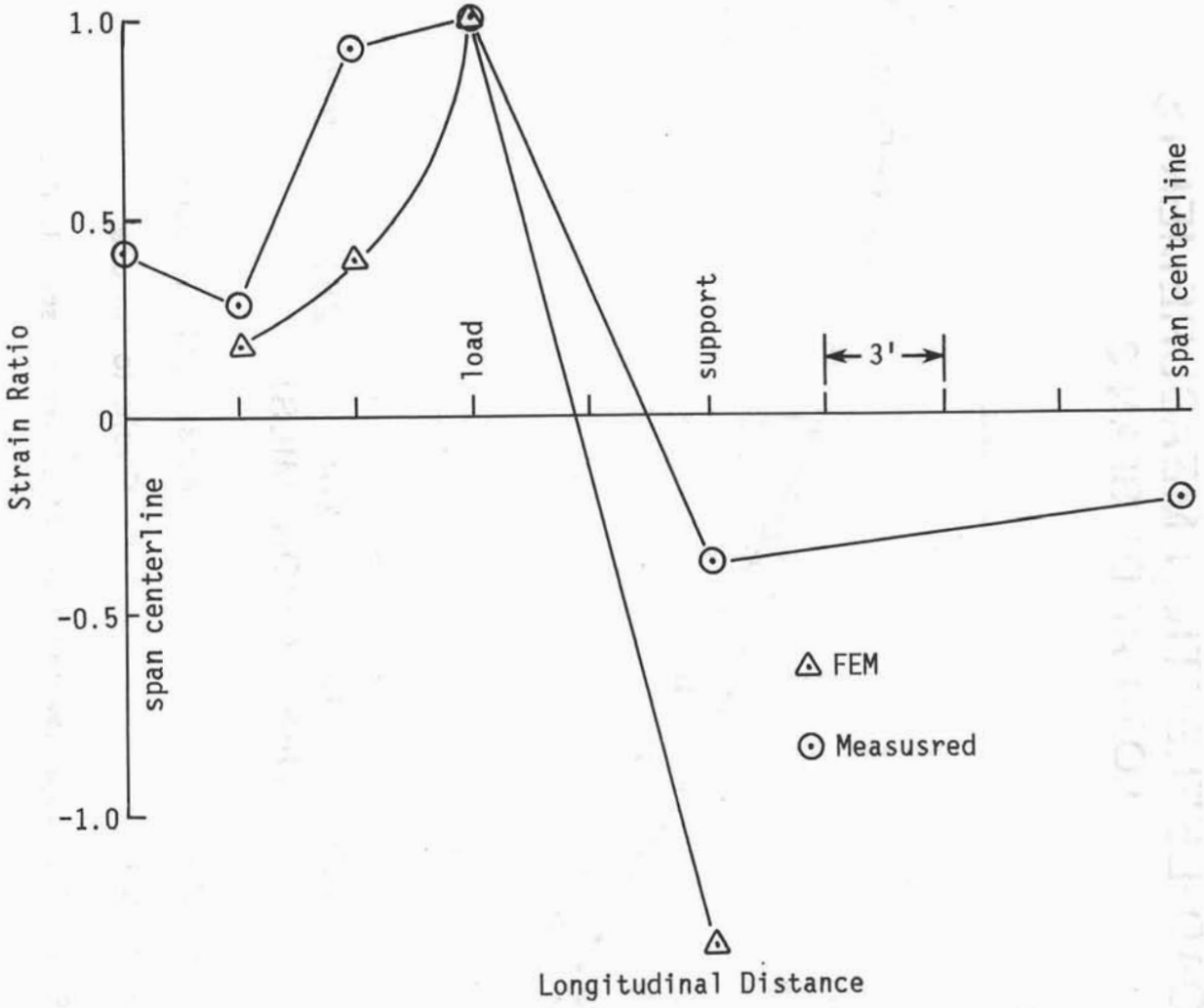

Figure 24. Longitudinal strain distribution of quarterspan load.

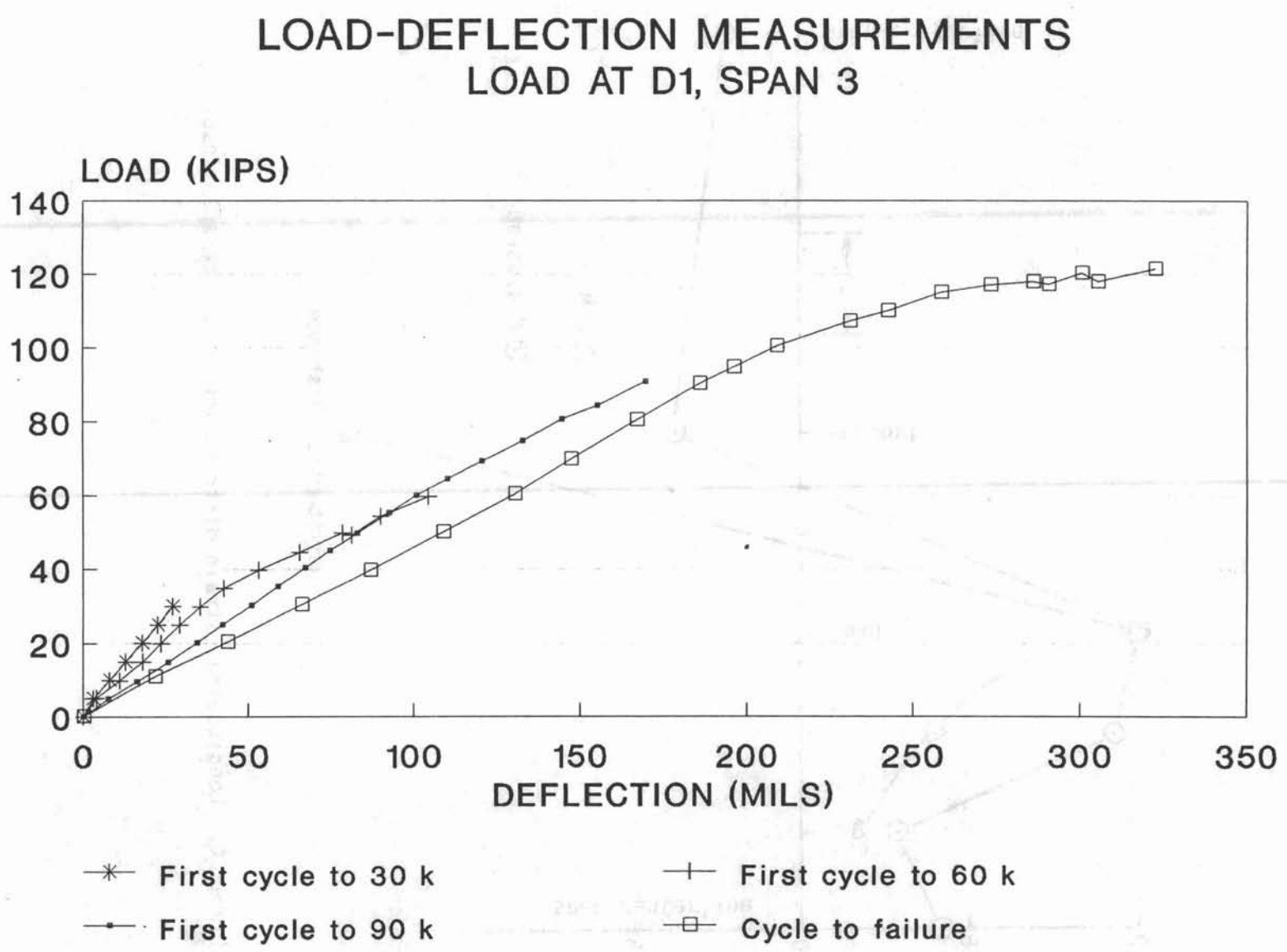

Figure 25. Experimental load-deflection at span 3, D1.

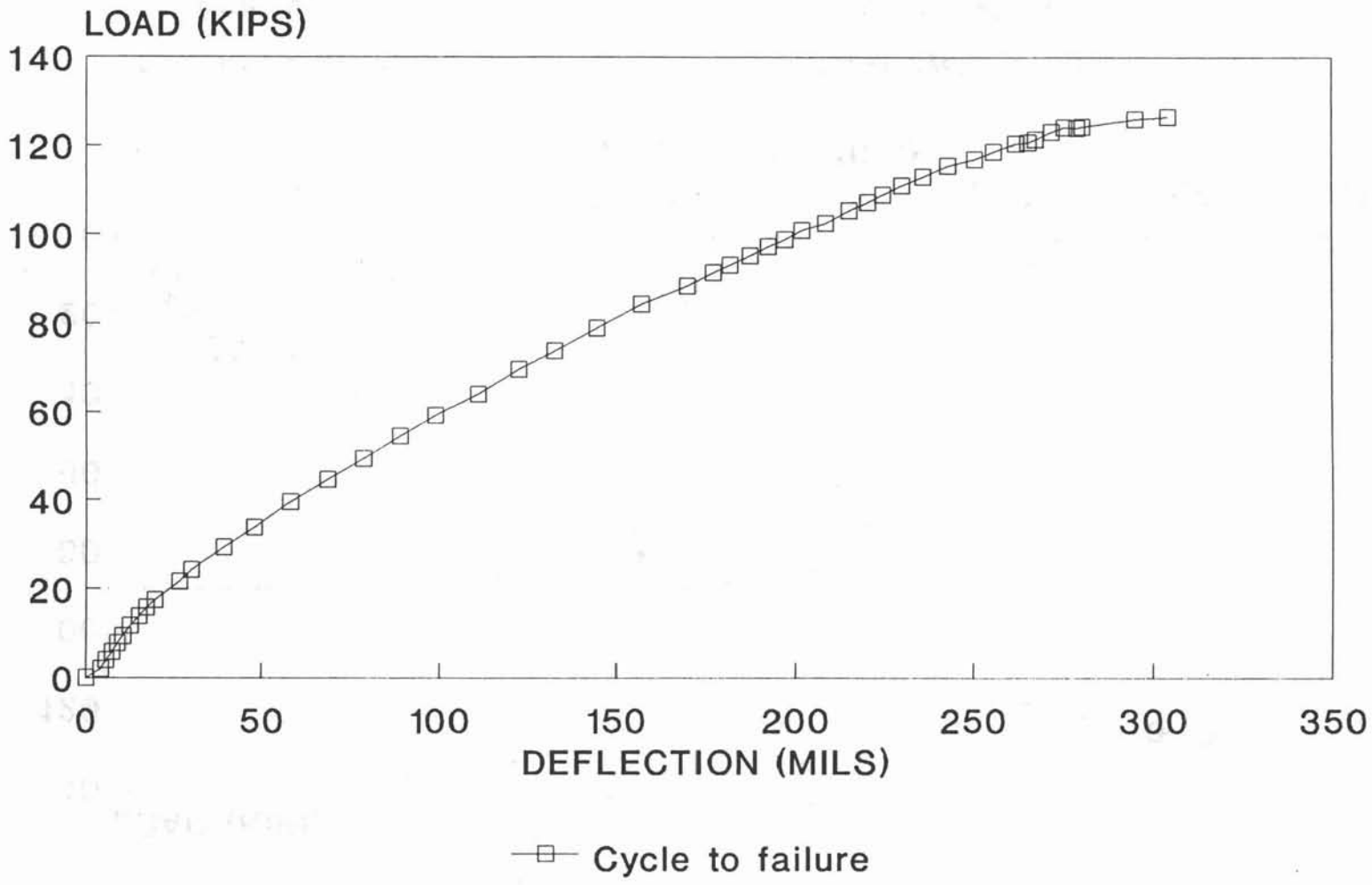

Figure 26. Experimental load-deflection at span 2, D15.

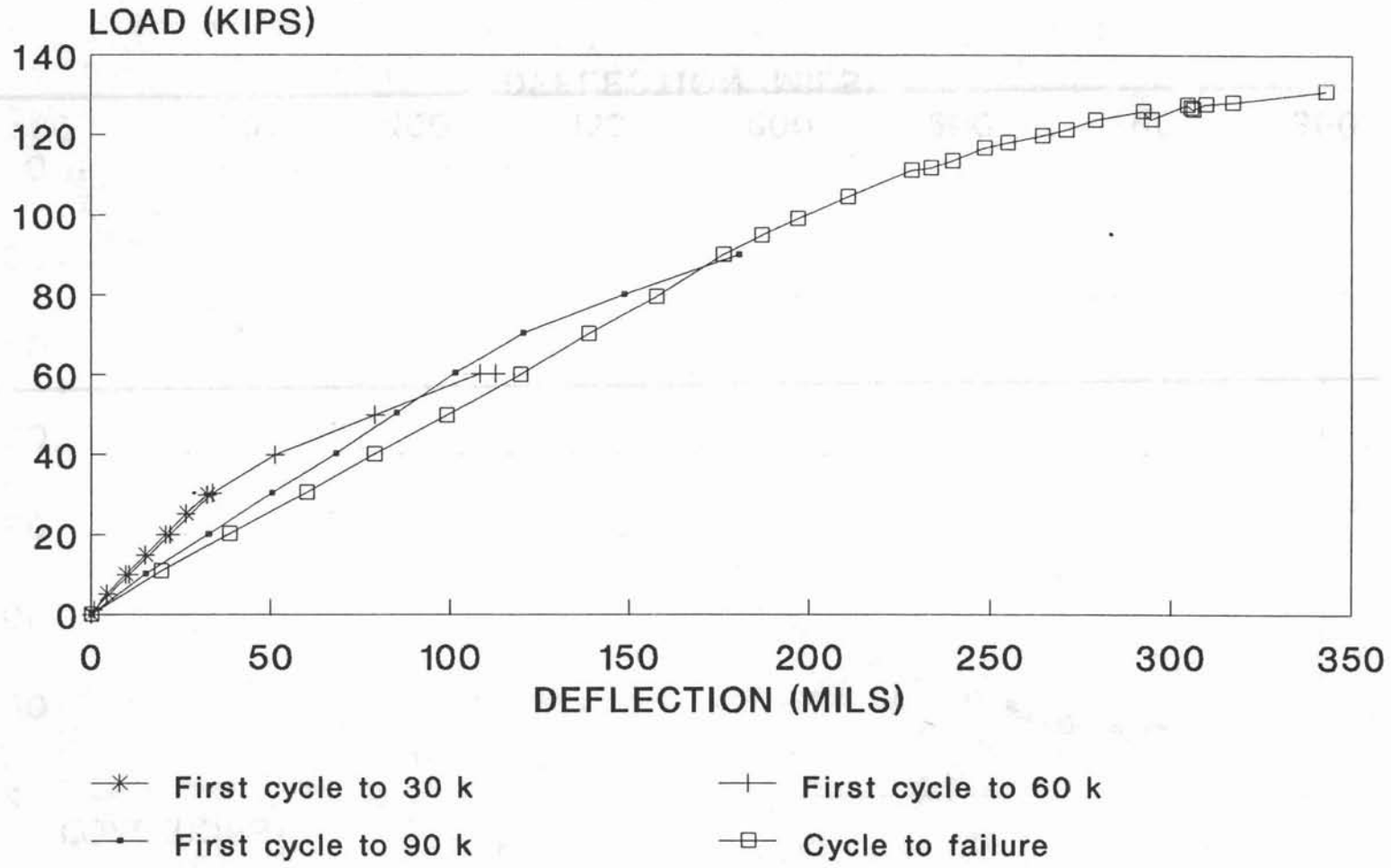

Figure 27. Experimental load-deflection at span 5, D4.

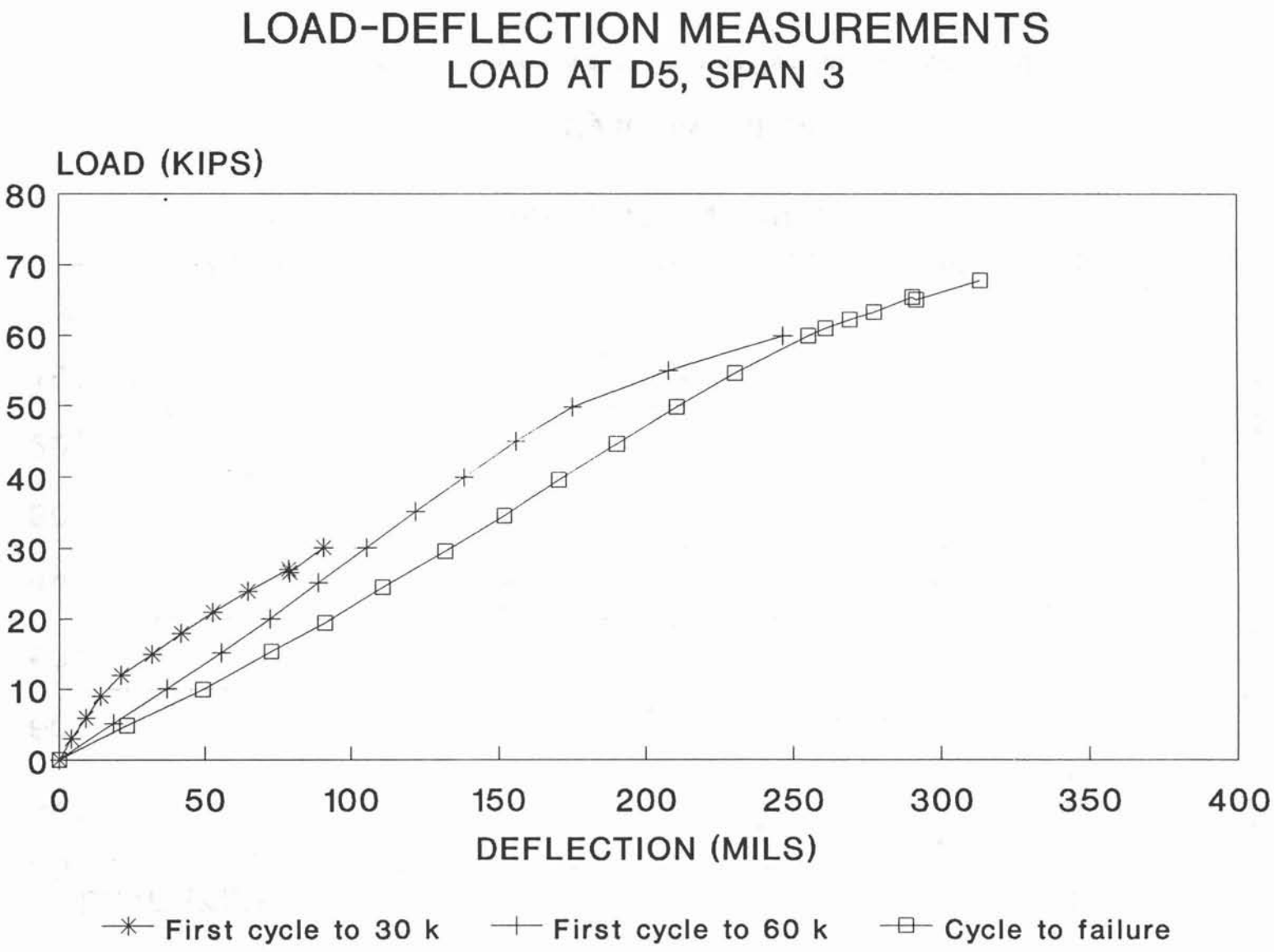

Figure 28. Experimental load-deflection at span 3, D5.

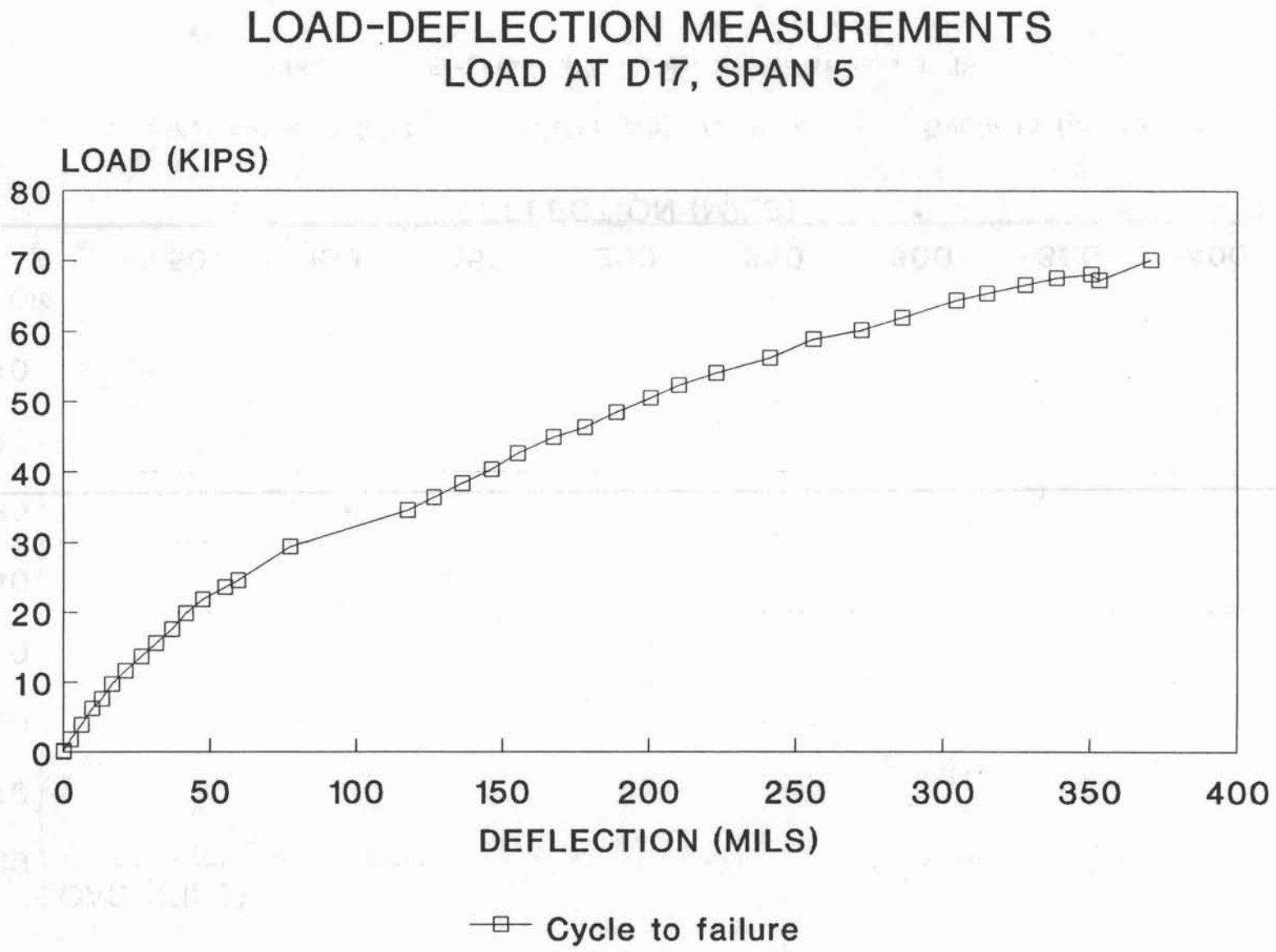

Figure 29. Experimental load-deflection at span 5, D17.

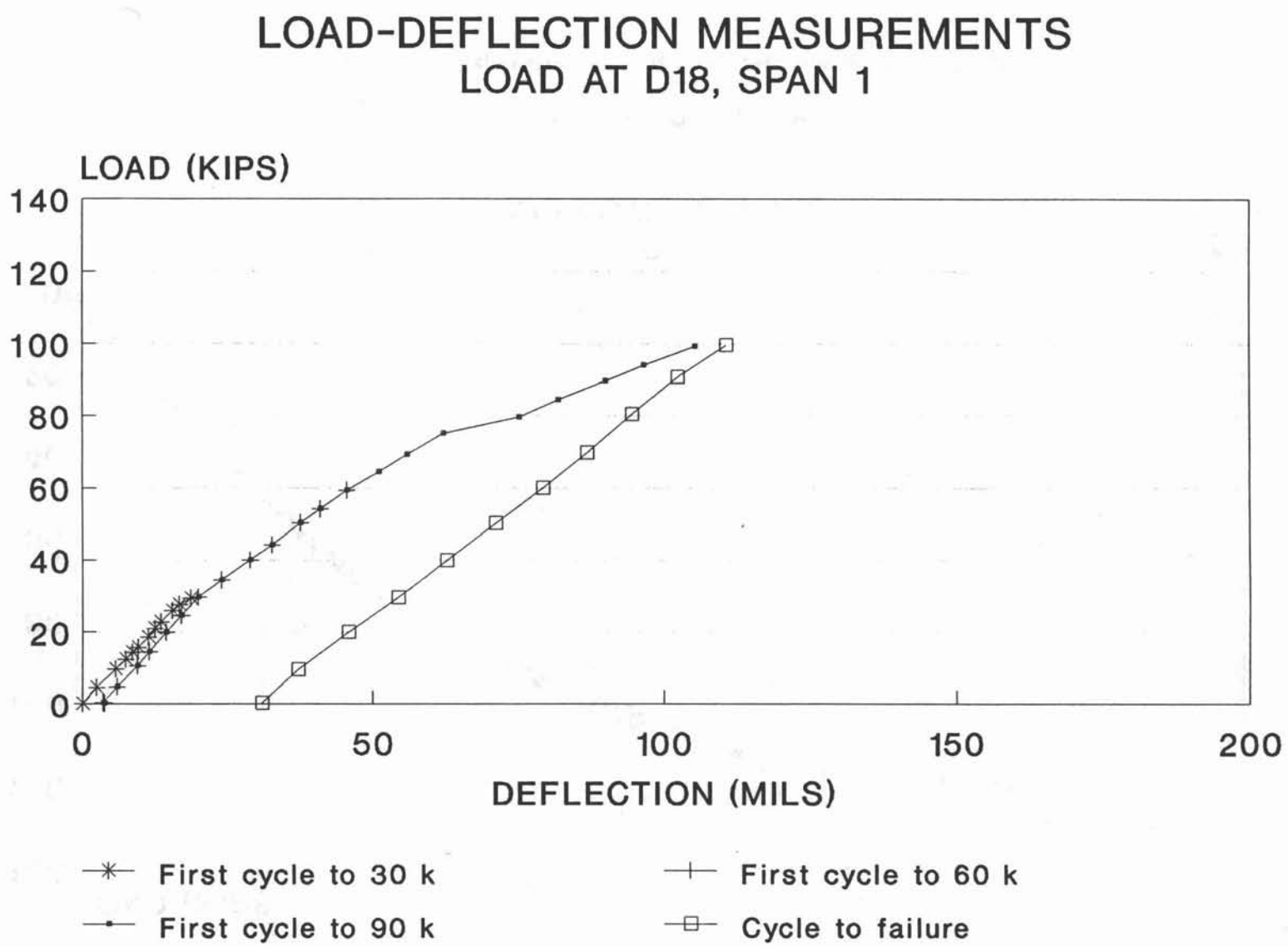

Figure 30. Experimental load-deflection at span 1, D18.

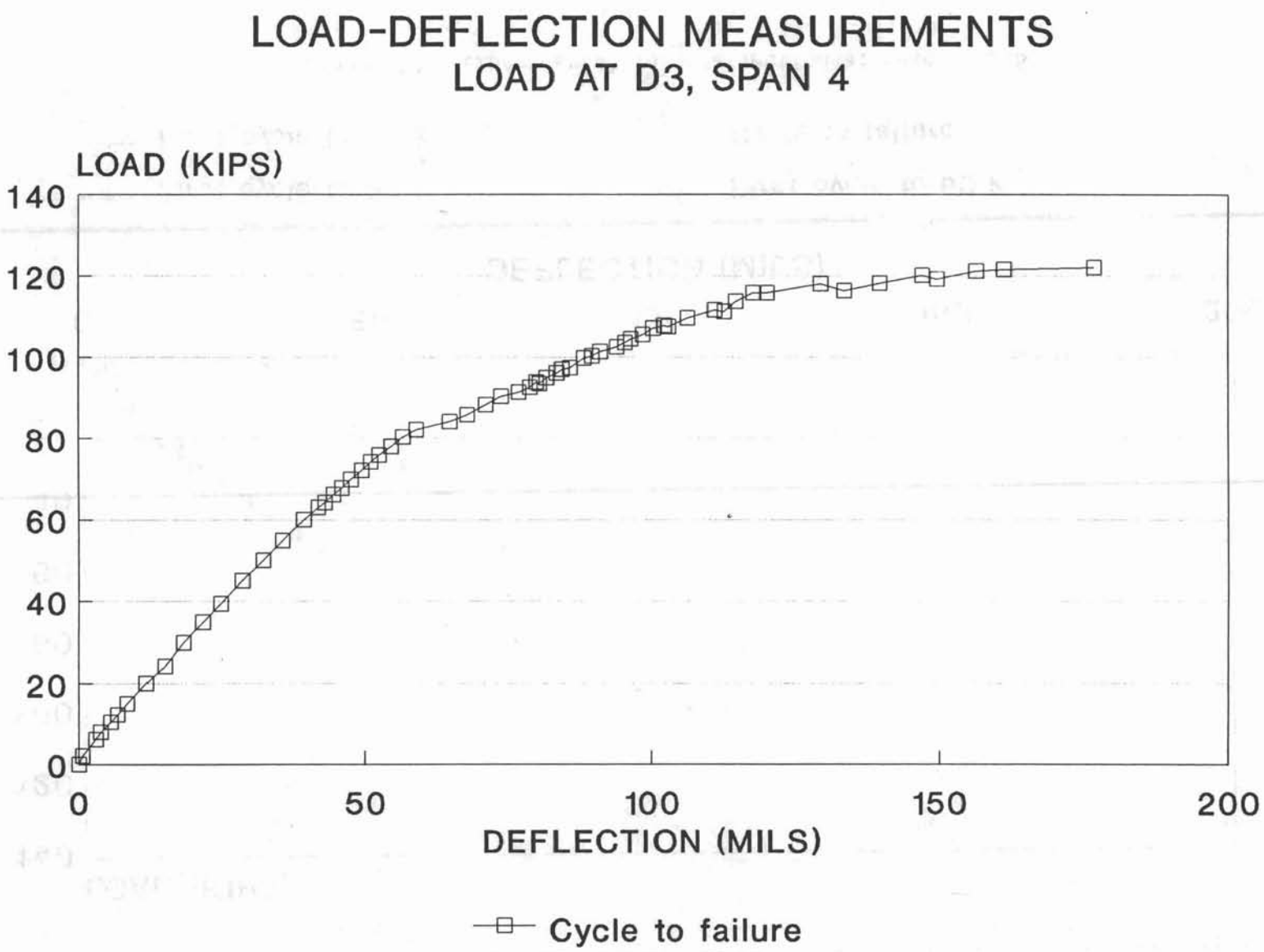

Figure 31. Experimental load-deflection at span 4, D3.

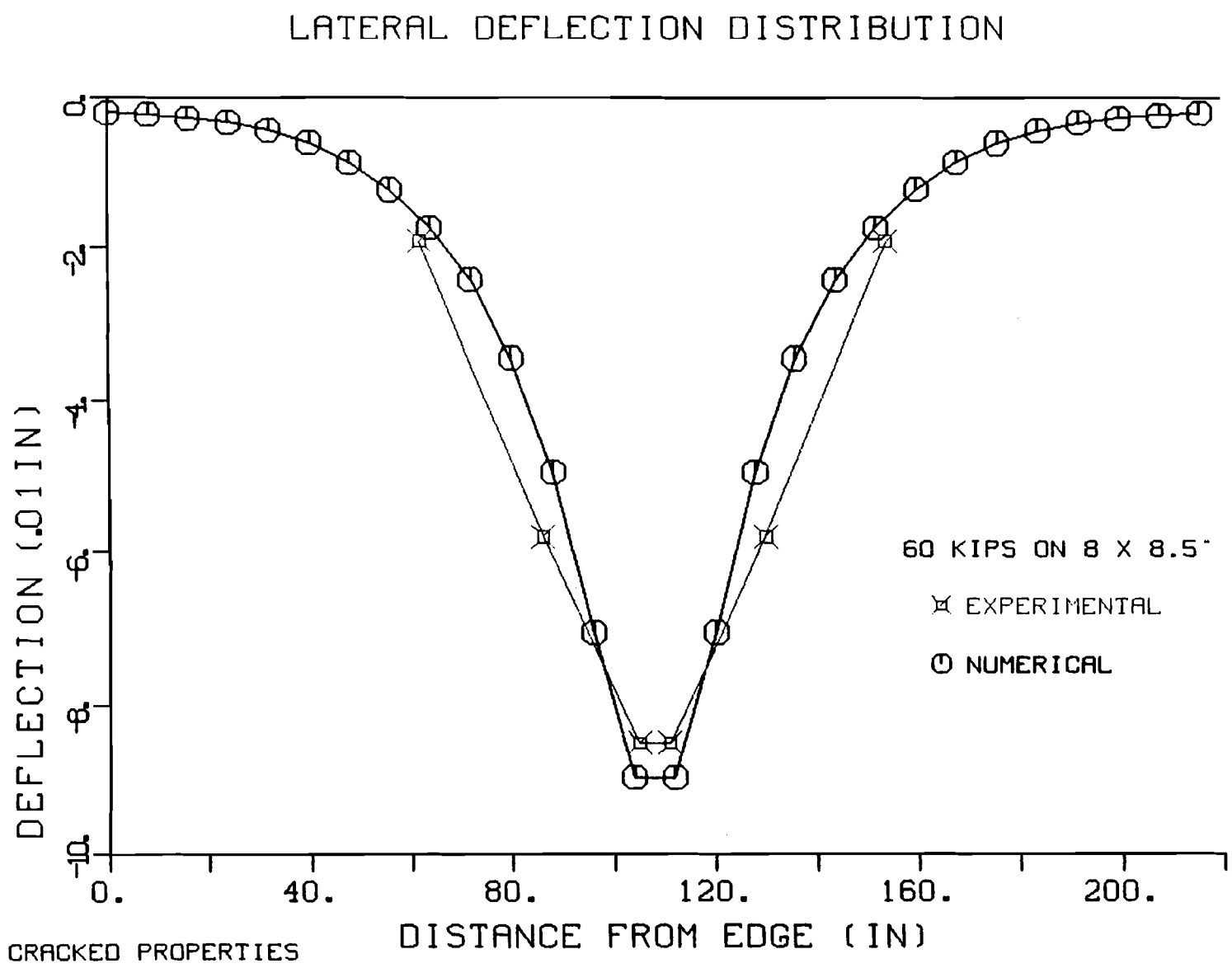

Figure 32. Lateral deflection distribution at span 3, D1.

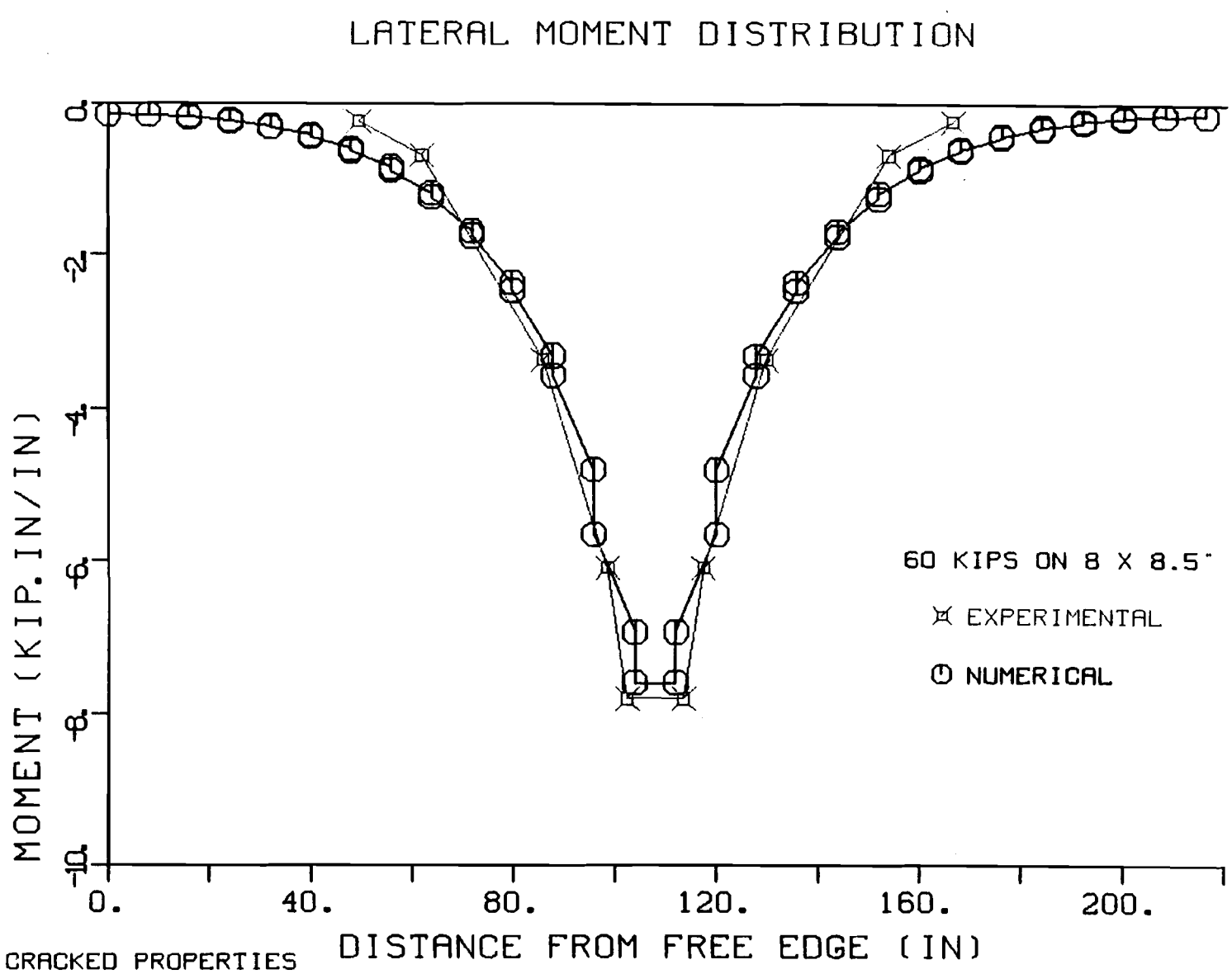

Figure 33. Lateral moment distribution at span 3, D1.

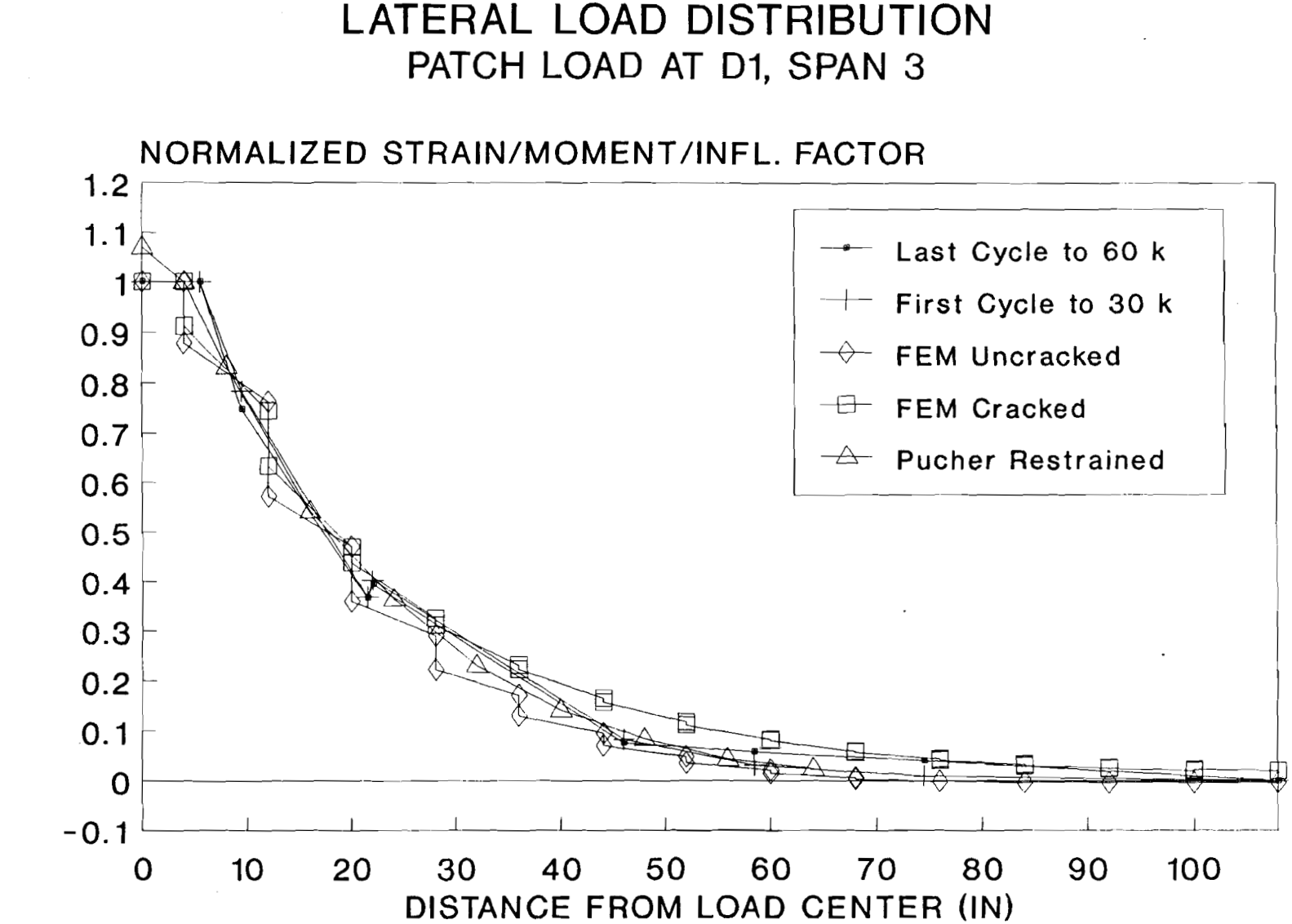

Pucher, restrained: E = 45"
Experimental: E = 46"
FEM uncracked/cracked: E = 41"/51"

Figure 34. Normalized lateral distribution at span 3, D1.

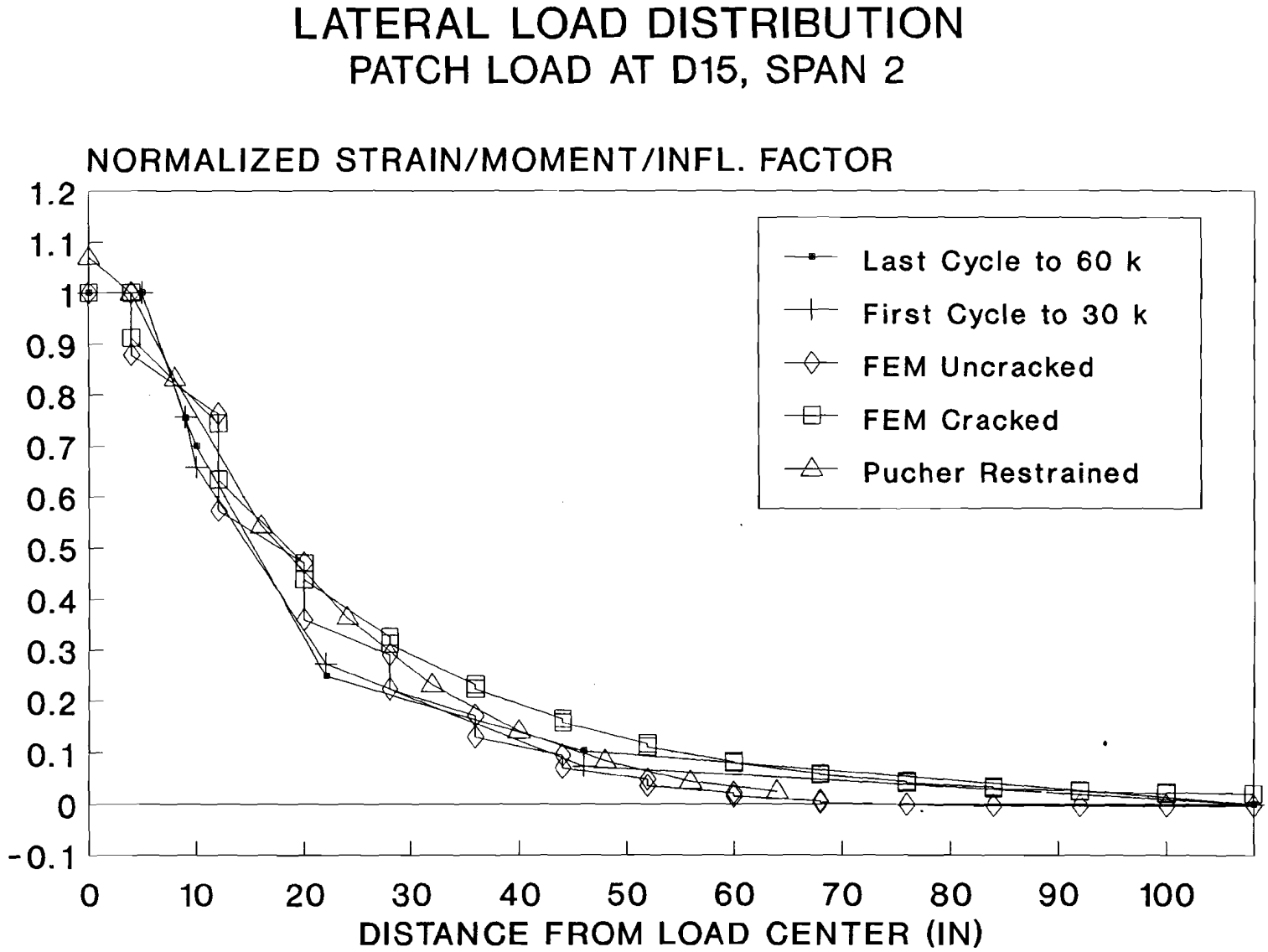

Pucher, restrained: E = 45"
Experimental: E = 43"
FEM uncracked/cracked: E = 41"/51"

Figure 35. Normalized lateral distribution at span 2, D15.

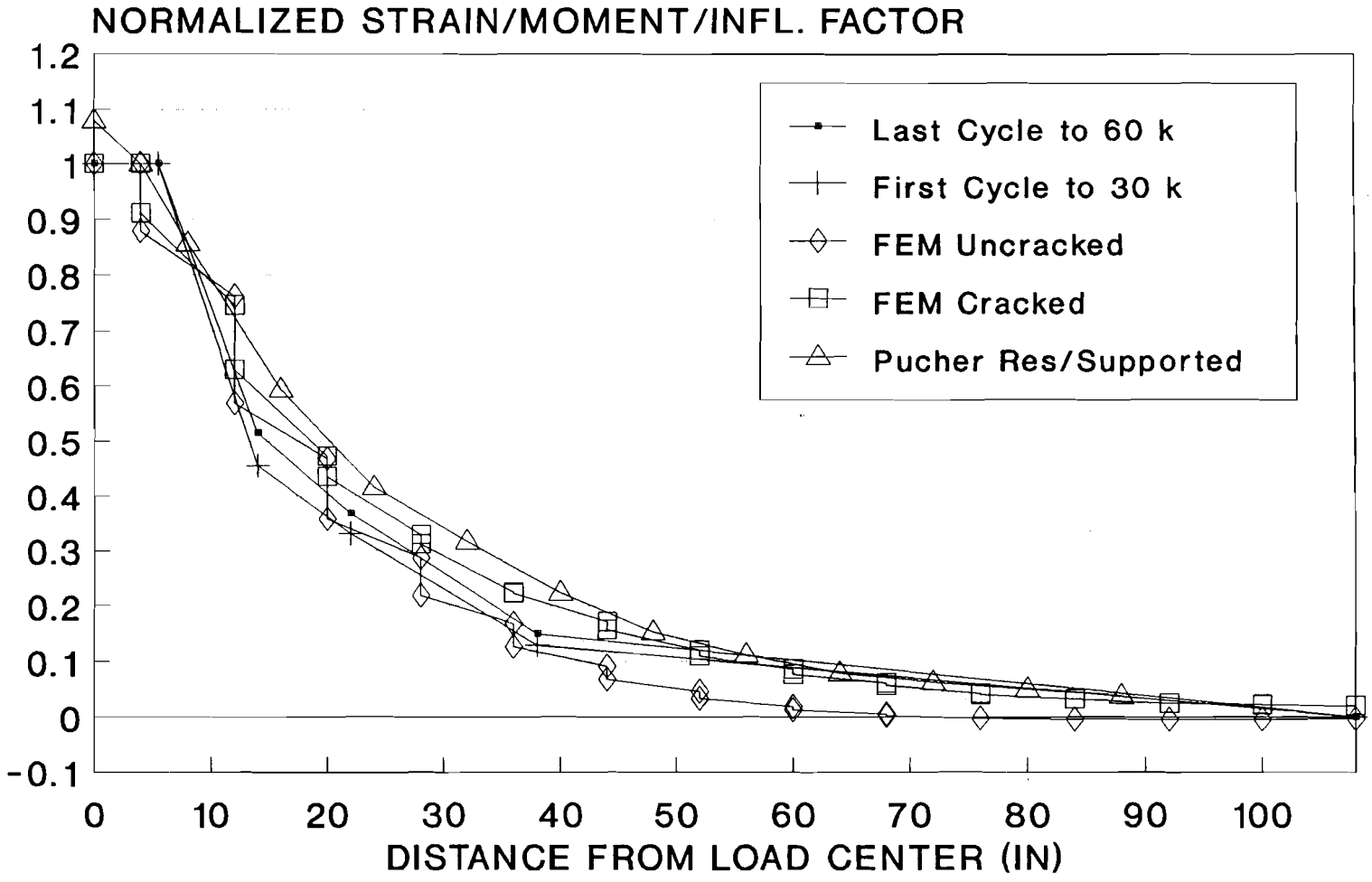

Pucher restrained/supported: E = 55"
Experimental: E = 50"
FEM uncracked/cracked: E = 41"/51"

Figure 36. Normalized lateral distribution at span 5, D4.

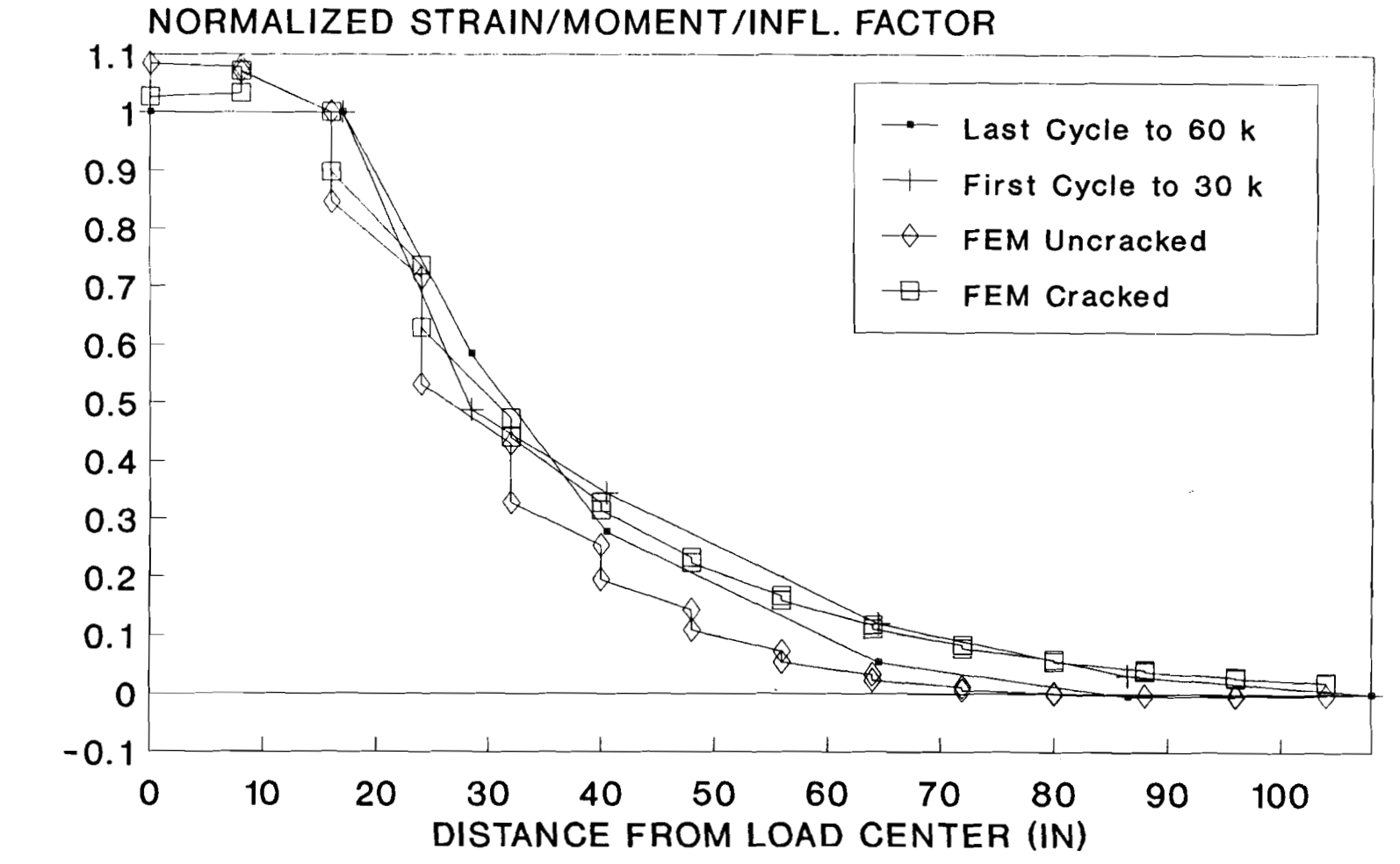

Pucher not available
Experimental: E = 36"
FEM uncracked/cracked: E = 30"/35"

Figure 37. Normalized lateral distribution at span 3, D5.

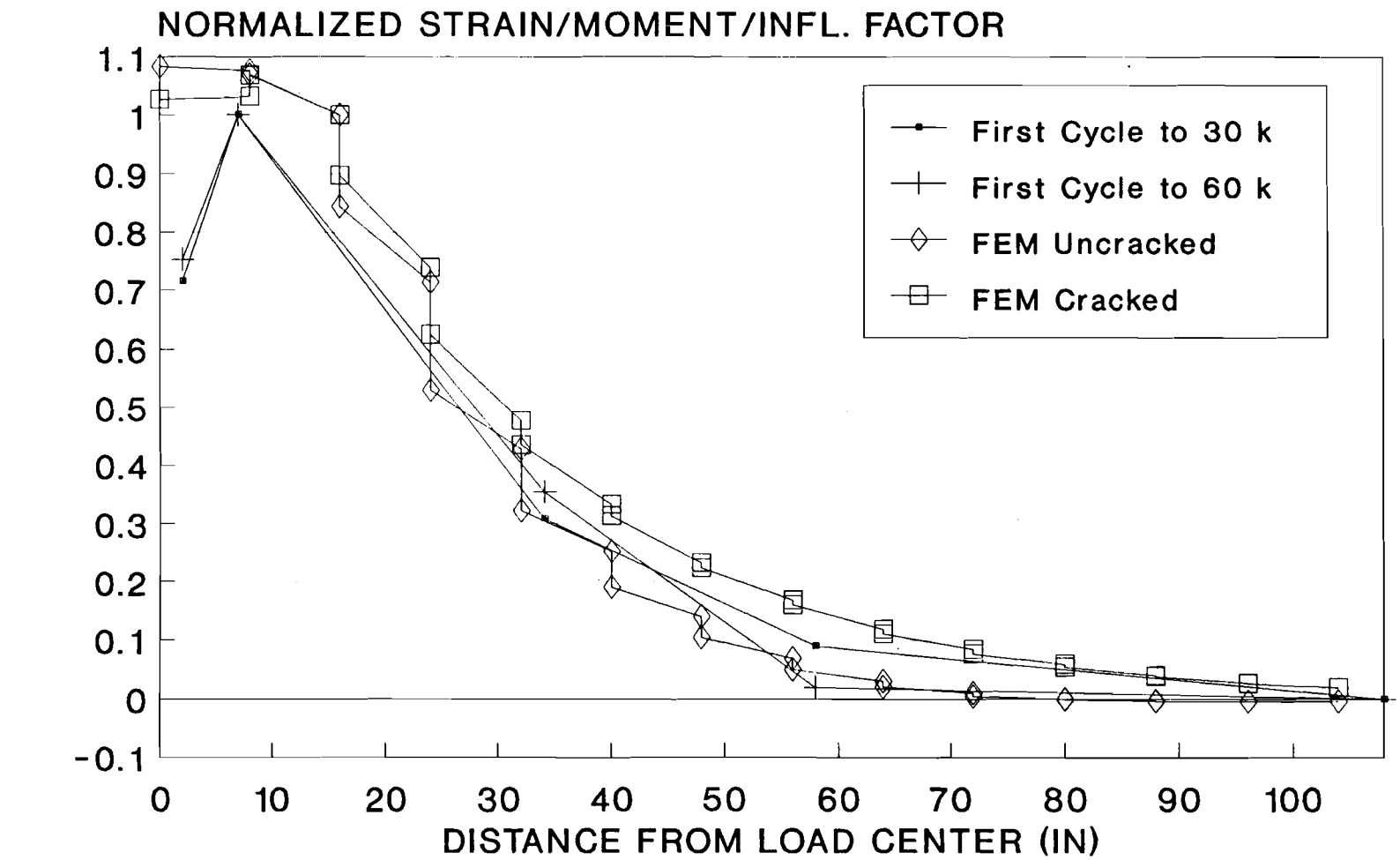

Pucher not available
Experimental: E = 31" (two gages lost)
FEM uncracked/cracked: E = 30"/38"

Figure 38. Normalized lateral distribution at span 5, D17.

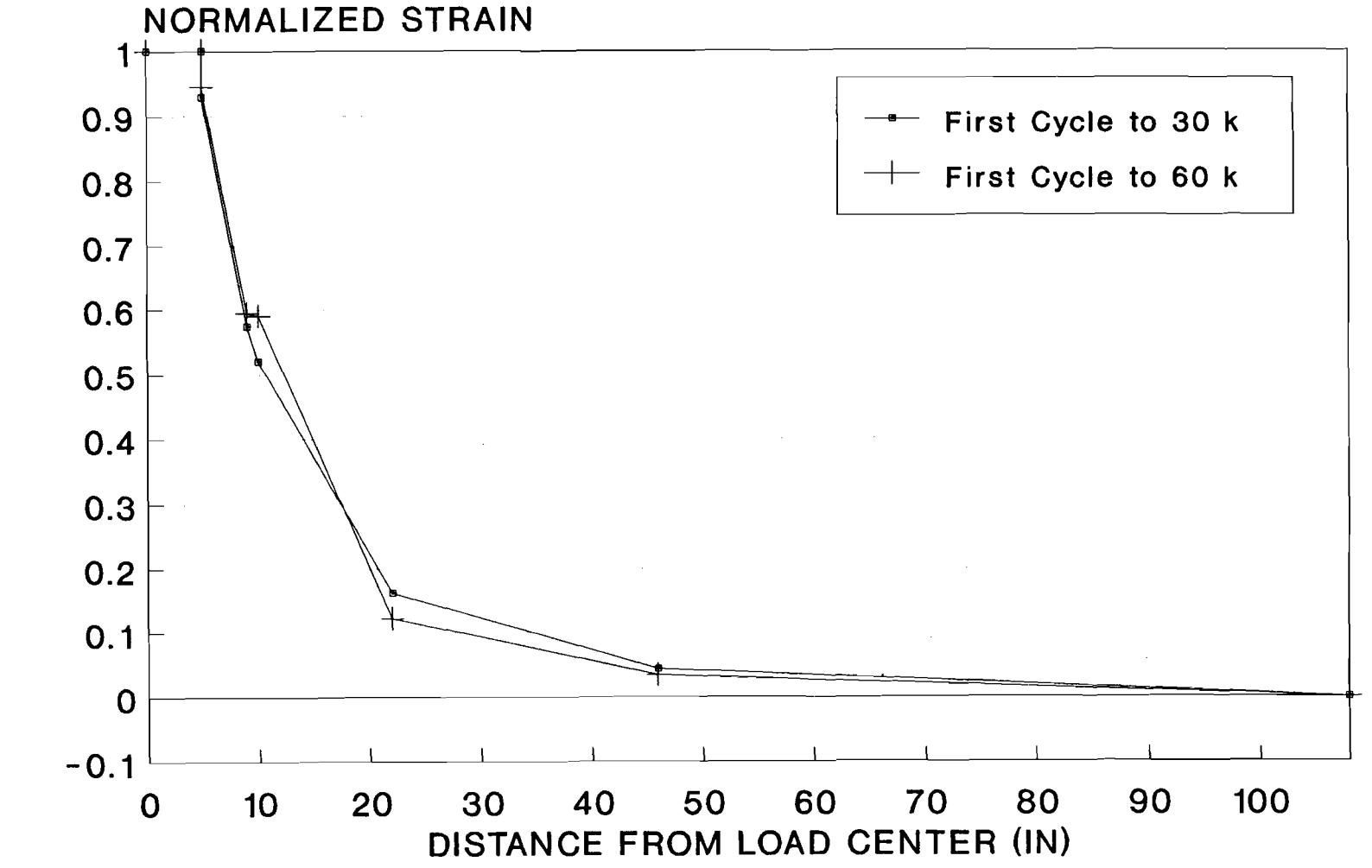

Figure 39. Normalized lateral distribution at span 1, D18.

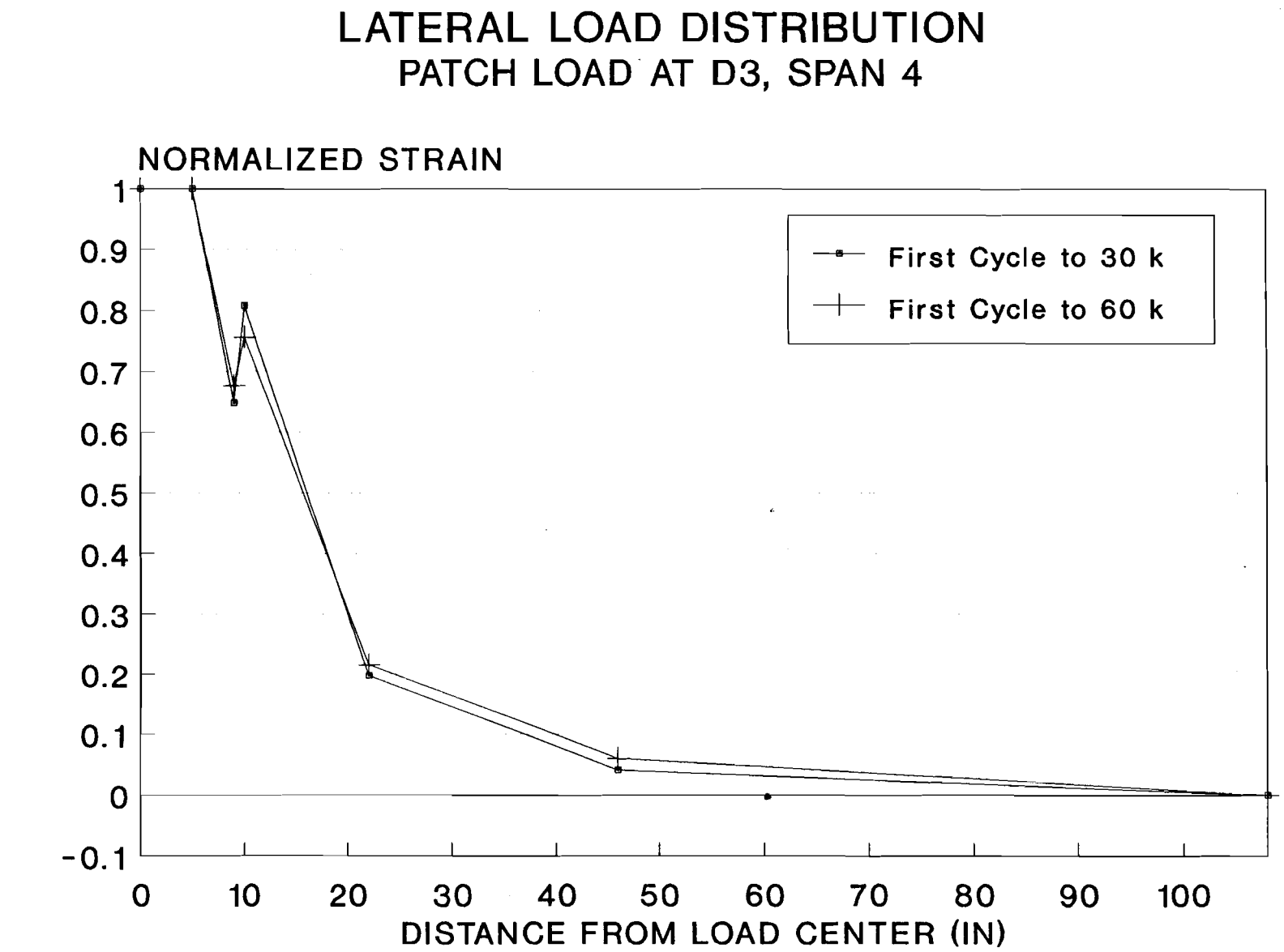

Figure 40. Normalized lateral distribution at span 4, D3.

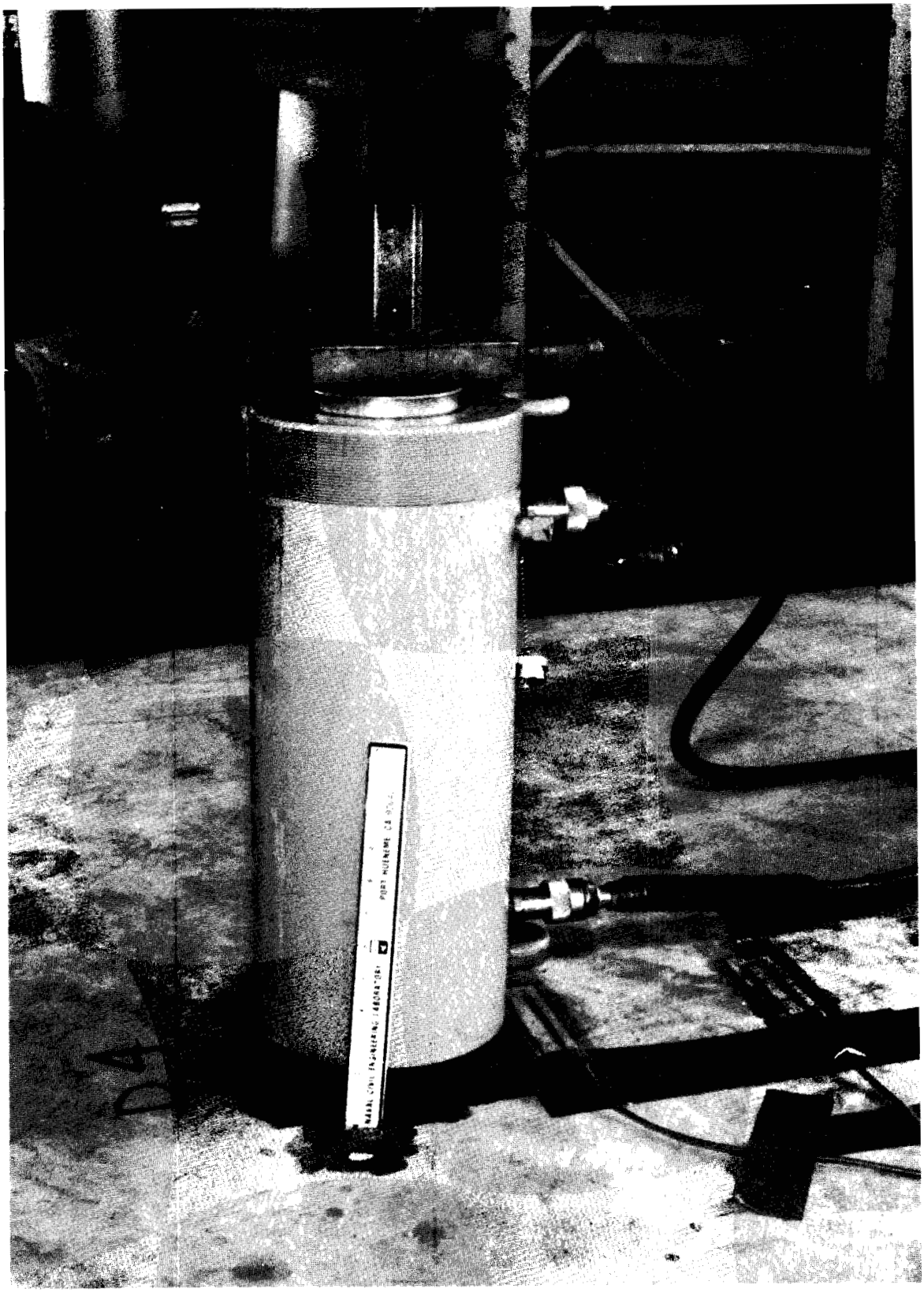

Figure 41. Punching shear failure at span 5, D4.

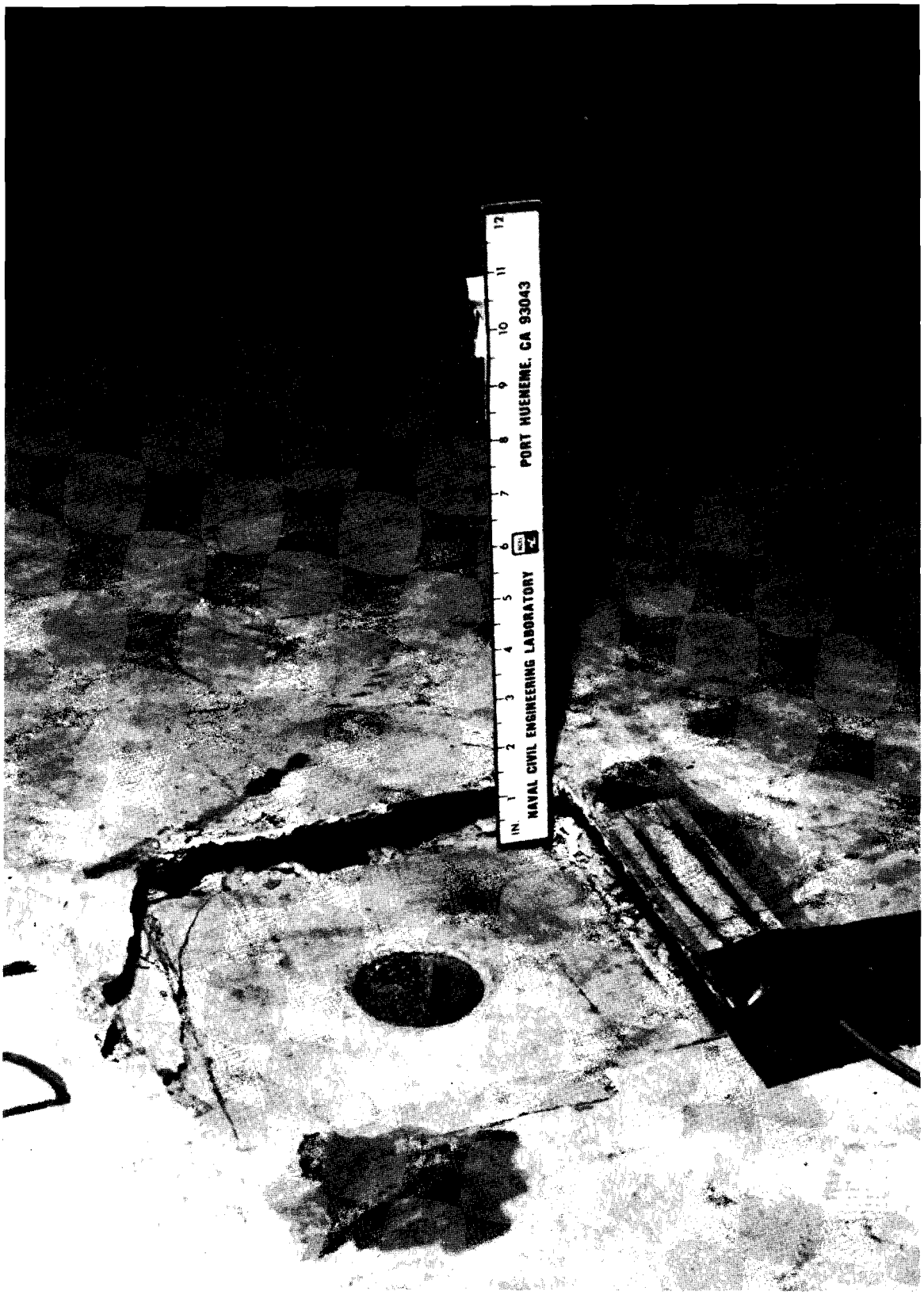

Figure 42. Top view of punching shear crack at span 5, D4.

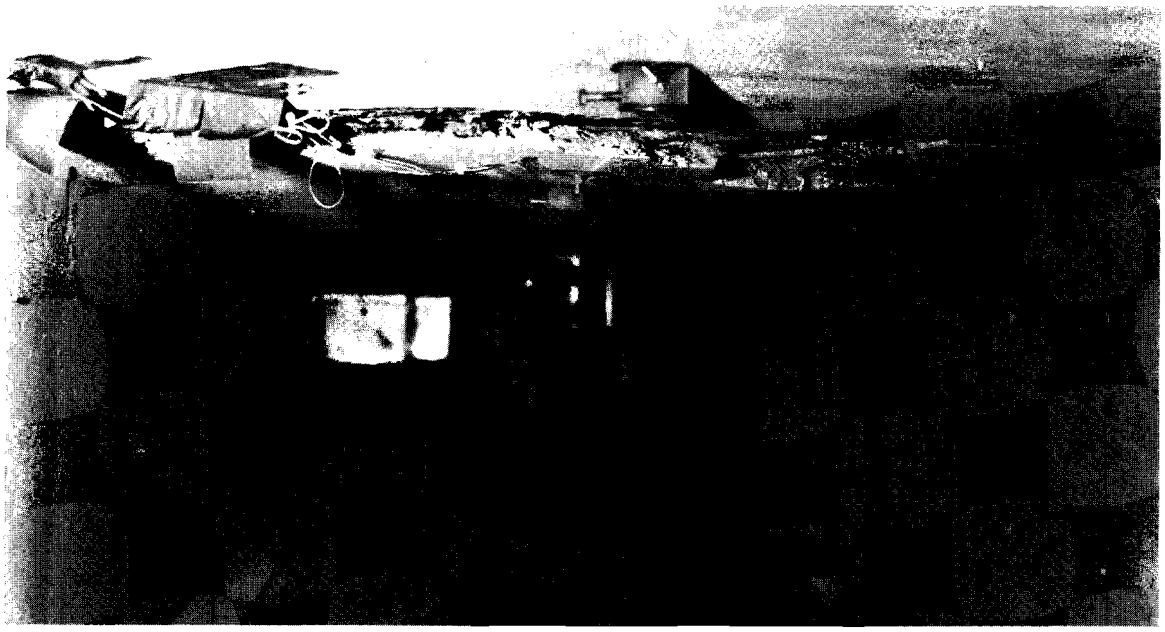

Figure 43. Bottom view of punching shear crack at span 5, D4.

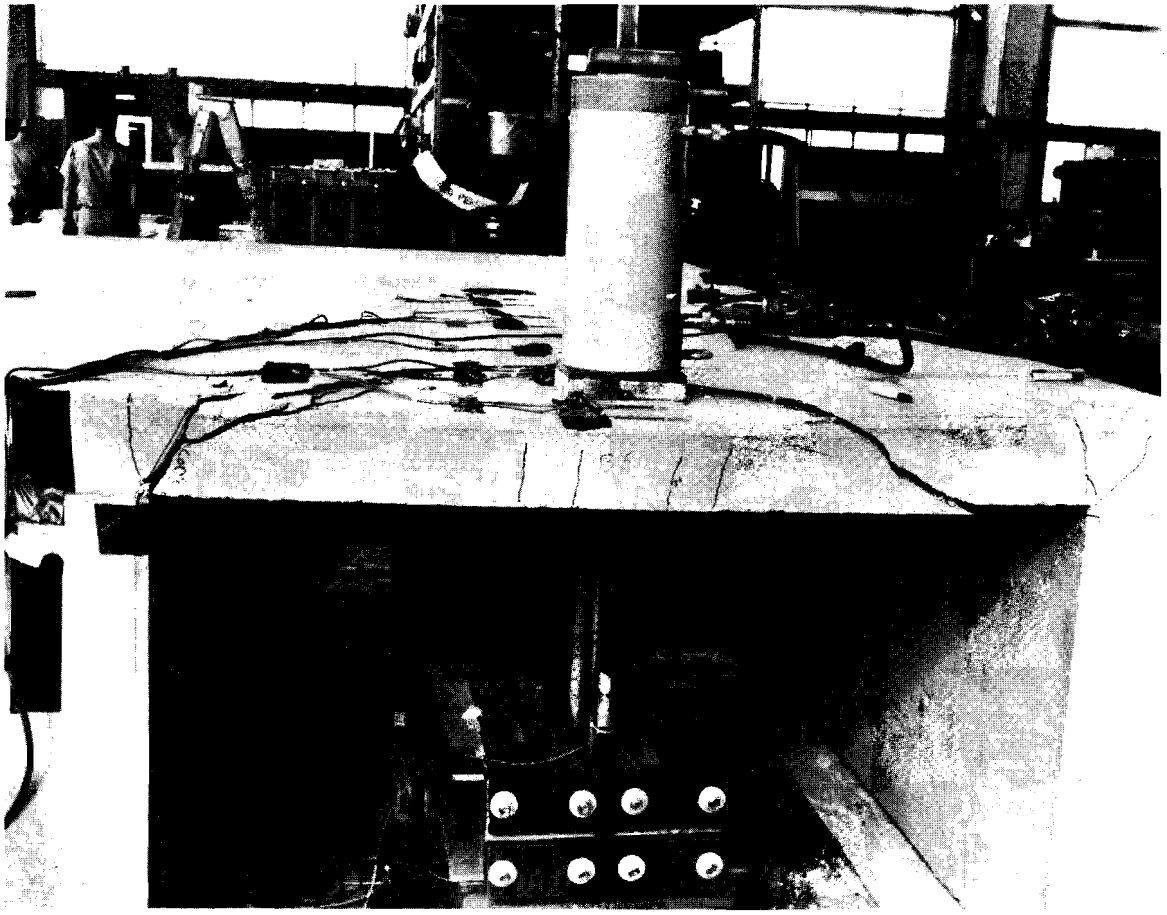

Figure 44. Punching shear failure at free edge of span 5, D17.

LATERAL LOAD DISTRIBUTION
INTERIOR MIDSPAN

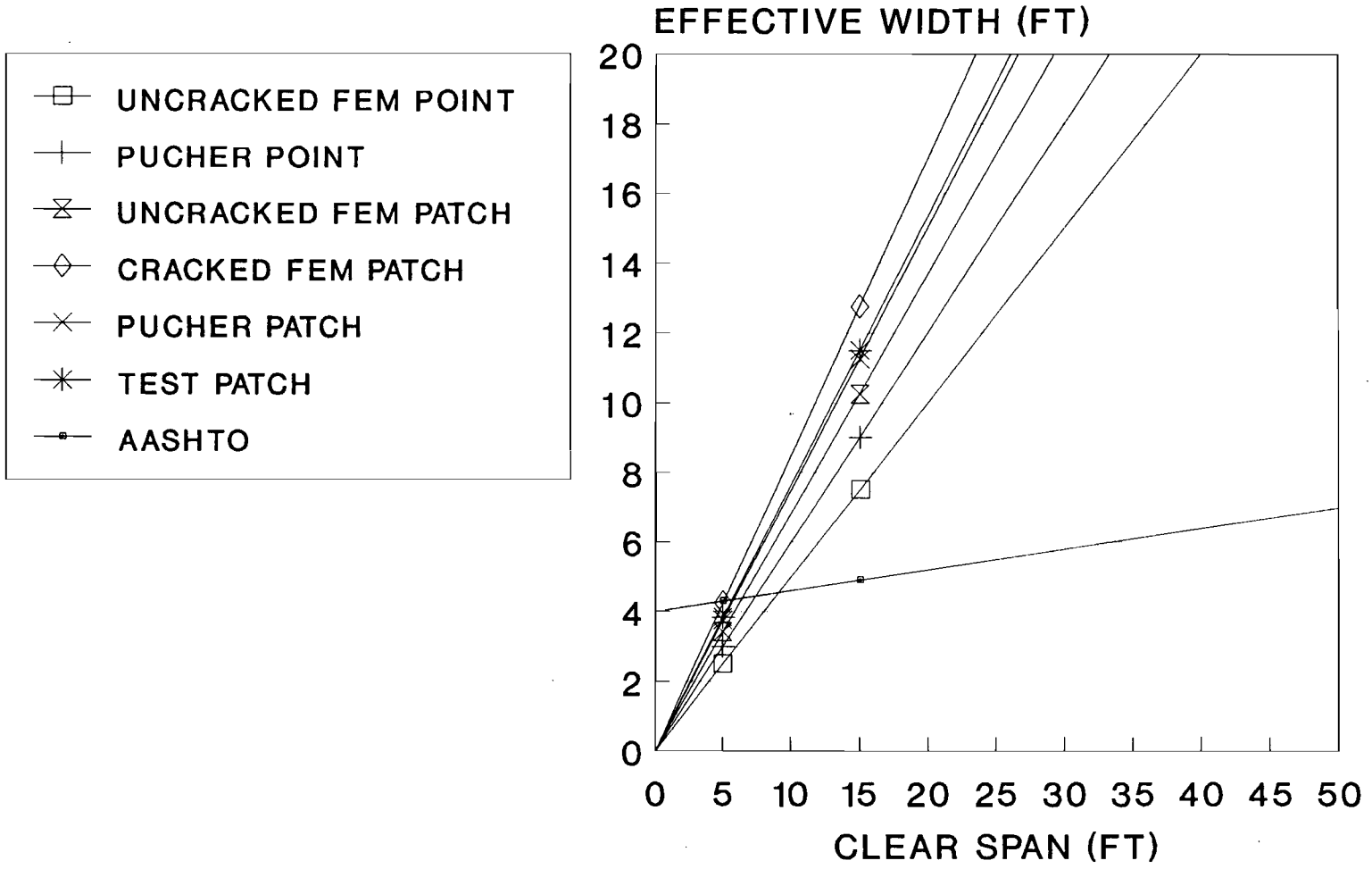

CRACKED/UNCRACKED CONCRETE PROPERTIES
RESTRAINED EDGES INFINITE STRIP (PUCHER)
POINT LOADS OR 8"x8" PATCH LOADS

Figure 45. Effective width versus span, interior midspan load.

LATERAL LOAD DISTRIBUTION
EXTERIOR MIDSPAN

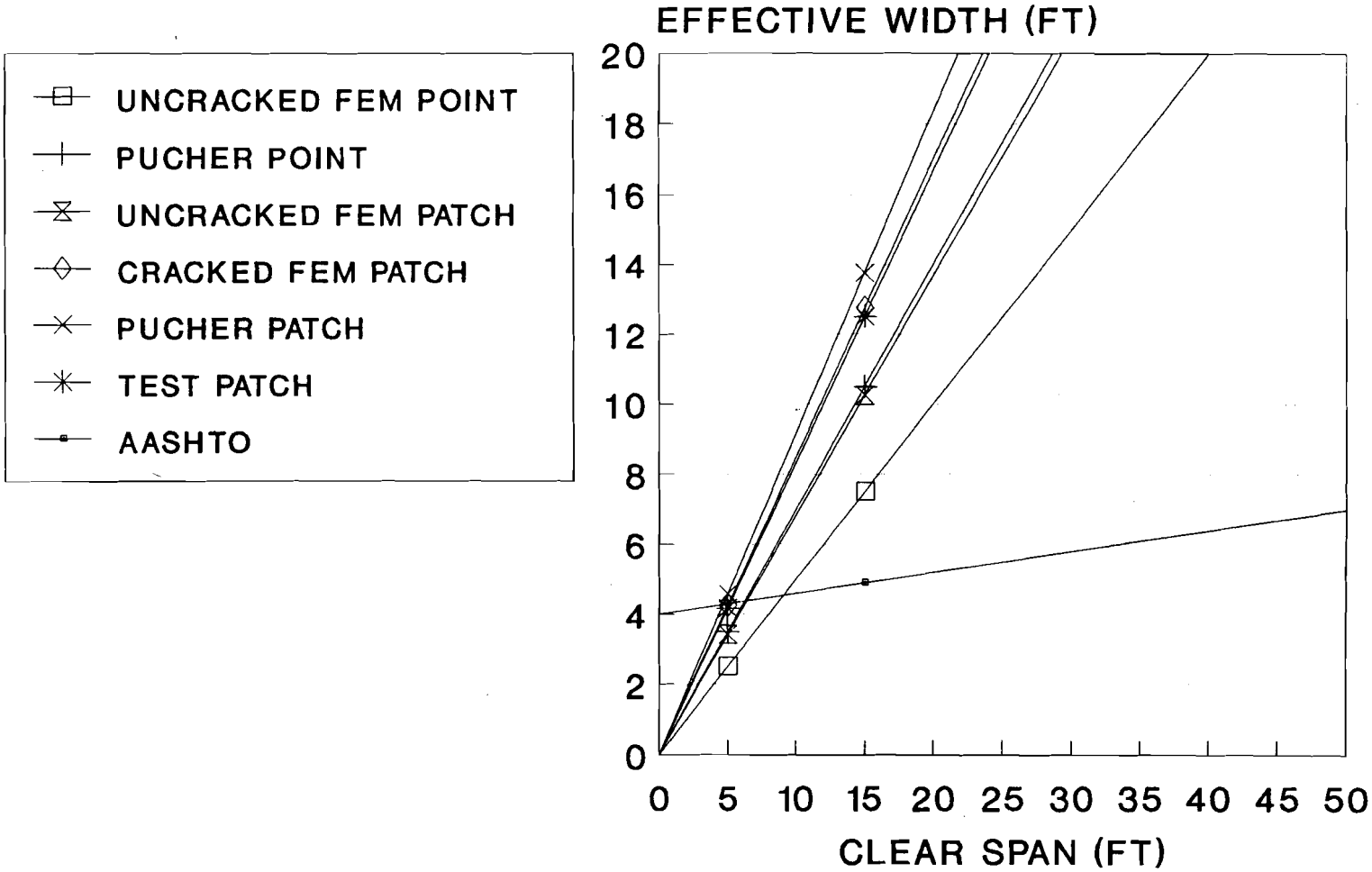

CRACKED/UNCRACKED CONCRETE PROPERTIES
RESTRAINED AND SUPPORTED STRIP (PUCHER)
POINT LOADS OR 8"x8" PATCH LOADS

Figure 46. Effective width versus span, exterior midspan load.

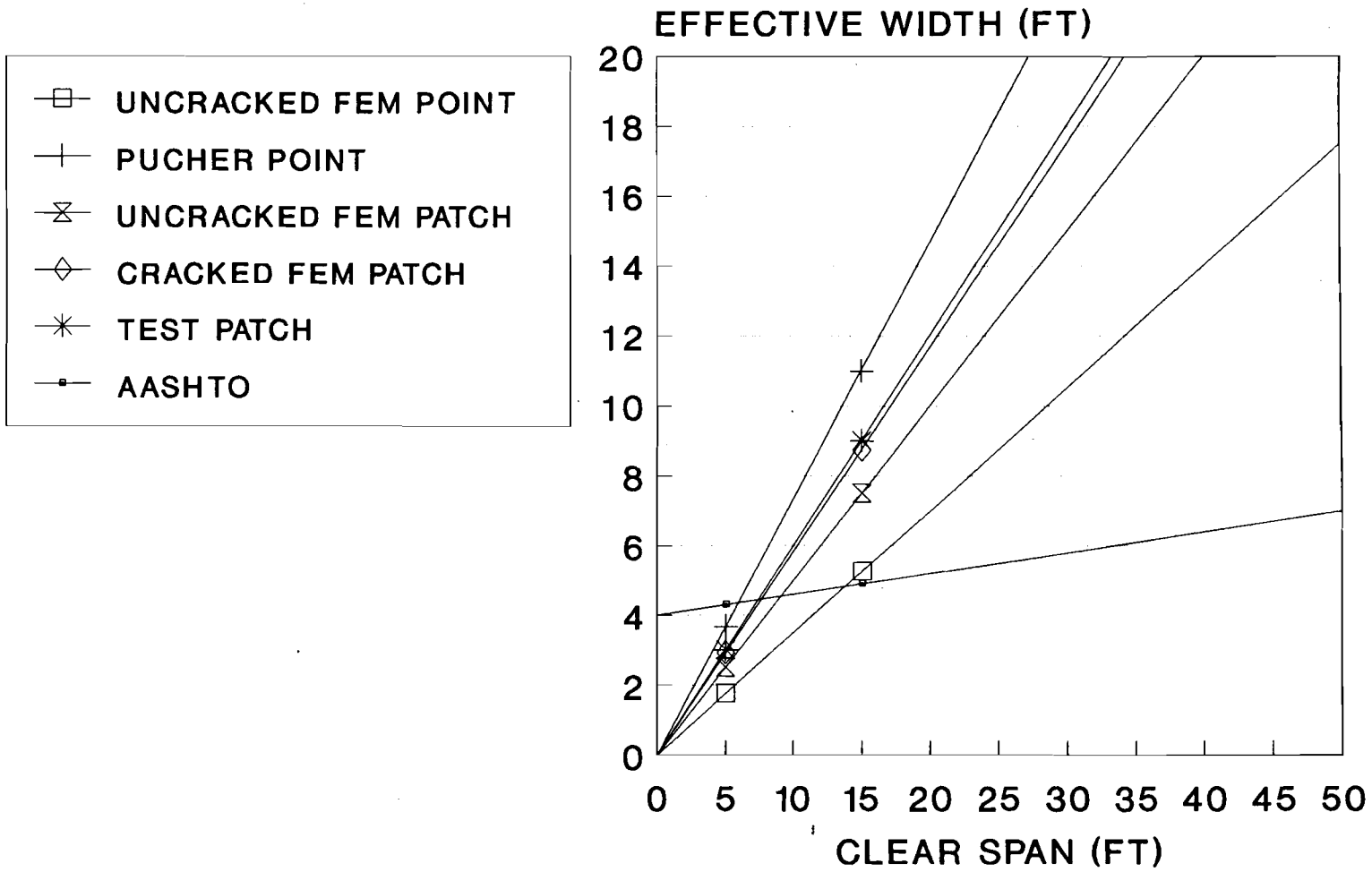

Figure 47. Effective width versus span, interior midspan edge load.

LATERAL LOAD DISTRIBUTION
EXTERIOR MIDSPAN EDGE

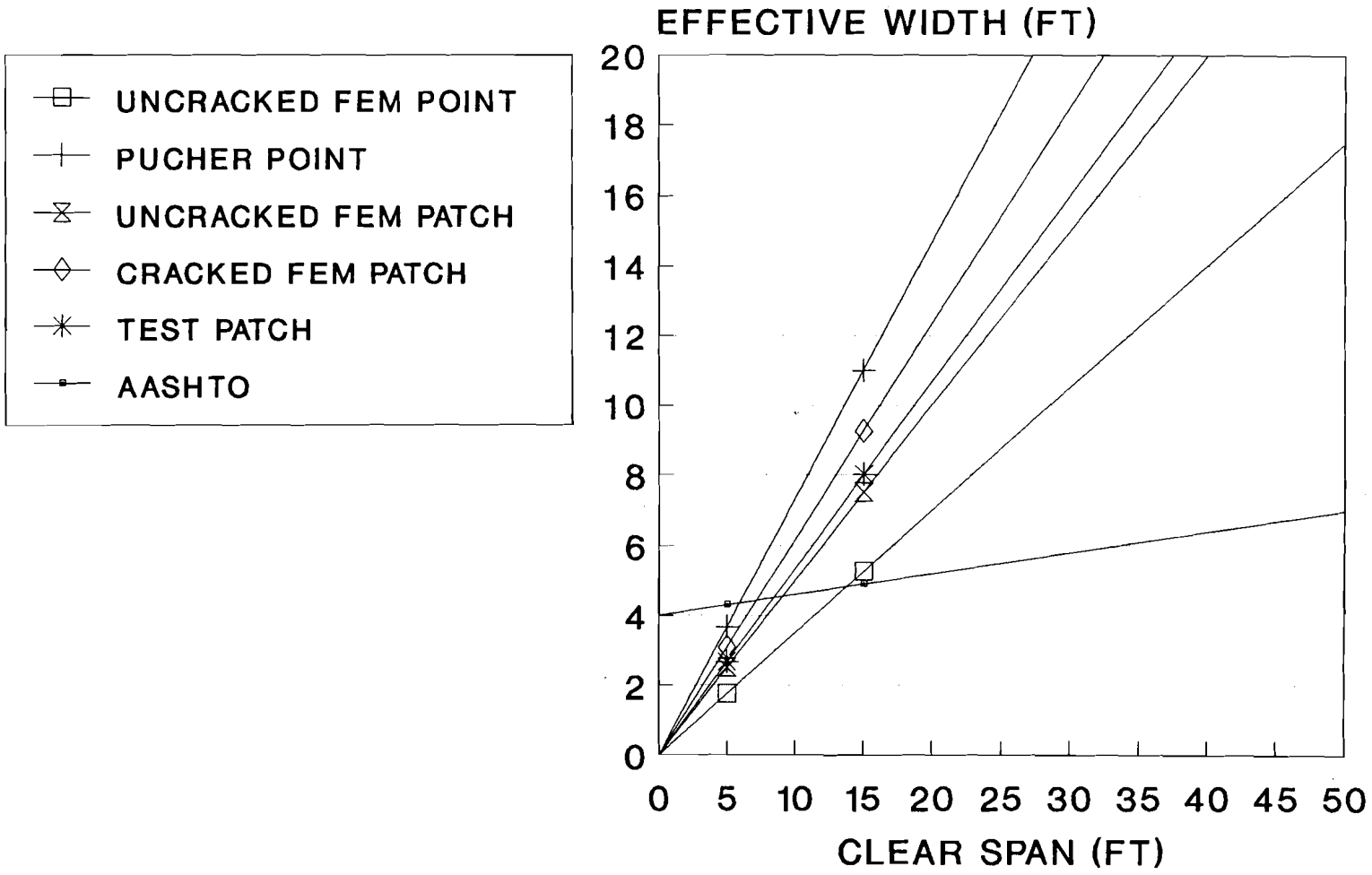

CRACKED/UNCRACKED CONCRETE PROPERTIES
SIMPLY SUPPORTED HALF STRIP (PUCHER)
POINT LOADS OR 8"x8" PATCH LOADS

Figure 48. Effective width versus span, exterior midspan edge load.

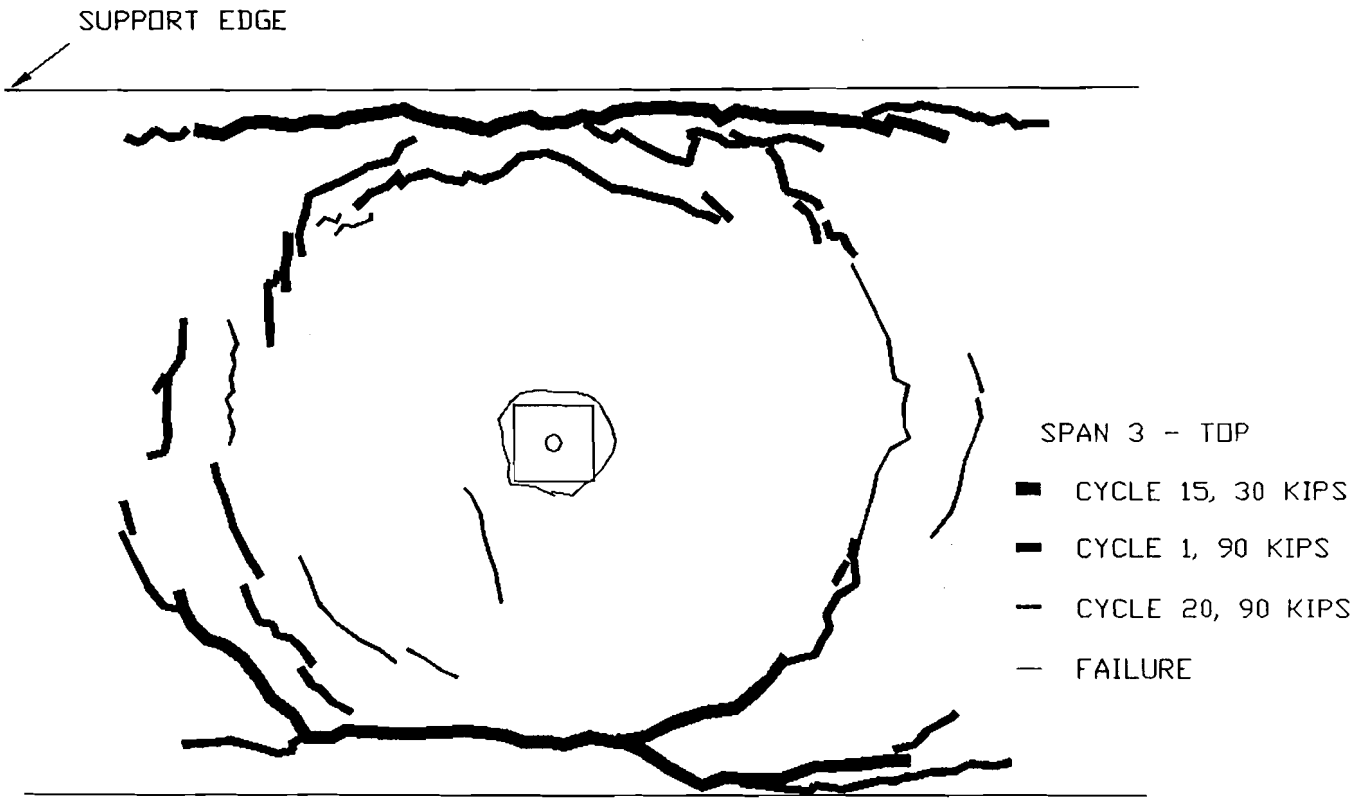

Figure 49. Crack patterns on deck top surface, span 3, D1.

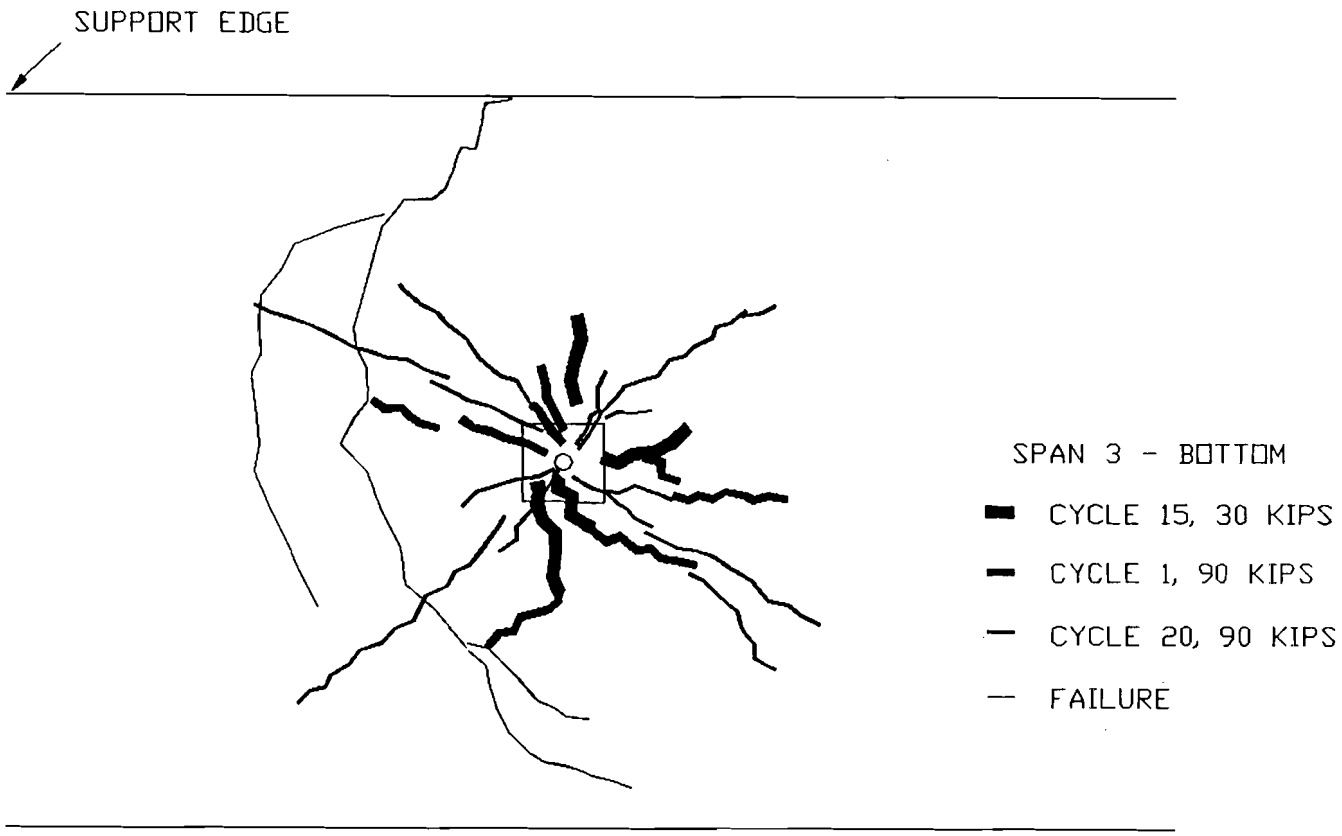

Figure 50. Crack patterns on deck bottom surface, span 3, D1.

DISTRIBUTION LIST

AFB / HQ TAC/DEMM (Pollard), Langley AFB, VA
AFESC / TIC Lib, Tyndall AFB, FL
AMERICAN CONCRETE / Lib, Detroit, MI
ARMY / R&D Lab, STRNC-UE, Natick, MA
ARMY CECOM R&D TECH LIBRARY / ASNC-ELC-I-T, Ft Monmouth, NJ
ARMY CERL / Lib, Champaign, IL
ARMY ENGRG DIST / CENPS-ED-SD, Seattle, WA; Lib, Seattle, WA; Phila, Lib, Philadelphia, PA
ARMY ENGRG DIV / CEHND-ED-CS, Huntsville, AL
ARMY EWES / CEWES-CD-P Vicksburg, MS; Lib, Vicksburg, MS; WESCD-P (Melby), Vicksburg, MS
ARMY MISSILE R&D CMD / Ch, Docs, Sci Info Ctr, Redstone Arsenal, AL
ARMY MMRC / DRXMR-SM (Lenoe), Watertown, MA
ARVID GRANT & ASSOC / Olympia, WA
ATLANTIC RICHFIELD CO / RE Smith, Dallas, TX
BATTELLE / D. Frink, Columbus, OH
BETHLEHEM STEEL CO / Engrg Dept, Bethlehem, PA
BLAKE, KIM / Martinez, CA
BRITISH EMBASSY / Sci & Tech Dept (Wilkins), Washington, DC
BROWN & ROOT / Ward, Houston, TX
BROWN, ROBERT / Tuscaloosa, AL
BULLOCK, TE / La Canada, CA
CASE WESTERN RESERVE UNIV / CE Dept (Perdikaris), Cleveland, OH
CBC / Code 155, Port Hueneme, CA
CHAO, JC / Houston, TX
CHILDS ENGRG CORP / K.M. Childs, Jr., Medfield, MA
CITY OF LIVERMORE / Dackins, PE, Livermore, CA
CLARK, T. / San Mateo, CA
CLARKSON COLL OF TECH / CE Dept, Potsdam, NY
COGUARD R&D CEN / Lib, Groton, CT
COLLEGE OF ENGINEERING / CE Dept (Grace), Southfield, MI
COLORADO STATE UNIV / CE Dept (Criswell), Ft. Collins, CO
COMCBLANT / Code S3T, Norfolk, VA
CONRAD ASSOC / Luisoni, Van Nuys, CA
CONSOER TOWNSEND & ASSOC / Schramm, Chicago, IL
CONSTRUCTION TECH LABS, INC / G. Corley, Skokie, IL
CORNELL UNIV / Civil & Environ Engrg, Ithaca, NY
DAMES & MOORE / Lib, Los Angeles, CA
DAVY DRAVO / Wright, Pittsburg, PA
DIA / DB-6E1, Washington, DC; DB-6E2, Washington, DC; VP-TPO, Washington, DC
DTRCEN / Code 172, Bethesda, MD
EDWARD K. NODA & ASSOC / Honolulu, HI
ENGINEERING DATA MANAGEMENT / Ronald W. Anthony, Fort Collins, CO
FLORIDA ATLANTIC UNIV / Ocean Engrg Dept (Su), Boca Raton, FL
FLORIDA INST OF TECH / CE Dept (Kalajian), Melbourne, FL
GEORGIA INST OF TECH / CE Schl (Kahn), Atlanta, GA; CE Schl (Swanger), Atlanta, GA; CE Schl (Zuruck), Atlanta, GA
GIORDANO, A.J. / Sewell, NJ
GRUMMAN AEROSPACE CORP / Tech Info Ctr, Bethpage, NY

HAN-PADRON ASSOCIATES / Dennis Padron, New York, NY
HARDY, S.P. / San Ramon, CA
HAYNES & ASSOC / H. Haynes, PE, Oakland, CA
HEUZE, F / Alamo, CA
HJ DEGENKOLB ASSOC / W. Murdough, San Francisco, CA
JOHN HOPKINS UNIV / CE Dept, Jones, Baltimore, MD
JOHN J MC MULLEN ASSOC / Lib, New York, NY
KAISER PERMANENTE MEDCIAL CARE PROGRAM / Oakland, CA
LAWRENCE LIVERMORE NATL LAB / FJ Tokarz, Livermore, CA
LEO A DALY CO / Honolulu, HI
LIN OFFSHORE ENGRG / P. Chow, San Francisco, CA
LONG BEACH PORT / Engrg Dir (Allen), Long Beach, CA; Engrg Dir (Lizzi), Long Beach, CA
MICHIGAN TECH UNIV / (Ligon), Houghton, MI; CO Dept (Haas), Houghton, MI
MT DAVISSON / CE, Savoy, IL
NAS / Code 421, San Diego, CA; Miramar, PWO, San Diego, CA
NAVFAC / N62, Argentina, NF, FPO New York,
NAVFACENGCOM / Code 04A1D, Alexandria, VA; Code 04A3, Alexandria, VA; Code 07, Alexandria, VA; Code 07M (Gross), Alexandria, VA
NAVFACENGCOM CHESDIV / Code 112.1, Washington, DC
NAVFACENGCOM SOUTHDIV / Code 04A3, Charleston, SC; Code 102H, Charleston, SC; Code 4023 (RDL), Charleston, SC
NAVMEDCOM / NWREG, Fac Engr, PWD, Oakland, CA
NAVOCEANSYSCEN / Code 9642B, San Diego, CA
NAVPGSCOL / PWO, Monterey, CA
NAVSCOLCECOFF / Code C35, Port Hueneme, CA
NAVSHIPREFAC / Lib, FPO San Francisco; SCE, FPO Seattle
NAVSHIPYD / Code 244.13, Long Beach, CA; Code 443, Bremerton, WA; Mare Is, Code 202.13, Vallejo, CA; Mare Is, Code 280, Vallejo, CA; Mare Is, PWO, Vallejo, CA; Norfolk, Code 380, Portsmouth, VA; Tech Lib, Portsmouth, NH
NAVSTA / CO, Long Beach, CA; Code N4214, Mayport, FL
NEW ZEALAND CONCRETE RSCH ASSN / Lib, Porirua,
NIEDORODA, AW / Gainesville, FL
NORTHDIV CONTRACTS OFFICE / ROICC, Colts Neck, NJ
NRL / Code 2511, Washington, DC; Code 4670, Washington, DC
NUHN & ASSOC / A.C. Nuhn, Wayzata, NM
NUSC DET / Lib, Newport, RI
OICC / Engr and Const Dept, APO New York,
OREGON STATE UNIV / CE Dept (Hicks), Corvallis, OR
PAYE-KOSANOWSKY, S / Pond Eddy, NY
PENNSYLVANIA STATE UNIV / Gotolski, University Park, PA; Rsch Lab, State College, PA
PILE BUCK, INC / Smoot, Jupiter, FL
PMB ENGRG / Lundberg, San Francisco, CA
PMTC / Code 1018, Point Mugu, CA
PORTLAND CEMENT ASSOC / AE Fiorato, Skokie, IL
PORTLAND STATE UNIV / Engrg Dept (Migliori), Portland, OR
PURDUE UNIV / CE Scol (Leonards), West Lafayette, IN
PWC / Code 1011, Pearl Harbor, HI; Code 102, Oakland, CA; Code 400, Oakland, CA; Code 412, San Diego, CA; Code 420, Oakland, CA; Code 421 (Kaya), Pearl Harbor, HI; Code 421 (Quin), San Diego, CA; Code 421 (Reynolds), San Diego, CA; Code 421, Norfolk, VA; Code 422, San Diego, CA; Code 423, San Diego, CA

SAN DIEGO PORT / Port Fac, Proj Engr, San Diego, CA
SAN DIEGO STATE UNIV / CE Dept (Krishnamoorthy), San Diego, CA
SANDIA LABS / Lib, Livermore, CA
SARGENT & HERKES, INC / JP Pierce, Jr, New Orleans, LA
SEATECH CORP / Peroni, Miami, FL
SEATTLE PORT / Dave Van Vleet, Seattle, WA
SEATTLE UNIV / CE Dept (Schwaegler), Seattle, WA
SHELL OIL CO / E. Doyle, Houston, TX
SIMPSON, GUMPERTZ & HEGER, INC / Hill, Arlington, MA
SOUTHWEST RESEARCH INSTITUTE / Thacker, San Antonio, TX; Energetic Sys Dept (Esparza), San Antonio, TX; King, San Antonio, TX; M. Polcyn, San Antonio, TX; Marchand, San Antonio, TX
STATE UNIV OF NEW YORK / CE Dept, Buffalo, NY
TEXAS A&M UNIV / CE Dept (Machemehl), College Station, TX; CE Dept (Niedzwecki), College Station, TX; Ocean Engr Proj, College Station, TX
TRW INC / Engr Lib, Cleveland, OH
TUDOR ENGRG CO / Ellegood, Phoenix, AZ
UNIV OF CALIFORNIA / CE Dept (Fenves), Berkeley, CA; CE Dept (Fourney), Los Angeles, CA; CE Dept (Gerwick), Berkeley, CA; CE Dept (Taylor), Davis, CA; CE Dept (Williamson), Berkeley, CA; Naval Archt Dept, Berkeley, CA
UNIV OF HAWAII / CE Dept (Chiu), Honolulu, HI; Manoa, Lib, Honolulu, HI; Ocean Engrg Dept (Ertekin), Honolulu, HI; Riggs, Honolulu, HI
UNIV OF ILLINOIS / Metz Ref Rm, Urbana, IL
UNIV OF MICHIGAN / CE Dept (Richart), Ann Arbor, MI
UNIV OF NEW MEXICO / NMERI (Bean), Albuquerque, NM
UNIV OF RHODE ISLAND / CE Dept (Kovacs), Kingston, RI
UNIV OF TEXAS / CE Dept (Thompson), Austin, TX; Construction Industry Inst, Austin, TX; ECJ 4.8 (Breen), Austin, TX
UNIV OF WASHINGTON / CE Dept (Mattock), Seattle, WA
UNIV OF WISCONSIN / Great Lakes Studies Cen, Milwaukee, WI
USDA / For Svc, Reg Bridge Engr, Aloha, OR
USNA / Ch, Mech Engrg Dept (C Wu), Annapolis, MD; PWO, Annapolis, MD
VALLEY FORGE CORPORATE CENTER / Franklin Research Center, Norristown, PA
VAN ALLEN, B / Kingston, NY
VSE / Ocean Engrg Gp (Murton), Alexandria, VA
VULCAN IRON WORKS, INC / DC Warrington, Cleveland, TN
WESTINGHOUSE ELECTRIC CORP / Lib, Pittsburg, PA
WINSTON CHEE / Gretna, LA
WISS, JANNEY, ELSTNER, & ASSOC / DW Pfeifer, Northbrook, IL
WOODWARD-CLYDE CONSULTANTS / West Reg, Lib, Oakland, CA

DISTRIBUTION QUESTIONNAIRE

The Naval Civil Engineering Laboratory is revising its primary distribution lists.

SUBJECT CATEGORIES

1 SHORE FACILITIES
1A Construction methods and materials (including corrosion control, coatings)
1B Waterfront structures (maintenance/deterioration control)
1C Utilities (including power conditioning)
1D Explosives safety
1E Aviation Engineering Test Facilities
1F Fire prevention and control
1G Antenna technology
1H Structural analysis and design (including numerical and computer techniques)
1J Protective construction (including hardened shelters, shock and vibration studies)
1K Soil/rock mechanics
1L Airfields and pavements
1M Physical security

2 ADVANCED BASE AND AMPHIBIOUS FACILITIES
2A Base facilities (including shelters, power generation, water supplies)
2B Expedient roads/airfields/bridges
2C Over-the-beach operations (including breakwaters, wave forces)
2D POL storage, transfer, and distribution
2E Polar engineering

3 ENERGY/POWER GENERATION
3A Thermal conservation (thermal engineering of buildings, HVAC systems, energy loss measurement, power generation)
3B Controls and electrical conservation (electrical systems, energy monitoring and control systems)
3C Fuel flexibility (liquid fuels, coal utilization, energy from solid waste)
3D Alternate energy source (geothermal power, photovoltaic power systems, solar systems, wind systems, energy storage systems)
3E Site data and systems integration (energy resource data, integrating energy systems)
3F EMCS design

4 ENVIRONMENTAL PROTECTION
4A Solid waste management
4B Hazardous/toxic materials management
4C Waterwaste management and sanitary engineering
4D Oil pollution removal and recovery
4E Air pollution
4F Noise abatement

5 OCEAN ENGINEERING
5A Seafloor soils and foundations
5B Seafloor construction systems and operations (including diver and manipulator tools)
5C Undersea structures and materials
5D Anchors and moorings
5E Undersea power systems, electromechanical cables, and connectors
5F Pressure vessel facilities
5G Physical environment (including site surveying)
5H Ocean-based concrete structures
5J Hyperbaric chambers
5K Undersea cable dynamics

ARMY FEAP
BDG Shore Facilities
NRG Energy
ENV Environmental/Natural Responses
MGT Management
PRR Pavements/Railroads

TYPES OF DOCUMENTS

D = Techdata Sheets; **R** = Technical Reports and Technical Notes; **G** = NCEL Guides and Abstracts; **I** = Index to TDS; **U** = User Guides; ☐ None - remove my name

INSTRUCTIONS

The Naval Civil Engineering Laboratory has revised its primary distribution lists. To help us verify our records and update our data base, please do the following:

- Add - circle number on list
- Remove my name from all your lists - check box on list.
- Change my address - line out incorrect line and write in correction **(DO NOT REMOVE LABEL).**
- Number of copies should be entered after the title of the subject categories you select.
- Are we sending you the correct type of document? If not, circle the type(s) of document(s) you want to receive listed on the back of this card.

Fold on line, staple, and drop in mail.

DEPARTMENT OF THE NAVY

Naval Civil Engineering Laboratory
Port Hueneme, CA 93043-5003

Official Business
Penalty for Private Use, $300

BUSINESS REPLY CARD
FIRST CLASS PERMIT NO. 12503 WASH D.C.

POSTAGE WILL BE PAID BY ADDRESSEE

NO POSTAGE NECESSARY IF MAILED IN THE UNITED STATES

Commanding Officer
Code L34
Naval Civil Engineering Laboratory
Port Hueneme, CA 93043-5003

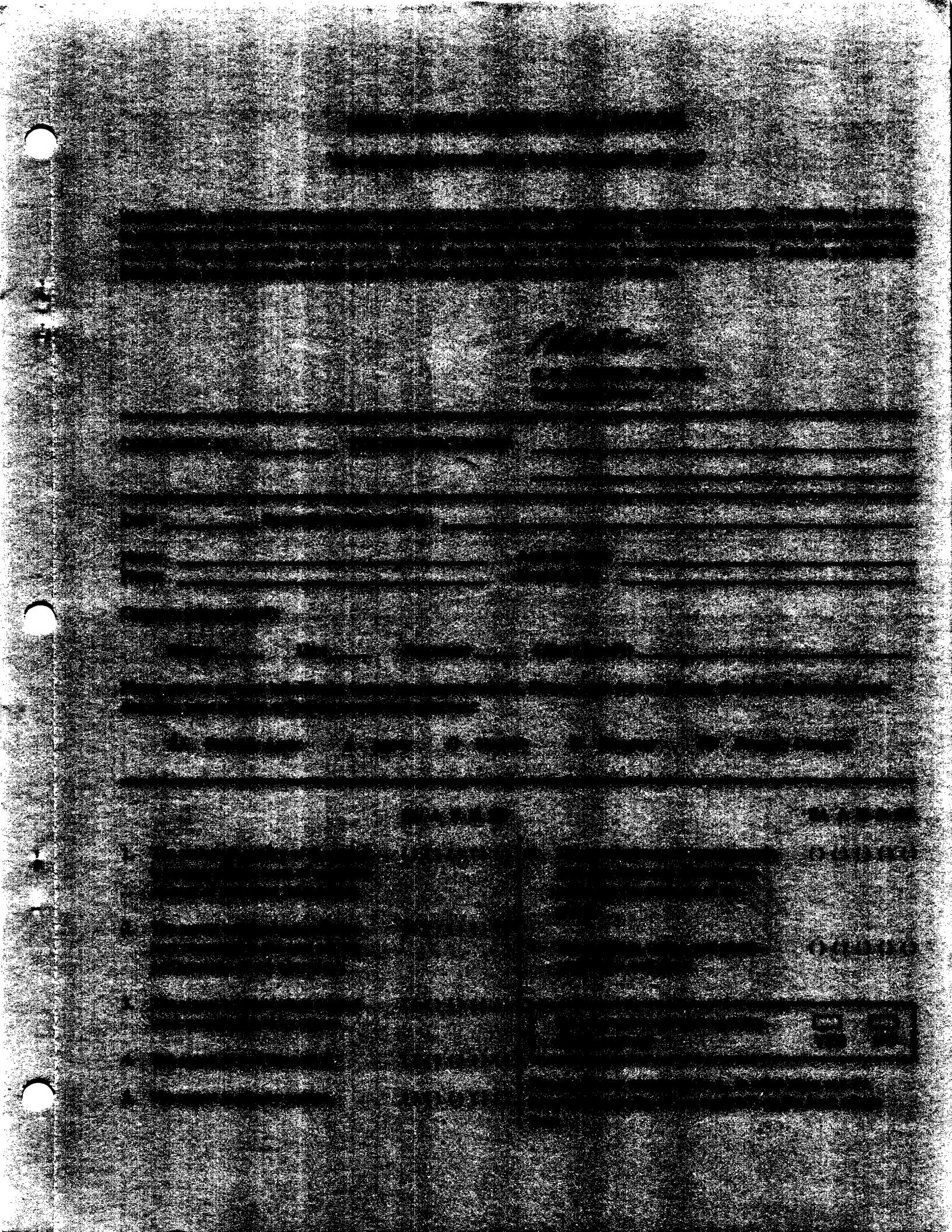

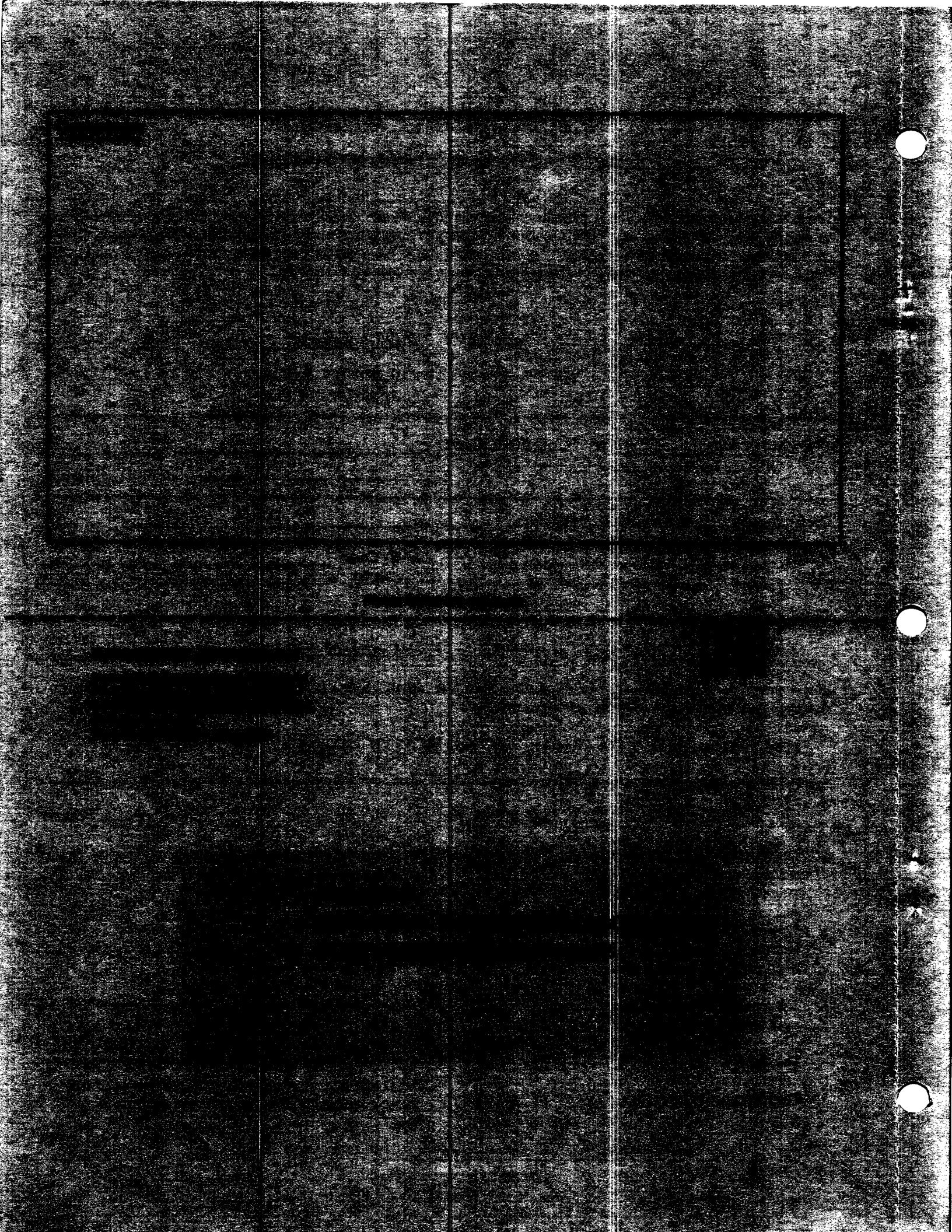

DEPARTMENT OF THE NAVY
Naval Civil Engineering Laboratory
Port Hueneme, CA 93043-5003
Official Business
Penalty for Private Use $300

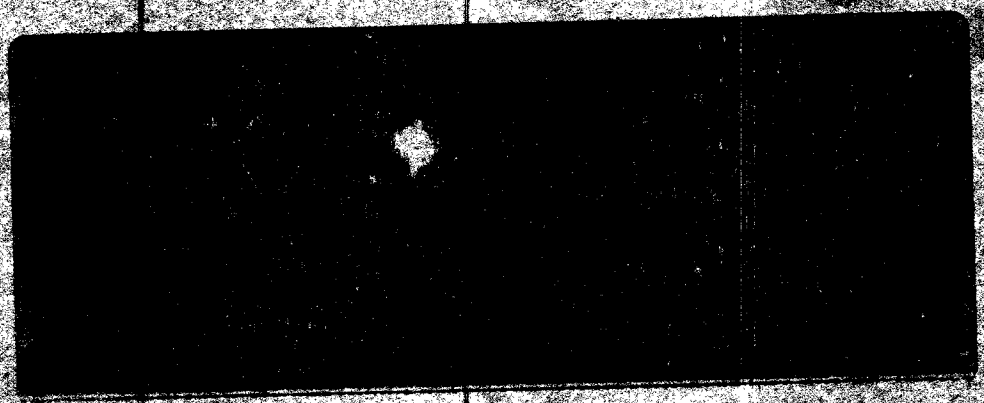

FIRST CLASS